The Galactic Population of Binaries Containing Neutron Stars

by

Eric D. Pfahl

B.A., Franklin & Marshall College (1998)

Submitted to the Department of Physics
in partial fulfillment of the requirements for the degree of

Doctor of Philosophy

at the

MASSACHUSETTS INSTITUTE OF TECHNOLOGY

May 2002
[JUNE 2002]

Author .....
Department of Physics
May 24, 2002

Certified by .....
Saul Rappaport
Professor of Physics
Thesis Supervisor

Accepted by .....
Thomas J. Greytak
Professor of Physics
Associate Department Head for Education

The Galactic Population of Binaries Containing Neutron Stars

by
Eric D. Pfahl

Submitted to the Department of Physics
on May 24, 2002, in partial fulfillment of the
requirements for the degree of
Doctor of Philosophy

Abstract

The research presented herein is a theoretical investigation of the formation, evolution, and ultimate fate of low-, intermediate-, and high-mass X-ray binaries (L/I/HMXBs). The primary theoretical tool used throughout is binary population synthesis. Results of these calculations are used to account for the numbers and properties of observed X-ray binaries and their descendants, as well as to direct future observational and theoretical work.

Combining binary population synthesis and binary stellar evolution calculations, I present a systematic population study of L/IMXBs in the Galactic plane. Since full stellar evolution calculations are used to model the X-ray binary phase, it is possible to make detailed comparisons between the theoretical models and observations. It is demonstrated quantitatively that IMXBs probably play a crucial role in shaping the population of LMXBs observed at the current epoch, as well as their descendant binary millisecond radio pulsars.

Recently, a new class of HMXBs has emerged, distinguished from other HMXBs by their wide, nearly circular orbits. I show that the discovery of a significant number of such systems is at odds with the conventional wisdom that most neutron stars receive very large "kick" speeds at birth. This problem may be rectified in a self-consistent way if the kick speed depends on the rotation rate of the pre-collapse core, which I propose is strongly influenced by the evolution of the neutron-star progenitor in a binary system.

The reasonable suggestion that certain globular clusters contain nearly 1000 neutron stars conflicts with the large mean kick speeds estimated from observations of isolated radio pulsars, which are 5 to 10 times the present cluster escape speeds. Therefore, most neutron stars born from single progenitors should have been ejected from their host clusters. I show that many more neutron stars are retained if a significant fraction are formed with massive stellar companions, but that the retained fraction is still too small to account for the inferred large numbers of neutron stars at the current epoch. Several alternative hypotheses are discussed, including the intriguing possibility that globular clusters we see today were ten times more massive in the distant past.

The *Chandra X-ray Observatory* has revealed hundreds of previously undetected point sources in a small field about the Galactic center. I show that the majority of these sources may be neutron stars accreting from the winds of unevolved companion stars. Infrared observations are proposed to search for the stellar counterparts of the X-ray sources.

Thesis Supervisor: Saul Rappaport
Title: Professor of Physics

Acknowledgments

First and foremost, I would like to convey my deep appreciation for my adviser, Saul Rappaport. Saul's inquisitive nature, sharp physical intuition, and kind demeanor have shown me a positive model for doing science, which is often as much of a social endeavor as it is intellectual.

I would like to acknowledge the MIT astrophysics faculty and graduate student community, who have helped to make my experiences as a graduate student *and* an MIT student both enjoyable and productive. Special thanks also go to my friends and collaborators, Philipp Podsiadlowski and Fred Rasio.

I am greatly indebted to my office mates, past and present, both for useful and illuminating scientific discussions, for entertaining my nearly continuous barrage of questions and commentary on miscellaneous topics, and, of course, for tolerating my unusual brand of humor. These fine folks include, John Fregeau, Jake Hartman, Jim Kiger, Mike Muno, Matt Muterspaugh, Mark Snyder, and Linqing Wen.

Lastly, but perhaps most importantly, I owe a great deal to my family and close friends for helping to shape my view of the world and my place in it.

Contents

List of Figures

List of Tables

Chapter 1

Introduction

Nearly forty years have passed since the first detection of X-ray sources beyond our own solar system. It quickly became clear that the brightest of these sources are accreting compact objects with binary stellar companions. With the maturity of X-ray astronomy came the discovery of hundreds of such binary X-ray sources, including the conspicuous low- and high-mass X-ray binaries, the more abundant but less luminous cataclysmic variables, and a dozen or so candidate black-hole binaries. While X-ray binaries are now rather common-place, many important unanswered questions still remain.

Theoretical motivations for studying X-ray binaries are two-fold. First, X-ray binaries are unique astrophysical laboratories for addressing fundamental questions regarding matter at extremely high densities, strong-field gravitation, and the plasma physics that shapes the accretion flow around and onto the compact object. Second, at a more global, statistical level, the population of X-ray binaries can offer specific, otherwise inaccessible, data about the formation and evolution of both binary and single stars. Here we focus on the latter course of study.

In order to account for the numbers and properties of observed X-ray binaries, it is necessary to understand quantitatively how such systems form and subsequently evolve. With these details in hand, it is possible to generate a theoretical population of X-ray binaries that can then be compared with observations. This procedure is referred to as *binary population synthesis*, whereby each of an ensemble of X-ray binary progenitors is followed analytically or numerically until it resembles the systems of interest or goes down a different evolutionary path. In later chapters, we demonstrate that binary population synthesis is a valuable scientific tool, not only for placing the populations of X-ray binaries and their descendants in a statistical framework, but also for identifying important new physical phenomena and guiding future observational and theoretical work.

All of the studies presented in this thesis specifically address only binary systems that contain neutron stars. Thus, the term "X-ray binary" will hereafter refer to only those systems with neutron-star accretors. However, it is important to mention that the basic theoretical techniques that we use to model populations of neutron-star X-ray binaries may also be applied to investigate populations of cataclysmic variables and binaries with

accreting black holes. We now give a brief and general overview of what is known empirically about X-ray binaries and how they are classified.

1.1 Observations of X-ray Binaries

Observed X-ray binaries exhibit a wide range of characteristics, including orbital periods from 11 minutes to $\sim$1 year, companion masses of $\sim$0.01–30 $M_\odot$, and X-ray luminosities from the detection sensitivities to $\sim 10^{38}$ ergs s^{-1} (see the catalogs of Liu et al. 2000, 2001). In the face of this large variety, workers in the field have grouped sources according to some common observed traits, such as the binary parameters or the X-ray spectral and variability properties. For the present work, the most important, and somewhat questionable, classification is based on the companion mass at the current epoch. Historically, a nominal distinction has been made between *low-* and *high-mass X-ray binaries* (L/HMXBs), depending on whether the inferred mass of the stellar companion is $\lesssim 1\ M_\odot$ or $\gtrsim 8\ M_\odot$, respectively. We now discuss how these systems are classified in practice and highlight some of the associated uncertainties.

1.1.1 High-Mass X-ray Binaries

The standard picture that applies to most HMXBs is that of a neutron star (NS) accreting from the wind of a massive ($\gtrsim 8\ M_\odot$), main-sequence stellar companion, with an orbital period of several tens of days or longer. The remainder of HMXBs have orbital periods of $\lesssim$10 days, and contain somewhat evolved, supergiant stars that may fill their Roche lobes. A massive companion is generally straightforward to identify optically if the binary lies within a few kiloparsecs in the Galactic plane; more distant Galactic sources may require infrared observations. When the companion is unidentified, the classification as an HMXB is based on the properties of the X-ray emission.

HMXBs are typically first detected as X-ray pulsars with hard, nonthermal X-ray spectra that extend beyond 10 keV (e.g., Nagase 1989). Strong X-ray pulsations and the occasional presence of a cyclotron absorption line at 10–30 keV suggest magnetic field strengths for the NS of $\gtrsim 10^{12}$ G. By measuring the secular variations in the apparent pulse period, it has been possible in more than twenty HMXBs to determine the orbital parameters and mass function, in some cases very precisely (see Bildsten et al. 1997 and Chapter 4). However, the set of HMXBs with well-measured orbits comprises only $\sim$20% of the $\sim$130 known systems in the Milky Way, SMC, and LMC (Liu et al. 2000). Moreover, there are excellent reasons to believe that we have detected only a few percent of the HMXBs in our Galaxy (see § 1.2.5).

Approximately 40% of the detected HMXBs are transient X-ray sources. Transient outburst phases are typically fairly short, lasting less than several months, with X-ray luminosities exceeding 10^{36} ergs s^{-1}. The outburst frequency sometimes directly reflects the orbital modulation in the accretion rate onto a NS in an eccentric orbit about its massive stellar companion (Bildsten et al. 1997). However, it often appears that the transient

behavior is driven by the activity of the star and its wind, and has no regular temporal patterns. In fact, quite a few sources have been detected only once in the history of X-ray astronomy.

1.1.2 Low-Mass X-ray Binaries and their Descendants

In an active LMXB, a Roche-lobe filling companion loses material through the inner Lagrange point and feeds the accretion disk that surrounds the NS. For most LMXBs, the companion is *not* detected at optical wavelengths, which indeed strongly suggests that it is low-mass star. The bulk of the optical emission is usually attributed to reprocessed X-rays from the accretion disk. Indirect pieces of evidence that have been used to classify sources as LMXBs are short orbital periods of $\lesssim$1 day, or the detection of type I X-ray bursts, which have only been seen in LMXBs.

The observational data that may be used to constrain models for the formation and evolution of LMXBs are really quite limited. Out of $\sim$150 observed systems, roughly 50 have measured orbital periods (Liu et al. 2001). Furthermore, in only a few LMXBs has the stellar companion been unambiguously detected spectroscopically, and its mass determined to better than 10–20%. Another important observed characteristic of the population of LMXBs is their scale height of $\gtrsim$500 pc in the Galactic disk, which is considerably larger than the scale height of their presumed massive progenitor binaries. This suggests that LMXBs receive a significant systemic impulse at the time the NS is formed, due to the combination of supernova mass loss and a possible NS "kick" (see § 1.2).

There are a significant number of active LMXBs for which very detailed X-ray data are available. However, it is extremely difficult to extract from this data important physical information regarding accretion disks or compact objects. X-ray spectral and flux variability are generally indicative of the complex and often erratic processes occurring in the accretion disk, for which we still lack a complete theoretical understanding. More regular patterns in the X-ray flux variability are observed as *quasi-periodic oscillations*, with characteristic frequencies that range from Hz to kHz (van der Klis 2000). Thus far, only physically motivated numerological arguments have been put forward to explain these oscillations; no scenario adequately accounts for the quasi-periodic X-ray emission. During type I X-ray bursts, more coherent, kHz oscillations are sometimes seen. These *burst oscillations* may directly reveal the NS spin, although much work still needs to be done in this active area of research (see M. Muno 2002, Ph.D. Thesis, MIT).

Coherent X-ray *pulsations* are detected in only a handful of LMXBs. The rarity of X-ray pulsars among LMXBs has been attributed to generally weak NS magnetic field strengths of $\lesssim 10^8$–10^9 G. Three of the LMXB/X-ray pulsars have pulse periods of $\sim$2 ms. It is not surprising that such systems exist, since the material accreted onto the NS has the specific angular momentum of the inner part of the accretion disk. The accretion of $\sim$0.1 $M_\odot$ is sufficient to yield millisecond spin periods. Long before the discovery of the two millisecond X-ray pulsars, it was suggested (van den Heuvel 1987 and references therein) that LMXBs are the progenitors of binary *millisecond radio pulsars*, with pulse periods of $\lesssim$10 ms, which

are often called "recycled" pulsars. Nearly 30 binary millisecond radio pulsars (MSRPs) are observed about the Galactic disk (e.g., Rappaport et al. 1995), and another ~50 MSRPs (binary and single) have been detected in globular clusters (Camilo et al. 2000; D'Amico et al. 2001b).

1.2 Theoretical Problems and Thesis Overview

The remainder of this thesis is directed toward understanding theoretically the origins, evolution, and ultimate fate of binary systems that harbor NSs. We employ statistical methods to highlight preferred evolutionary channels and to constrain uncertain model parameters such that we can properly account for the abundance and variety of the observed populations of X-ray binaries and their descendants. The work presented herein is directly motivated by recent X-ray and radio observations. Many of the sources that have inspired our work do not follow preconceived trends, and in some cases even suggest a theoretical paradigm shift. As much as possible, we have tried to raise new questions and suggest new avenues of research, both theoretical and observational, based upon our theoretical results. We now briefly summarize each chapter of this thesis.

1.2.1 Formation of X-ray Binaries

X-ray binaries in our Galaxy form and evolve in two very different dynamical regimes. In the *Galactic plane*, strong dynamical interactions between stars and binaries can be neglected entirely. Therefore, in the plane, each binary containing a NS descends from a massive *primordial binary*, wherein one star is sufficiently massive (~8–20 $M_\odot$) to produce a NS remnant. In a *globular cluster*, on the other hand, an incipient X-ray binary is formed when a single NS is captured into a binary system, via either a *three-body exchange interaction* (e.g., Rasio et al. 2000) or possibly *two-body tidal capture* (Fabian et al. 1975). While we do not specifically consider the dynamical formation of X-ray binaries in the following chapters, we provide a comprehensive study in Chapter 5 of how NSs are retained in globular clusters (see also § 1.2.4).

The evolutionary steps that precede the formation of a NS in a binary system, beginning with a massive primordial binary, are fully described Chapter 2; here, we provide a short summary. Each primordial binary undergoes a phase of mass transfer when the initially more massive star (the NS progenitor) evolves to fill its Roche lobe. The mass transfer may be stable or dynamically unstable, depending on the initial mass ratio of the two stars and their evolutionary states when mass transfer begins. If a merger of the two stars is avoided, the mass transfer terminates when the stellar envelope of the NS progenitor is removed, leaving the star's hydrogen-exhausted core. After consuming its remaining nuclear fuel, the core explodes as a Type Ib or Ic supernova, leaving a NS remnant. The binary is strongly perturbed by the supernova explosion, and may be disrupted, due to the impulsive mass loss and a possible NS "kick" of magnitude $\gtrsim$100 km s^{-1}. If the binary remains bound, then the system is an incipient low-, intermediate-, or high-mass X-ray binary, if the mass

of the companion is $\lesssim 2\ M_\odot$, $\sim$2–8 $M_\odot$, or $\gtrsim 8\ M_\odot$, respectively.

1.2.2 Intermediate-Mass X-ray Binaries

It was long thought that mass transfer via Roche-lobe overflow would be dynamically unstable if the donor star is significantly more massive than the NS, and therefore that such systems would not survive to resemble the X-ray binaries we presently observe (see, however, Kalogera & Webbink 1996). Until recently, this view largely persisted, as only one exception—Her X-1, with a companion of mass $\sim 2\ M_\odot$—has so far been identified. The situation changed after optical observations of Cyg X-2 ($P_{\rm orb} = 9.84$ days) revealed the spectral type and mass ($\sim 0.6\ M_\odot$) of the donor star (Casares et al. 1998; Orosz & Kuulkers 1999). It was soon realized that the star is much hotter and more luminous than an initially low-mass star of the same radius evolving in isolation. Motivated by these results, several theoretical groups reinvestigated the old paradigm for LMXB evolution (King & Ritter 1999; Podsiadlowski & Rappaport 2000; Tauris et al. 2000; Podsiadlowski et al. 2002). They found that mass transfer may, in fact, be dynamically stable for companion masses up to $\sim 4\ M_\odot$, with the mass transfer initially proceeding on the thermal timescale of the donor. Detailed evolutionary calculations show that Cyg X-2 probably began its life as an X-ray binary with a donor of mass $\sim$3–4 $M_\odot$. That is, Cyg X-2, previously a prototype LMXB, was originally an *intermediate-mass X-ray binary* (IMXB).

The example of Cyg X-2 suggests that perhaps many, even the majority, of the observationally classified LMXBs are descended from IMXBs. This is extremely important, since it turns out that the evolutionary parameter space available for forming an incipient LMXB with a companion mass of $\lesssim 1\ M_\odot$ is really very small (e.g., Bhattacharya & van den Heuvel 1991; Kalogera & Webbink 1998). Allowing for initially more massive donors, one finds that this fine tuning problem all but disappears.

In Chapter 3, we present a systematic population study of L/IMXBs in the Galactic plane. Our investigation utilizes a library of previously calculated evolutionary sequences for L/IMXBs that covers a wide range of initial orbital periods and donor masses. By incorporating evolutionary calculations of the X-ray binary phase, we can assess in detail the role of IMXBs and the implications thereof, as well as quantify discrepancies between the theoretical population models and the observations.

1.2.3 HMXBs and Neutron-Star Kicks

Among the HMXBs with measured orbits, there seem to be three distinct classes of systems, distinguished by their orbital parameters: (i) binaries with supergiant companions, orbital periods of $P_{\rm orb} \lesssim 10$ days, and eccentricities of $e \lesssim 0.1$ (Bildsten et al. 1997); (ii) moderately wide, eccentric binaries with $P_{\rm orb} \sim$ 20–100 days and $e \sim$ 0.3–0.5 (Bildsten et al. 1997); (iii) a recently identified class with long periods of $P_{\rm orb} \sim$ 30–250 days and quite low eccentricities of $e \lesssim 0.2$. Chapter 4 is devoted to a full discussion of the latter class of HMXBs. We demonstrate the statistical significance of these systems, and show that their detection is at odds with the conventional wisdom regarding NS kicks.

A Maxwellian distribution in kick speeds, with a mean of ~200–300 km s^{-1}, adequately accounts for the kinematics of isolated radio pulsars and the Galactic scale height of LMXBs (e.g., Johnston 1996; Hansen & Phinney 1997; Arzoumanian et al. 2002). However, a Maxwellian with a mean speed of 50 km s^{-1} is required in order to account for the 6 observed long-period, low-eccentricity HMXBs. In Chapter 4, we describe an evolutionary scenario in which members of the new class of HMXBs are produced in sufficient numbers, and in which the the abundance and properties of other known NS populations are self-consistently reproduced. A physical model is proposed that may explain the dichotomous NS kicks, wherein the kick magnitude depends on the rotation rate of the pre-collapse core, which in turn is largely determined by the evolution of the NS progenitor in a binary system.

1.2.4 Neutron-Star Retention in Globular Clusters

Recent radio and X-ray observations of globular clusters have found evidence for surprisingly large numbers of NSs, in the form of MSRPs and low-luminosity X-ray sources (e.g., Camilo et al. 2000; Grindlay et al. 2001b). Together with the dozen well-known cluster LMXBs (Deutsch et al. 2000), these objects likely represent only a small fraction of the NSs present in the Galactic globular cluster system. Observational selection effects and theoretical formation statistics for LMXBs and MSRPs indicate that of order 1000 NSs may reside in certain massive clusters, which amounts to $\gtrsim$10–20% of the total number formed at early times. This is extremely problematic, since globular clusters presently have central escape speeds of $\lesssim$50 km s^{-1}, while the inferred mean kick speeds of isolated radio pulsars are $\gtrsim$200 km s^{-1}. A fundamental, unresolved question is how a large number of NSs are retained in globular clusters.

Chapter 5 gives a complete overview of the NS *retention problem*. Using binary population synthesis, we present a detailed quantitative assessment of how binary systems influence the net NS retention fraction. It has been suggested (Drukier 1996; Davies & Hansen 1998), though not quantitatively confirmed, that the retention problem may be solved if a significant fraction of NSs are formed in binary systems with massive companions; such a companion can effectively anchor a NS to the host cluster. Our calculations show that binaries do indeed lead to a greatly increased retention fraction over single NS progenitors when the characteristic kick speed is large. However, we find that the percentage of NSs retained is still only ~1–5%, which may not be sufficient to explain the numbers observed. We therefore speculate on alternative solutions to the retention problem.

If, as we propose in Chapter 4, a sizable fraction of NSs born in binary systems receive very small kicks, then the retention problem is not so severe. Using the dichotomous kick scenario described in Chapter 4, we find that the retention fraction is increased by a factor of ~4–5. The severity of the retention problem may be further reduced if we allow for NS formation via *accretion-induced collapse* of a massive white dwarf, although this process and its outcomes are very poorly understood. Finally, we note the interesting possibility that some of the globular clusters that presently have a mass of 10^6 $M_\odot$ are the surviving remnants of clusters with an initial mass in stars of $\gtrsim 10^7$ $M_\odot$. In this case, a small initial

retention fraction evolves into a large *inferred* retention fraction as the cluster loses $\gtrsim$90% of its mass before the current epoch.

1.2.5 Wind-Accreting Neutron Stars

Observations with the *Chandra X-ray Observatory* (Wang et al. 2002) have recently revealed $\gtrsim$500 previously undetected, faint point sources in a $0.8^\circ \times 2^\circ$ field about the Galactic center, the nature of which are unknown. Based on the extragalactic $\log N$–$\log S$ curve in X-rays (Brandt et al. 2001), we estimate that only 10–20% of the *Chandra* sources are background AGN. We propose that the remaining Galactic sources are wind-accreting NSs (WNSs), of which HMXBs are the best known examples.

We describe in Chapter 6 our motivations for suggesting that many, if not most, of the *Chandra* sources are WNSs, as opposed to LMXBs, black-hole binaries, or cataclysmic variables. Our arguments are supported by a binary population synthesis study of WNSs. Each theoretically produced WNS is characterized by the orbital parameters and companion mass. The NS accretes from the wind of its stellar companion via the Bondi-Hoyle-Lyttleton process (Hoyle & Lyttleton 1941; Bondi & Hoyle 1944), where the emerging X-ray luminosity sensitively depends on the wind speed and the orbital separation. By incorporating some reasonable spatial distribution of the WNSs, we calculate a theoretical X-ray flux distribution. Somewhat surprisingly, the distribution may be dominated by systems with intermediate-mass companions over a wide range in flux. We propose that an infrared observing campaign be undertaken to search for the stellar counterparts to the *Chandra* sources in order to identify their true nature and possibly corroborate our model.

Chapter 2

Massive Binary Population Synthesis

This chapter is adapted from material in the paper, "A Comprehensive Study of Neutron-Star Retention in Globular Clusters," by Eric Pfahl, Saul Rappaport, & Philipp Podsiadlowski, to appear in *The Astrophysical Journal.*

2.1 Introduction

From an operational standpoint, the formation of a NS in a binary system involves three distinct evolutionary steps. First, we begin with a *primordial binary*, where the initially more massive component (the *primary*) has a mass $\gtrsim 8\ M_\odot$, so that it ultimately produces a NS remnant. Second, we follow the phase of *mass transfer* from the primary to the initially less massive star (the *secondary*). Third, we compute the binary parameters following the *SN explosion* of the primary, where the often strong dynamical influence of the SN may unbind the binary system. In this chapter, we discuss each of these formation steps, which are implemented in the Monte Carlo binary population synthesis code that is utilzed in each study presented in this thesis. Below, we encapsulate our lack of detailed knowledge in the form of a set of free parameters, for which we quote reasonable values that are applied in our *standard model* of NS binary formation.

2.2 Primordial Binaries

We define a *massive* primordial binary as a system where at least one component has a large enough main-sequence mass that it would yield a NS remnant if left to evolve in isolation. The main-sequence mass threshold for NS formation is $\sim 8\ M_\odot$, but may be as low as $\sim 6\ M_\odot$ in the low-metallicity environment of a globular cluster (e.g., Marigo et al. 2001 and references therein). Hereafter, we refer to the initially more massive component of the

binary as the *primary* and the initially less massive component as the *secondary*. The main-sequence masses of the primary and secondary are denoted by M_1 and M_2, respectively, and we define the corresponding mass ratio as $q = M_2/M_1 < 1$.

2.2.1 Component Masses

Various authors (e.g., Kraicheva et al. 1978; Duquennoy & Mayor 1991) have found that the primary masses in close binaries are consistent with the initial mass function (IMF) of single stars. We draw primary masses from a single power-law IMF, which is appropriate for massive stars (see Miller & Scalo 1979; Scalo 1986; Kroupa et al. 1993):

$$p(M_1) = (x-1)(M_{1,\min}^{-x+1} - M_{1,\max}^{-x+1})^{-1} M_1^{-x} \ , \tag{2.1}$$

where we adopt $M_{1,\min} = 8\ M_\odot$. We choose values of x in the range 2–3, where $x = 2.35$ corresponds to a Salpeter IMF (Salpeter 1955). For our standard model, we adopt $x = 2.5$. An isolated star with $M_1 > M_{1,\max}$ is assumed to leave a black hole remnant rather than a NS. The precise value of $M_{1,\max}$ is unknown, but is probably $\gtrsim 30\ M_\odot$. Because the IMF sharply decreases with increasing mass, our results do not depend strongly on the value of $M_{1,\max}$.

It is generally believed that the main-sequence masses of binary components are correlated (e.g., Abt & Levy 1978; Garmany, Conti, & Massey 1980; Eggleton, Fitchett, & Tout 1989). Observations of massive binaries suggest that equal masses may be favored (e.g., Abt & Levy 1978; Garmany et al. 1980), presumably as a result of the formation process. However, serious selection effects hamper the determination of the true mass-ratio distribution, and other authors have found that low-mass companions to massive primaries appear to be more likely (e.g., Mason et al. 1998; Preibisch et al. 2000). For the distribution function, $p(q)$, we consider both increasing and decreasing functions of q, as encapsulated by the power-law form

$$p(q) = (1+y)q^y \ , \tag{2.2}$$

for $y > -1$.

Guided by the important work of Garmany et al. (1980), we adopt $y = 0$ for our standard model. These authors found that 40% of the O stars in a magnitude limited sample have binary companions, and that 85% of these systems have $q > 0.4$. When one takes into account the difficulty of detecting low-mass companions, the results of Garmany et al. (1980) seem consistent with a fairly flat distribution of mass ratios.

2.2.2 Eccentricity

It is often assumed in population studies of the sort we have undertaken that the orbits of primordial binaries are circular. However, since the process of binary formation is only poorly understood, there is no a priori justification for suggesting that massive primordial binaries should have small eccentricities. The situation is less clear in globular clusters, where dynamical interactions may influence binary formation (e.g., Price & Podsiadlowski

1995; Bonnell et al. 1998). However, it is expected that the binary will eventually circularize if the orbit is sufficiently compact that mass transfer will take place. From here on, we only consider circular primordial binaries.

There exists at least one important caveat to the circularization assumption stated above. Eccentricities of $\sim$0.5 are seen among the wide, interacting VV Cephei binaries, which consist of a massive red supergiant and an early-type B star (e.g., Cowley 1969; Cowley et al. 1977). The VV Cephei systems are the widest of the known massive, interacting binaries, with periods $\gtrsim$10 yr, and their significant eccentricities may indicate that not enough time has elapsed for the system to circularize. The growth of the large red-supergiant envelope occurs over a relatively short timescale of $<10^5$ yr, while the circularization timescale varies as $(a/R)^8$ (e.g., Zahn 1977), where a is the binary semimajor axis and R is the radius of the red supergiant. Therefore, the components of the observed VV Cephei binaries have experienced strong tidal interactions only very recently, in terms of the evolutionary history of the more massive star.

2.2.3 Orbital Separation

Observations of young, detached binary systems indicate that the distribution of orbital periods, and thus the distribution of semimajor axes, a, is logarithmically flat (Abt & Levy 1978; see, however, Duquennoy & Mayor 1991):

$$p(a) = \left[\ln\left(\frac{a_{\rm max}}{a_{\rm min}}\right)\right]^{-1} a^{-1} \ . \tag{2.3}$$

Since we assume that the primordial binaries are circular, a is just the orbital separation. For given component masses, the lower limit, $a_{\rm min}$, is determined from the constraint that neither star overflows its Roche lobe on the main sequence. The upper limit, $a_{\rm max}$, is somewhat arbitrary; in practice, we assume $a_{\rm max} = 10^3$ AU.

2.3 Overview of Massive Binary Stellar Evolution

Owing to its larger mass, the primary will be the first star to leave the main sequence. The subsequent binary evolution depends on the size of the Roche lobe that surrounds the primary. For circular orbits, the volume-equivalent radius of the Roche lobe of the primary is well approximated by the formula due to Eggleton (1983):

$$\frac{R_{\rm L1}}{a} \equiv r_{\rm L1} = \frac{0.49}{0.6 + q^{2/3}\ln(1+q^{-1/3})} \ , \tag{2.4}$$

where a in this equation represents the constant orbital separation. The radius of the Roche lobe of the secondary, $R_{\rm L2}$, is obtained by replacing q in eq. (2.4) with $1/q$.

Left to evolve in isolation, the primary would grow to a maximum radius of $\sim$500–2000 $R_\odot$; the value depends sensitively on mass, metallicity, and especially assumptions

about stellar winds. So, if the orbit is sufficiently compact ($R_{\rm L1} \lesssim 20$ AU), the primary will grow to fill its Roche lobe. The value of $R_{\rm L1}$ is used to determine the evolutionary state of the primary when it begins to transfer matter through the inner Lagrange point.

It is particularly important to distinguish between mass transfer that is dynamically *stable* (proceeding on the nuclear or thermal timescale of the primary) and mass transfer that is dynamically *unstable* (proceeding on the dynamical timescale of the primary). For the case where the mass donor is more massive than the accretor, dynamical instability is typically attributed to one of two root causes. If the star grows faster than its Roche lobe (or the Roche lobe shrinks faster than the star), a phase of runaway mass transfer may ensue. In particular, stars with deep convective envelopes tend to expand in response to mass loss (e.g., Paczyński & Sienkiewicz 1972; Hjellming & Webbnik 1987), while the Roche lobe generally shrinks. Also, for systems with extreme mass ratios, the primary may not be able to achieve synchronous rotation with the orbit, causing the components to spiral together; this is the classic Darwin tidal instability (Darwin 1879; see also Hut 1981) . The evolutionary state of the primary when it fills its Roche lobe is a good indicator of the physical character of the subsequent mass transfer and binary stellar evolution.

Following Kippenhahn & Weigert (1966; see also Lauterborn 1970 and Podsiadlowski, Joss, & Hsu 1992), we distinguish among three evolutionary phases of the primary at the onset of mass transfer. Case A evolution corresponds to core hydrogen burning, Case B refers to the shell hydrogen burning phase, but prior to central helium ignition, and case C evolution begins after helium is exhausted in the core. These three cases (see Figs. 2-1 and 2-2) provide a rough framework for categorizing binary stellar evolution during mass transfer. Of course, not all systems will undergo Roche lobe overflow. A large fraction of binaries will be sufficiently wide that the primary and secondary evolve as isolated stars prior to the first SN. We refer to such detached configurations as case D.

Of the three broad categories of mass transfer, case A evolution is potentially the most problematic. Perhaps the most likely outcome is a merger of the two stars following a contact phase, wherein both stars fill their Roche lobes, leaving a massive single star (Pols 1994; Wellstein et al. 2001). For a recent detailed discussion of the complex evolutionary processes that occur during case A mass transfer and the possible outcomes, see Nelson & Eggleton (2001) and Wellstein, Langer, & Braun (2001). Fortunately, the subtleties of case A evolution may essentially be overlooked presently. The range in orbital separations admitted by case A is $\sim$3–20 $R_\odot$, which comprises $\sim$5–10% of the primordial binary population. In addition, if the majority of case A systems merge as expected, then a detailed consideration of case A evolution is unnecessary, since our focus is on binary systems.

Two important subcases comprise case B. *Early* case B (case B_e) mass transfer occurs when the primary fills its Roche lobe as it evolves through the Hertzsprung gap. In this case, the envelope of the primary is still mostly radiative and the mass transfer is thought to be initially stable for a wide range of mass ratios. *Late* case B (case B_l) mass transfer occurs when the primary fills its Roche lobe as it evolves up the first giant branch. Case B_l mass transfer is characterized by a deep convective envelope, in which case it is likely that mass transfer will initially take place on the dynamical timescale of the primary, leading

to a common-envelope (CE) phase (see § 2.4). The range in orbital separations of case B systems is ~20–1000 $R_\odot$, which contains ~20–30% of the primordial binary population.

For stars of mass $\lesssim$12–15 $M_\odot$, core helium burning is typically accompanied by a significant decrease in stellar radius (see Fig. 2-1), so that the primary cannot fill its Roche lobe during this time. After helium is exhausted in the core, the star develops a deep convective envelope and begins to ascend the Hayashi track. We refer to this phase as late case C (case C_l). We assume that case C_l mass transfer is dynamically unstable, as we do for case B_l (see, however, Podsiadlowski et al. 1992, 1994).

For stars more massive than ~12–15 $M_\odot$, stellar evolution calculations do not provide a self-consistent physical picture that simultaneously accounts for observations of massive stars in high- and low-metallicity environments (e.g., the Milky Way and the SMC, respectively). One important problem is to explain the ratio of blue to red supergiants among massive stars, as a function of metallicity (see Langer & Maeder 1995). For these massive stars, it is possible for helium to ignite in the core while the star is traversing the Hertzsprung gap and is still mostly radiative. It is unclear how the radius behaves during the subsequent phase of core helium burning. The radius may shrink somewhat, so that Roche lobe overflow is impossible during this phase. However, the radius may continue to increase after a short plateau (a so-called "failed blue loop" in the HR diagram; see Fig. 2-2). Therefore, it is theoretically possible for mass transfer to begin during core helium burning, but the allowed range in stellar radii is sufficiently small that we neglect this possibility. Following core helium exhaustion, the star still has a radiative envelope. Early case C (case C_e) mass transfer is possible before the primary reaches the base of the asymptotic giant branch and begins to ascend the Hayashi track, at which point the star is mostly convective and falls into the case C_l category. Cases C_e and C_l account for ~15% and ~10% of the primordial binaries, respectively.

For solar metallicity, stars of mass $\gtrsim$20–25 $M_\odot$ may shed their hydrogen-rich envelopes following core helium exhaustion as a result of prodigious wind mass loss (Maeder 1992). However, for the low metallicities of globular clusters ($Z \lesssim 0.001$ typically), stellar wind mass loss is probably only important above ~30–40 $M_\odot$ (Maeder 1992), although it should be emphasized that such mass loss is quite uncertain, both theoretically and observationally. For most NS progenitors, especially those that undergo mass transfer in a binary system, stellar winds are not a very important consideration, and thus in our simulations we do not consider stellar winds prior to the SN explosion.

The mass of the primary and its radius at the onset of Roche-lobe overflow are sufficient to determine the category of mass transfer. Using the fitting formulae of Hurley et al. (2000), we compute the radius of an isolated star with the mass of the primary at different stages of its evolution (e.g., main sequence, core helium ignition, base of the asymptotic giant branch). The Roche-lobe radius of the primary falls into some range and determines if mass transfer is categorized as case A, B_e, B_l, C_e, C_l, or D.

It is worth adding a note here regarding the possible outcomes of contact evolution. Unless the initial mass ratio is close to unity, it is likely that the majority of case A, B_e, and C_e systems will evolve into a contact configuration (Pols 1994; Nelson & Eggleton 2001;

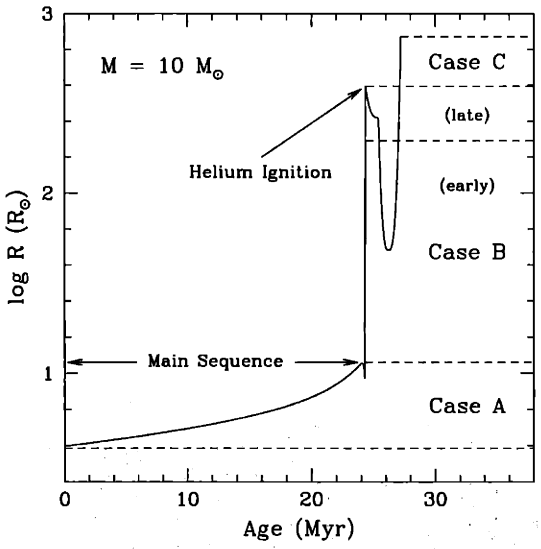

Figure 2-1: Evolution of the radius as a function of time for a star of mass 10 $M_{\odot}$, calculated with the fitting formulae of Hurley et al. (2000). The range of radii for each case of mass transfer is labeled. Note that the radius decreases by a factor of $\sim$10 immediately following central helium ignition.

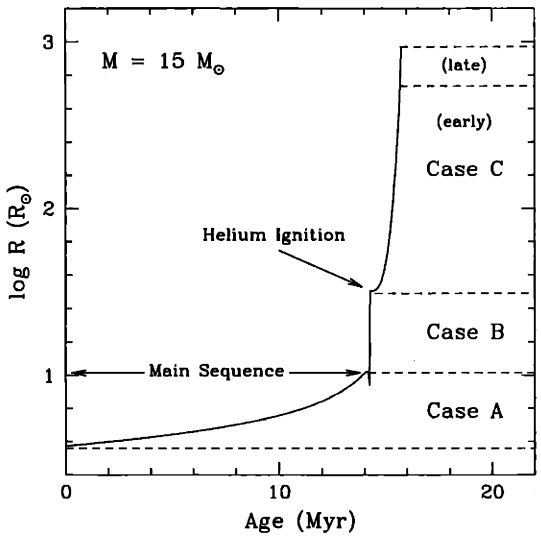

Figure 2-2: Evolution of the radius as a function of time for a star of mass 15 $M_{\odot}$, calculated with the fitting formulae of Hurley et al. (2000). Helium ignites in the core while that star is evolving through the Hertzsprung gap. Steady helium burning proceeds rapidly, and the radial evolution is barely perturbed during this phase. This type of evolution permits *early*, or radiative, case C mass transfer.

Wellstein et al. 2001). Shortly after the primary first fills its Roche lobe, the mass transfer rate rises to values of order $M_1/\tau_{\rm th,1} \sim 10^{-3}$–$10^{-4}\ M_\odot\ {\rm yr}^{-1}$, where $\tau_{\rm th,1}$ is the thermal timescale of the primary. Most of the envelope of the primary is removed during this initial rapid phase. The secondary reacts to donated material on its own thermal timescale, and thus can only accrete in an equilibrium fashion if it is very nearly coeval with the primary at the onset of Roche lobe overflow (i.e., $q \sim 1$). If the secondary is essentially unevolved at the time the primary fills its Roche lobe, the transferred gas will fill up the Roche lobe of the secondary and thus initiate a contact phase.

Some attempts have been made to follow the evolution of both stars during the contact phase (see Kähler 1989 for an overview of the important issues), but since the problem requires certain three-dimensional hydrodynamical elements, no complete physical description of this process has emerged. However, there are two distinct possible outcomes: (i) evolution during contact is dynamically stable, with some fraction of the material ejected from the system, or (ii) there is sufficient drag on the secondary—owing to the extended common stellar envelope surrounding the system—that the binary components spiral together on a dynamical timescale, possibly resulting in the ejection of the common envelope or a merger of the two stars. Dynamical spiral-in cannot be the generic consequence of contact evolution, since then we would have great difficulty in explaining the observed long-period high-mass X-ray binaries in the Galaxy (see § 4). We expect that there is some critical mass ratio, q_c, that separates stable and dynamically unstable mass transfer for those systems that experience a contact phase. In our simulations, we typically choose $q_c = 0.5$ for all case B_e and C_e systems, which implies that 50% of these binaries undergo dynamically unstable mass transfer for a flat distribution in initial mass ratios. As we will show in the next section, dynamically unstable case B_e and C_e mass transfer almost always leads to a merger of the two stars.

2.4 Analytic Prescriptions for Mass Transfer

Dynamically stable mass transfer can be reasonably well characterized by two dimensionless parameters, not necessarily fixed during the evolution. In a given time step, the secondary accretes a fraction β of the mass lost by the primary. Generally, β is a function of the component masses, the rate at which mass is transferred from the primary, and the evolutionary state of the secondary. The complementary mass fraction, $1-\beta$, escapes the binary system, taking with it specific angular momentum α, in units of the orbital angular momentum per unit reduced mass, $(GM_b a)^{1/2}$, where $M_b = M_1 + M_2$ is the total binary mass.

For a circular orbit, the orbital angular momentum is given by

$$J = \frac{M_1 M_2}{M_b}(GM_b a)^{1/2}\ . \tag{2.5}$$

Logarithmic differentiation yields

$$\frac{\delta J}{J} = \frac{\delta M_1}{M_1} + \frac{\delta M_2}{M_2} - \frac{1}{2}\frac{\delta M_b}{M_b} + \frac{1}{2}\frac{\delta a}{a} , \tag{2.6}$$

where it is assumed that the orbits remains circular during mass transfer. From the definition of the mass *capture fraction*, β, it is clear that $\delta M_2 = -\beta\,\delta M_1$ and $\delta M_b = (1-\beta)\,\delta M_1$. We neglect the tidal coupling between the rotation of the Roche lobe-filling primary and the orbit. Therefore, variation in the orbital angular momentum is attributed solely to systemic mass loss, and it follows that

$$\delta J = \alpha\,(G M_b a)^{1/2} \delta M_b . \tag{2.7}$$

We consider one of two modes of angular momentum loss during stable mass transfer: mass that is lost from the system takes with it (1) a constant fraction of the specific orbital angular momentum (constant α), or (2) the specific angular momentum of the secondary. Constant values of α and $\beta > 0$ lead to one possible analytic solution (Podsiadlowski et al. 1992) of eq. (2.6):

$$\left(\frac{a'}{a}\right)_1 = \frac{M_b'}{M_b}\left(\frac{M_1'}{M_1}\right)^{C_1}\left(\frac{M_2'}{M_2}\right)^{C_2} , \tag{2.8}$$

where

$$\begin{aligned} C_1 &\equiv 2\alpha(1-\beta) - 2 \\ C_2 &\equiv -2\alpha\left(\frac{1}{\beta} - 1\right) - 2 . \end{aligned} \tag{2.9}$$

Primes on the masses and semimajor axis indicate the values after some amount of mass has been transferred. Figure 2-3 illustrates the evolution of $(a'/a)_1$ as a function of the fractional mass loss, $\Delta M_1/M_1 \equiv 1 - M_1'/M_1$, from the primary. For our standard model, we use eq. (2.8) to evolve the orbit, with $\alpha = 1.5$, a value characteristic of mass loss through the L2 point, and $\beta = 0.75$. These values imply that $(a'/a)_1 \sim 1$ for $\Delta M_1/M_1 \sim 0.8$, a characteristic fractional envelope mass.

A second analytic solution can be obtained for the case where β is constant and where matter lost from the system takes away the specific angular momentum of the accreting star (perhaps in the form of jets or an axisymmetric wind). In this scenario we have

$$\left(\frac{a'}{a}\right)_2 = \left(\frac{M_b'}{M_b}\right)^{-1}\left(\frac{M_1'}{M_1}\right)^{-2}\left(\frac{M_2'}{M_2}\right)^{-2/\beta} . \tag{2.10}$$

It can be shown that eq. (2.10) is a weak function of β, and so $(a'/a)_2$ closely follows the $\beta = 1$ solution (see Fig. 2-3) within a factor of two for a wide range of initial mass ratios.

Mass that is removed from the primary on a dynamical timescale cannot be assimilated by the secondary, which can only accept matter on its much longer thermal readjustment

timescale. Consequently, the transferred material fills the Roche lobe of the secondary and a common-envelope (CE) phase is initiated (Paczyński & Sienkiewicz 1972). As a result of hydrodynamic drag, the secondary spirals in toward the core of the primary, depositing a fraction $\eta_{\rm CE} \lesssim 1$ of the initial orbital binding energy into the CE as frictional luminosity (e.g., Meyer & Meyer-Hofmeister 1979; Sandquist et al. 2000). If sufficient energy is available to unbind the envelope, what remains is a compact binary consisting of the secondary, which we assume is unaltered during the spiral-in process, and the hydrogen-depleted core of the primary. On the other hand, if the CE remains gravitationally bound to the system, drag forces will perpetuate the spiral-in and the two stars will merge.

A simple energy relation determines the outcome of the CE and spiral-in (e.g., Webbink 1984):

$$-\frac{GM_1M_e}{\lambda\, a\, r_{\rm L1}} = \eta_{\rm CE}\left[-\frac{GM_cM_2}{2a'} + \frac{GM_1M_2}{2a}\right] , \tag{2.11}$$

where M_e and M_c are the envelope-mass and the core-mass of the primary, respectively. The left-hand side of eq. (2.11) is the envelope binding energy, taking into account both gravitational and thermal contributions, where λ is a parameter that depends on the structure of the envelope. Solving eq. (2.11) for a'/a, we find

$$\left(\frac{a'}{a}\right)_{\rm CE} = \frac{M_cM_2}{M_1}\left(M_2 + \frac{2M_e}{\lambda\,\eta_{\rm CE}\, r_{\rm L1}}\right)^{-1} . \tag{2.12}$$

If the secondary fills its Roche lobe for the computed final orbital separation, a', this effectively indicates that insufficient energy was available to unbind the CE, and we assume that a merger is the result. Figure 2-4 illustrates the dependence of $(a'/a)_{\rm CE}$ on the initial mass ratio, q, for four values of the initial fractional envelope mass, M_e/M_1.

For the NS progenitors considered here, detailed calculations by Dewi & Tauris (2000) show that $\lambda \sim 0.1$–0.5 over a wide range of evolutionary states. We utilize a fixed value of $\lambda = 0.5$ for the studies presented in Chapters 4, 5, and 6, where dynamically unstable mass transfer is of minor importance. On the other hand, the common-envelope phase is a crucially important aspect of low- and intermediate-mass X-ray binary formation. Thus, in Chapter 3, we give results for a range of λ values.

The majority of systems with $q < q_c$ that undergo case B_e or C_e mass transfer end up merging, a result that we can demonstrate as follows. Typical fractional primary envelope masses are $\sim$0.7, and thus Fig. 2-4 indicates that dynamically unstable mass transfer causes the orbit to shrink by a factor of $\lesssim$50 for $q \lesssim 0.5$. Case B_e and C_e binaries have $a \lesssim 500\ R_\odot$, and so we see that most systems with $q < q_c$ should merge, since for orbital separations $\lesssim 10\ R_\odot$ the secondary is likely to be overfilling its Roche lobe. Therefore, binaries with wider orbits, which undergo case B_l or C_l mass transfer, are more likely to survive the common-envelope phase.

If the primary mass takes its minimum value of 8 $M_\odot$, then case B_e or C_e mass transfer is stable for systems where the secondary mass is $>q_c 8\ M_\odot$. An 8-$M_\odot$ primary sheds its $\sim$6-$M_\odot$ envelope, of which $\beta 6\ M_\odot$ is accreted by the secondary. Thus, we see that the

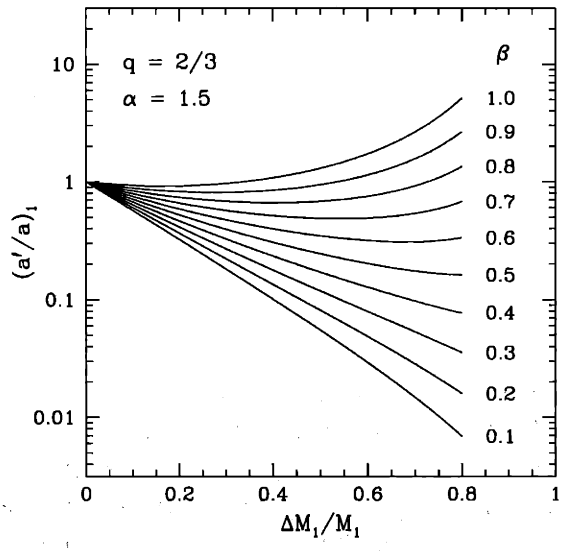

Figure 2-3: Curves representing the dependence of the final-to-initial orbital separation, $(a'/a)_1$, on the fractional mass loss from the primary, $\Delta M_1/M_1$, shown for ten different values of the mass capture fraction, β. The initial mass ratio was chosen to be $q = 2/3$, and the dimensionless angular momentum-loss parameter was set to $\alpha = 1.5$, a value characteristic of mass loss through the L2 point.

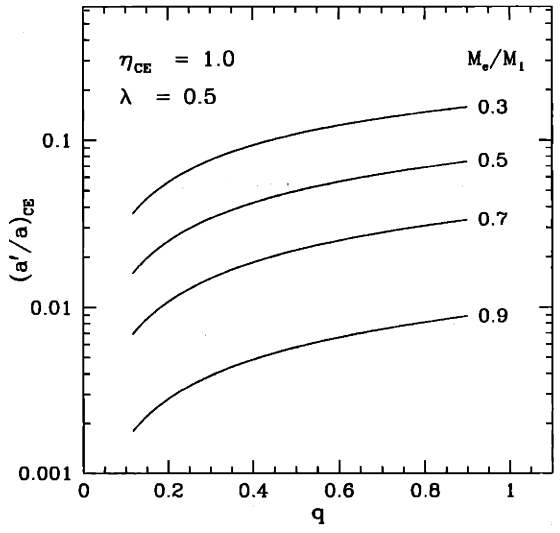

Figure 2-4: The final-to-initial orbital separation $(a'/a)_{\rm CE}$ for common-envelope evolution as a function of the initial mass ratio, q. The function is plotted for four different values of the fractional envelope mass, M_e/M_1, of the primary. For this plot, we have chosen $\eta_{\rm CE} = 1.0$ and $\lambda = 0.5$.

minimum secondary mass following stable mass transfer is approximately $q_c 8\ M_\odot + \beta 6\ M_\odot$. For our reference values of $q_c = 0.5$ and $\beta = 0.75$, this minimum mass is 8.5 $M_\odot$. It follows that if we observe an X-ray binary where the secondary is of low- or intermediate-mass, then the system has likely undergone dynamically unstable case B_l or C_l mass transfer prior to the formation of the NS.

In all cases where a stellar merger is avoided, we assume that the entire hydrogen-rich envelope of the primary is removed, either transferred stably through the inner Lagrange point or expelled during a CE phase. By the time the primary reaches the end of the main sequence, its core is well developed, with a mass given approximately by (Hurley et al. 2000)

$$M_c \simeq 0.12\, M_1^{1.35}\ . \tag{2.13}$$

We assume that this is the mass of the exposed helium core following case B mass transfer. For case C and D evolution, the mass of the core may be larger by ~0.5–1 $M_\odot$ as a result of shell nuclear burning.

Following case B mass transfer, the exposed core of the primary is a nascent helium star. Helium stars with mass $\gtrsim$5 $M_\odot$ probably experience mass loss in the form of a Wolf-Rayet wind, where the timescale for mass loss is comparable to the evolutionary timescale (~10^6 yr) of the star (see Langer 1989). However, we find hat such massive helium stars are not produced in sufficient numbers to strongly effect our results on NS retention, and so we neglect Wolf-Rayet winds in the present study. Stellar winds are less important for helium stars of lower mass. Although, if the core is exposed following case B mass transfer and $M_c \lesssim 3\ M_\odot$, the star may grow to giant dimensions (Habets 1986b) upon central helium exhaustion and possibly fill its Roche lobe, initiating a phase of case BB mass transfer (De Greve & De Loore 1977; Delgado & Thomas 1981; Habets 1986a). For the maximum radius of a helium star, we adopt a slightly modified version of the fitting formula derived by Kalogera & Webbink (1998):

$$\log(R_{\rm He,max}/R_\odot) = \begin{cases} 2.3 & M_c \le 2.5 \\ 0.057\,[\log(M_c/M_\odot) - 0.17]^{-2.5} & M_c > 2.5\ . \end{cases} \tag{2.14}$$

This relation is consistent with the results of Habets (1986b). It is expected that $\lesssim$0.5 $M_\odot$ is transferred to the secondary during the case BB phase (e.g., Habets 1986a). We consider case BB mass transfer by assuming that a fixed amount of mass (e.g., 0.3 $M_\odot$) is transferred conservatively (i.e., no loss of mass or orbital angular momentum) to the secondary, and we expand the orbit accordingly. The inclusion of this process does not significantly influence our results.

2.5 Supernova Explosion

At the end of the mass-transfer phase, the result may be a stellar merger or a binary consisting of the secondary and the core of the primary. Subsequently, the remaining

nuclear fuel in the primary's core is consumed, leading to core collapse and a SN explosion. The post-SN orbital parameters are computed by taking into account the mass lost from the primary and the kick delivered to the newly-formed NS. In all of the simulations discussed in this thesis, we neglect the effects of the SN blast wave on the secondary, which is a very reasonable assumption for the majority of binaries that we consider (e.g., Wheeler et al. 1975; Fryxell & Arnett 1981; Livne et al. 1992; Marietta et al. 2000). We further assume that the orientations of the kicks are distributed isotropically, as there is no clear observational indication that the kicks are preferentially aligned with respect to the spin of the NS progenitor.

One of two distinct outcomes follows the explosion (see Appendix A for a description of our computational formalism): (i) the NS and the secondary are gravitationally bound, with new orbital parameters and a new CM velocity, or (ii) the binary is disrupted, with the NS and secondary receding along hyperbolic trajectories relative to the new CM. Even if the binary formally bound ($e < 1$) following the SN, the binary is not necessarily a viable, incipient low-, intermediate-, or high-mass X-ray binary. When the characteristic kick speed is large, the mean eccentricity for the bound post-SN binaries may be $\gtrsim$0.7. In a significant fraction of these systems, the closest approach of the NS immediately after the SN is smaller than the radius of the secondary, with the likely outcome that the NS spirals in to the envelope of the secondary to form a Thorne-Żytkow object (Leonard, Hills, & Dewey 1994; Brandt & Podsiadlowski 1995). The fate of the NS is unlcear in this case. In Chapter 5, we provide a more detailed discussion and references regarding the formation of Thorne-Żytkow objects, especially as the evolutionary endpoints of high-mass X-ray binaries.

2.6 Double Neutron Star Formation

High-mass X-ray binaries are the natural progenitors of double NS binaries. After evolving off of the main-sequence, the secondary quickly grows to giant dimensions. The extreme mass ratio guarantees that a common-envelope phase and spiral-in will occur not long after the secondary fills its Roche lobe. The common envelope will be successfully dispersed by the engulfed NS if the orbital period is $\gtrsim$100 d (e.g., Taam et al. 1978) at the onset of the spiral-in. If collapse to a black hole, via "hypercritical" accretion (e.g., Chevalier 1993; Fryer et al. 1996; Brown et al. 2000), and merger are avoided, the NS will emerge in a tight orbit with the hydrogen-exhausted core of the secondary. A double NS binary is then formed if the system remains bound following the SN explosion of the secondary's core.

Chapter 3

Low- and Intermediate-Mass X-ray Binaries

3.1 Introduction

Roughly 150 low-mass X-ray binaries (LMXBs) have been observed in the Galaxy (Liu et al. 2001), with orbital periods from 11 minutes to $\sim$1 year, donor masses of $\sim$0.01–2 $M_\odot$, and X-ray luminosities from the detection sensitivities ($\sim 10^{32}$ ergs s^{-1} for a distance of $\sim$1 kpc) to $\sim 10^{38}$ ergs s^{-1}. Over the past twenty years or so, there have been many theoretical studies of LMXBs aimed at accounting for their abundance and variety. During this time, a standard picture for their formation and evolution was established. However, recent observational and theoretical work challenge the conventional wisdom and have prompted a renewed interest in the origins of observed LMXBs. Specifically, it has been realized that many, perhaps even the majority, of the identified LMXBs may have descended from systems with *intermediate-mass* donor stars.

It was long thought that mass transfer via Roche-lobe overflow would be dynamically unstable if the donor star is significantly more massive than the neutron star (NS), and therefore that such systems would not survive to resemble the X-ray binaries we presently observe. Until recently, this view largely persisted (see, however, Pylyser & Savonije 1988, 1989), as only one exception—Her X-1, with a companion of mass $\sim$2 $M_\odot$—has so far been identified. This issue was reopened after optical observations of Cyg X-2 revealed the spectral type and mass ($\sim$0.6 $M_\odot$) of the secondary (Casares et al. 1998; Orosz & Kuulkers 1999), which turns out to be much hotter and more luminous than a giant that descended from a star of mass $<$1.5 $M_\odot$. Evolutionary calculations (King & Ritter 1999; Podsiadlowski & Rappaport 2000; Kolb et al. 2000) show that Cyg X-2 probably began its life as an X-ray binary with a donor of mass $\sim$3.5 $M_\odot$. That is, Cyg X-2, previously a prototype LMXB, was originally an intermediate-mass X-ray binary (IMXB).

In the past, the evolution of X-ray binaries and the criteria for dynamically unstable mass transfer were computed using analytic techniques (e.g., Rappaport et al. 1982; Kalogera & Webbink 1996). This is a satisfactory approach as long as the structure of the donor star and

its response to mass loss can be described using relatively simple prescriptions. However, this is not possible in general. The clear realization that intermediate-mass donor stars can stably transfer matter to a NS accretor came largely as a result of recent calculations that utilized full stellar evolution codes (e.g., Tauris & Savonije 1999; Tauris et al. 2000; Podsiadlowski & Rappaport 2000; Podsiadlowski et al. 2002). Only with such codes can the evolution of the donor be followed realistically during the rapid phase of thermal timescale mass transfer that characterizes the early evolution of IMXBs.

All previous binary population synthesis studies of LMXBs have focused on the issues of formation, and, at best, considered only qualitatively the evolution during mass transfer onto the NS. Such studies are therefore limited in their applicability to observations. In our population study, we take the next logical steps of (i) allowing for the possibility that IMXBs play a major role in shaping the population of observed LMXBs, and (ii) incorporating detailed binary stellar evolution calculations of the X-ray binary phase.

The present work is a natural extension of the systematic evolutionary study of LMXBs and IMXBs given in Podsiadlowski et al. (2002), where we describe our library of 100 binary evolution sequences computed with a standard Henyey-type stellar evolution code. By combining population synthesis models of the formation of incipient LMXBs and IMXBs with detailed calculations of the subsequent mass transfer phase, it is possible for the first time to generate theoretical distributions of observable quantities at the current epoch, such as donor mass, orbital period, and X-ray luminosity.

This Chapter is organized as follows. In § 3.2, we discuss the important aspects of L/IMXB formation. The subsequent evolution during the X-ray binary phase is considered in § 3.3 using an analytic approach. We quantify the different mechanisms that drive mass transfer, determine the conditions for which mass transfer is dynamically unstable, and show why the evolution of the donor star must be computed self-consistently. The library of 100 L/IMXBs evolutionary sequences calculated by Podsiadlowski et al. (2002), and some of the important conclusions of that study, are discussed in § 3.4. Preliminary results and conclusions of our combined binary population synthesis and evolutionary study are given in § 3.5.

3.2 Formation of L/IMXBs

An operational discussion of how binaries containing NSs form in the Galactic disk is given in Chapter 2. We now highlight and expand on the most important points that are relevant for L/IMXB formation in the Galactic disk. Of particular importance is the common-envelope phase that precedes the formation of the NS, as well as the mass loss and NS kick associated with the SN explosion. Results of our population synthesis calculations for producing incipient L/IMXBs are shown in § 3.5.

3.2.1 Common-Envelope Evolution

The majority of LMXBs with measured orbital periods have $P_{\rm orb} \lesssim 10$ days, corresponding to separations of $\lesssim 30\ R_\odot$. These orbits could not have accommodated an evolved, massive NS progenitor, which might grow to radii of $\sim 1000\ R_\odot$ in isolation. In the context of cataclysmic variables, it was suggested (Paczyński 1976) that such tight orbits can be explained by common-envelope (CE) evolution (see § 2.3 and § 2.4). For reasons given in § 2.4, which we reiterate below, it is reasonable to assume that all incipient L/IMXBs of interest are formed following a CE phase, wherein the primordial secondary—ultimately the donor star in the X-ray binary—spirals into the envelope of the NS progenitor.

As in Chapter 2, we let M_1 and M_2 be, respectively, the masses of the primary and secondary in the primordial binary, and we denote the initial mass ratio by $q \equiv M_2/M_1 < 1$. We assumed in § 2.3 that there is some critical mass ratio, q_c, below which the mass transfer is dynamically unstable regardless of the evolutionary state of the primary. A fixed value of $q_c = 0.5$ was adopted, but, in fact, a more correct number is probably somewhat closer to unity. This critical mass ratio implies the existence of a *minimum* final secondary mass for binaries that experience *stable* mass transfer. If the mass transfer is case B_e or C_e (see § 2.3) and the secondary mass is $M_2 > q_c M_1$, then the mass transfer is stable and the secondary accretes a mass of βM_e, where M_e is the mass of the primary's envelope and β is the (constant) mass capture fraction. Therefore, stable mass transfer results in a final secondary mass of $q_c M_1 + \beta M_e$. The minimum final secondary mass for systems that undergo stable mass transfer is obtained when $M_1 = 8\ M_\odot$, the mass threshold for NS formation, and $M_e = 6\ M_\odot$, the corresponding envelope mass. This minimum mass is approximately $q_c 8\ M_\odot + \beta 6\ M_\odot = 8.5\ M_\odot$ for $q_c = 0.5$ and $\beta = 0.75$. With our adopted parameter values, we see that all primordial binaries with intermediate-mass secondaries will evolve through a CE phase.

From the standard energy relation (§ 2.11) that describes the spiral-in, we derive the ratio of the final to the initial orbital separation:

$$\left(\frac{a'}{a}\right)_{\rm CE} = \frac{M_c M_2}{M_1}\left(M_2 + \frac{2M_e}{\lambda\,\eta_{\rm CE}\,r_{\rm L1}}\right)^{-1}\ , \tag{3.1}$$

where M_c is the core mass of the primary, and $a r_{\rm L1}$ is the Roche-lobe radius about the primary. Note that the two crucial parameters that characterize the CE—λ, the structure parameter, and $\eta_{\rm CE}$, the CE ejection efficiency—appear only in the product $\lambda\eta_{\rm CE}$. In the present study, we use a fixed value of $\eta_{\rm CE} = 1$ and allow $\lambda = 0.1$–0.5 (see below) to vary as a free parameter. For low- and intermediate-mass secondaries, a useful approximation of eq. (3.1) is

$$\left(\frac{a'}{a}\right)_{\rm CE} \sim \frac{1}{2}\lambda\,\eta_{\rm CE}\,r_{\rm L1}\,q\frac{M_c}{M_e}\ , \tag{3.2}$$

wherein $(a'/a)_{\rm CE}$ is proportional to both λ and q. When λ is made smaller, the CE is more tightly bound, and ejection of the CE requires more orbital shrinkage. Likewise, for a smaller mass ratio, more shrinkage is required to deposit the same amount of orbital energy

into the CE.

The massive NS progenitors we are considering have $M_c/M_e \sim 0.3$–0.5. Initial mass ratios of $q \lesssim 0.5$ and $\lambda < 0.5$ give $(a'/a)_{\rm CE} \lesssim 0.02$ (see Fig. 2-4). A sufficient mathematical condition for the merger of the primary and secondary is that the secondary overfills its Roche lobe for the calculated post-CE orbital separation. Main-sequence secondaries of mass $M_2 \gtrsim 1\ M_\odot$ have radii given by $R_2 \simeq (M_2/M_\odot)^{0.6}\ R_\odot$. Taking $M_c > 2\ M_\odot$ and equating the radius of the secondary to the Roche-lobe radius, we find that the minimum orbital separation is $\gtrsim$3–6 $R_\odot$ for $M_2 = 1$–$5\ M_\odot$, which corresponds to orbital separations of $\gtrsim$300–600 $R_\odot$ at the onset of the CE phase. Therefore, we expect that the majority systems that survive the CE undergo case B_l or C_l mass transfer (see Figs. 2-1 and 2-2).

Dewi & Tauris (2000; see also Tauris & Dewi 2001 and Dewi & Tauris 2001) have computed λ as a function of the radius of an evolving star, over a stellar mass range of 3–100 $M_\odot$. For stars of mass 8–20 $M_\odot$, the values are $\lambda \sim 0.05$–0.5 for the particular, and quite reasonable, definition of the core mass used by Dewi & Tauris (2000). While λ may change by an order of magnitude during the course of a star's evolution, the variation is within a factor of $\sim$2 for the range in primary radii that are important for L/IMXB formation. Furthermore, there is a tendency for λ to decrease as the stellar mass increases. We do not attempt to include in our calculations the variation of λ with radius or mass, but rather take a constant value of λ for each population synthesis calculation.

If a merger of the two stars is avoided following the spiral-in, the outcome is a detached binary consisting of the (unaltered) secondary and the core of the primary. Following case B_e or B_l mass transfer, the primary's core is a nascent helium star (see § 2.3). Helium stars of mass $\sim$2–3 $M_\odot$ expand significantly and may fill their Roche lobes following the CE and spiral-in, thus initiating a phase of case BB mass transfer (see § 2.4). More massive ($\gtrsim$5 $M_\odot$) helium stars experience mass loss in the form of a Wolf-Rayet wind. The inclusion of these two processes in our study would not significantly influence the main results, and so they are not considered presently, but may be incorporated into future investigations.

3.2.2 Supernova Explosion

After the core consumes its remaining nuclear fuel, it explodes as a Type Ib or Ic SN and leaves a NS remnant. Impulsive mass loss and the NS kick strongly perturb the binary and may cause its disruption. Because the mass of the primary's core may be greater than or comparable to the mass of the secondary, the effect of SN mass loss on the binary is especially significant, and some important quantitative results can be obtained rather simply by neglecting NS kicks. It is straightforward to show (e.g., Blaauw 1961; Boersma 1961) that for a circular pre-SN orbit the eccentricity, $e_{\rm SN}$, after the SN is simply

$$e_{\rm SN} = \frac{M_c - M_{\rm NS}}{M_2 + M_{\rm NS}}\ , \tag{3.3}$$

where $M_{\rm NS}$ is the mass of the NS. The system is unbound ($e_{\rm SN} > 1$) when $M_c > M_2 + 2M_{\rm NS}$. Letting $M_2 = 1\ M_\odot$ and $M_{\rm NS} = 1.4\ M_\odot$, we see that for core masses of $M_c > 3.8\ M_\odot$

(primary masses of $M_1 \gtrsim 13\ M_\odot$) disruption of the binary is guaranteed. In such a situation, a kick of appropriate magnitude and direction is *required* in order to keep the system bound. For intermediate-mass donors, a wider range of pre-SN core masses is permitted when kicks are neglected. Following the CE phase, the core of the primary will have orbital speeds about the binary center-of-mass (CM) of $v_c \sim 100$–200 km s^{-1}. It can be also be shown that after the SN, the CM of the binary acquires a speed of $v_{\rm CM} = e_{\rm SN} v_c$, so that eccentricities of $e_{\rm SN} \lesssim 1$ correspond to large post-SN systemic speeds of order 100 km s^{-1}.

When NS kicks are considered in addition to SN mass loss, it becomes more probable that a given binary will be disrupted, and those binaries that do remain bound will have larger CM speeds. We utilize a Maxwellian distribution in kick speeds,

$$p(v_k) = \sqrt{\frac{2}{\pi}} \frac{v_k^2}{\sigma^3} e^{-v_k^2/2\sigma^2} \ , \tag{3.4}$$

where the directions of the kicks are assumed to be distributed isotropically. Dispersions of $\sigma \sim 100$–200 km s^{-1} are consistent with the data on pulsar proper motions (e.g., Hansen & Phinney 1997; Arzoumanian et al. 2002). In our study, we consider $\sigma = 50$, 100, and 200 km s^{-1}. For each binary system, the magnitude and direction of the kick are chosen by Monte Carlo methods. The post-SN orbital parameters are then calculated using the formalism described in Appendix A.

Significant SN mass loss and large NS kicks are likely to yield a substantial fraction of bound post-SN binaries with eccentricities of $\gtrsim$0.5. Given the post-SN eccentricity, we check if the radius of the secondary is larger than its Roche lobe at periastron by some amount; if so, we assume that the NS immediately spirals into the envelope of the unevolved secondary. The product of the merger may be a Thorne-Żytkow object (Thorne & Zytkow 1975, 1977), which we do not mention further in this Chapter (see Chapter 5). In our simulations, we assume a coalescence results if the secondary overfills its Roche lobe at periastron by >10%, a reasonable but otherwise ad hoc value. This allows for the possibility that tidal circularization and perhaps some mass loss will prevent the objects from merging. The details of eccentric binary evolution with mass transfer is well beyond the scope of this investigation. However, we note in passing that Cir X-1 is most likely a young X-ray binary undergoing episodic mass transfer as a result of having a highly eccentric ($e_{\rm SN} \gtrsim 0.8$) orbit (Shirey 1998). There is also some evidence that the stellar companion in Cir X-1 is of intermediate mass.

If the coalescence of the NS and secondary is avoided, we neglect mass loss from the system and assume that the binary eventually circularizes while conserving *orbital* angular momentum. The final orbital separation is then $a_{\rm SN}(1 - e_{\rm SN}^2)$, where $a_{\rm SN}$ is the semimajor axis after the SN. Moreover, we assume that the secondary rotates synchronously with the circularized orbit. As we are neglecting the rotational angular momentum of the secondary, our treatment of orbital circularization is not completely correct, but is quantitatively adequate for our purposes. Further evolution of the circularized orbit may be driven by orbital angular momentum loss via *magnetic braking* (discussed in the next section) if the mass of the secondary is $\lesssim$1.5 $M_\odot$. Systems that contain low-mass secondaries, with main-sequence

lifetimes of $\sim$10 Gyr, will become potentially observable X-ray binaries only if magnetic braking causes the orbit to shrink enough for the star to fill its Roche lobe. Clearly, there is no such problem for intermediate-mass secondaries, which have nuclear lifetimes of $\lesssim 10^9$ yr. We now go on to describe the processes that govern the phase of mass transfer that begins when the secondary fills its Roche lobe.

3.3 Overview of Binary Stellar Evolution

While a full numerical treatment is required to adequately model the stellar evolution processes during mass transfer in a L/IMXB, a great deal of quantitative insight is gained by using an *analytic* approach. In addition to highlighting and quantifying the mechanisms that drive mass transfer, the analytic calculations presented below may also be used to determine under what conditions the mass transfer becomes unstable on the dynamical time scale of the donor. Furthermore, in what follows it will become clear why a simplistic treatment of the evolution of the secondary is not possible in general.

3.3.1 Analytic Formalism

During dynamically stable mass transfer, we imagine that the donor star precisely fills its Roche lobe in an orbit with semimajor axis a. The instantaneous masses of the NS accretor and the donor star are denoted by M_a and M_d, respectively, and the total binary mass is given by $M_b = M_a + M_d$. A fraction β of the material lost from the companion through the inner Lagrange point is accreted onto the NS, so that

$$\dot{M}_a = -\beta \dot{M}_d \ , \quad \dot{M}_b = (1-\beta)\dot{M}_d \ . \tag{3.5}$$

Changes in the masses of the components have an immediate influence on the orbital separation and the size of the Roche lobe about the secondary. The volume-equivalent radius, $R_{\mathrm{L}d}$, of the donor's Roche lobe is given by (Eggleton 1983)

$$\frac{R_{\mathrm{L}d}}{a} \equiv r_{\mathrm{L}d} = \frac{0.49}{0.6 + q^{-2/3}\ln(1+q^{1/3})} \ , \tag{3.6}$$

where $q = M_d/M_a$ is the binary mass ratio. The differential equation that relates the rates of change of $R_{\mathrm{L}d}$, M_d, and a may be written as

$$\frac{\dot{R}_{\mathrm{L}d}}{R_{\mathrm{L}d}} = \frac{\dot{a}}{a} + (1+\beta q)\,\zeta(q)\,\frac{\dot{M}_d}{M_d} \ , \tag{3.7}$$

where

$$\zeta(q) \equiv \frac{d\ln r_{\mathrm{L}d}}{d\ln q} = \frac{1}{3}\left[\frac{2\ln(1+q^{1/3}) - 1/(1+q^{-1/3})}{0.6q^{2/3} + \ln(1+q^{1/3})}\right] \ . \tag{3.8}$$

Equation (3.7) directly couples stellar and orbital evolution if we impose the constraint that $R_{Ld} = R_d$, where R_d is the radius of the secondary. We now discuss the physical process that drive changes in a and R_d.

For a circular binary, the orbital angular momentum, J, is given by

$$J = \frac{M_a M_d}{M_b}(G M_b a)^{1/2} . \tag{3.9}$$

In what follows, we neglect the rotational angular momentum of the donor star. Logarithmic differentiation of eq. (3.9) with respect to time yields

$$\begin{aligned} \frac{\dot{J}}{J} &= \frac{\dot{M}_a}{M_a} + \frac{\dot{M}_d}{M_d} - \frac{1}{2}\frac{\dot{M}_b}{M_b} + \frac{1}{2}\frac{\dot{a}}{a} \\ &= \left[1 - \beta q - \frac{1}{2}\frac{q(1-\beta)}{1+q}\right]\frac{\dot{M}_d}{M_d} + \frac{1}{2}\frac{\dot{a}}{a} . \end{aligned} \tag{3.10}$$

Clearly, when there is no mass transfer, the orbital separation changes only as a result of the loss of orbital angular momentum; specifically, we see that $\dot{a}/a = 2\dot{J}/J$. Three independent mechanisms are responsible for removing angular momentum from the binary orbit, which we now summarize:

Mass Loss (ML).—When mass is lost from the system (i.e., $\dot{M}_b < 0$), it takes with it some amount of angular momentum. It is reasonable to suppose that the ejected material has some fraction, α, of the specific orbital angular momentum of the NS. This would be the case if, for instance, mass were lost in the form of a wind from the vicinity of the NS, or a more collimated outflow, such as a jet. It is straightforward to show that

$$\left(\frac{\dot{J}}{J}\right)_{\rm ML} = \frac{\alpha(1-\beta)q^2}{1+q}\frac{\dot{M}_d}{M_d} , \tag{3.11}$$

where, for simplicity, α is taken to be a constant, independent of the component masses and time. For $\beta = 1$, we say that the mass transfer is *conservative*; that is, the mass of the system is conserved, and $(\dot{J}/J)_{\rm ML} = 0$.

Gravitational Radiation (GR).—In the quadrupole approximation, it can be shown that gravitational waves take away orbital angular momentum at a rate given by (e.g., Faulkner 1971; Landau & Lifshitz 1975)

$$\left(\frac{\dot{J}}{J}\right)_{\rm GR} = -\frac{32(2\pi)^{8/3}G^{5/3}}{5c^5} M_a M_d M_b^{-1/3} P_{\rm orb}^{-8/3} , \tag{3.12}$$

where $P_{\rm orb}$ is the orbital period. Neglecting mass transfer and other sinks of orbital angular

momentum, we find that the corresponding timescale, $\tau_{\rm GR}$, for orbital contraction is

$$\tau_{\rm GR} \equiv \left|\frac{a}{\dot{a}}\right|_{\rm GR} = \frac{1}{2}\left|\frac{J}{\dot{J}}\right|_{\rm GR} \simeq 2.3\times10^{7}\,{\rm yr}\,\frac{(1+q)^{1/3}}{q}\left(\frac{P_{\rm orb}}{1\,{\rm hr}}\right)^{8/3}\,, \tag{3.13}$$

where we have taken the NS mass to be $M_a = 1.4\ M_\odot$. For $q = 1$ and $P_{\rm orb} = 10\,{\rm hr}$, the timescale is $\tau_{\rm GR} \sim 10\,{\rm Gyr}$, or roughly a Hubble time. Furthermore, note that $\tau_{\rm GR}$ increases for decreasing q.

Magnetic Braking (MB).—If the wind from an isolated star is forced by coronal magnetic field lines to corotate with the star out to large distances, then a small amount of mass may carry away a significant fraction of the star's rotational angular momentum. This process, known as magnetic braking, is observed (e.g., Skumanich 1972; Smith 1979) to operate in low-mass ($\sim$ 0.4–1.5 $M_\odot$) main-sequence stars, which have appreciable convection zones that may lead to magnetic field generation via a dynamo process. For a Roche-lobe filling star in a binary system, tidal interactions will cause the star to rotate synchronously with the orbit, and thus any angular momentum that is lost from the star due to MB will likewise be lost from the orbit. Applied to the binary orbit, the standard braking law derived by Verbunt & Zwaan (1981; see also Rappaport et al. 1983) is given by

$$\left(\frac{\dot{J}}{J}\right)_{\rm MB} \simeq -2\times10^{-34}\,r_{{\rm L}d}^{4}M_a^{-1}M_b^{5/3}P_{\rm orb}^{-2/3}\,, \tag{3.14}$$

where all variables are to be given in CGS units. The corresponding timescale, $\tau_{\rm MB}$, for orbital contraction is given by

$$\tau_{\rm MB} \simeq 5\times10^{8}\,{\rm yr}\,r_{{\rm L}d}^{-4}(1+q)^{-5/3}\left(\frac{P_{\rm orb}}{1\,{\rm hr}}\right)^{2/3}\,, \tag{3.15}$$

where, as in eq. (3.13), we have set $M_a = 1.4\ M_\odot$. Because of its weaker dependence on $P_{\rm orb}$, angular momentum loss via MB is more important than GR for sufficiently long orbital periods. When q is varied from 0.5 to 2.0, the period for which $\tau_{\rm MB} = \tau_{\rm GR}$ changes from $\sim$24 hr to $\sim$16 hr.

Like the orbital angular momentum, the donor radius changes by virtue of three different and independent processes, one of which depends explicitly on the mass lost from the star:

Adiabatic Mass Loss.—When mass is removed from the donor, the stellar radius changes on a dynamical timescale (of order an hour) as the star adjusts to a new hydrostatic equilibrium configuration. This change thus occurs essentially *adiabatically*, as the thermal readjustment timescale of a $\sim$ 1-$M_\odot$ star is $\sim 10^7$ yr (see eq. [3.17]). We suppose that at each instant the adiabatic radial response of the donor is governed by the power-law relation

$R_d \propto M_d^{\xi_{\rm ad}}$, where $\xi_{\rm ad}$ is referred to as the *adiabatic index*, so that

$$\left(\frac{\dot{R}_d}{R_d}\right)_{\rm ad} = \xi_{\rm ad}\frac{\dot{M}_d}{M_d} \ . \tag{3.16}$$

For $\xi_{\rm ad} < 0$, the secondary expands in response to mass loss, and conversely for $\xi_{\rm ad} > 0$. Negative adiabatic indices occur for stars that are convective or are supported by nonrelativistic degeneracy pressure, as in the case of a white dwarf. Stars of mass $\gtrsim 1\ M_\odot$ that are near the main sequence have radiative envelopes and large, positive values of $\xi_{\rm ad}$ near the surface. In this case, the removal of a small amount of mass will cause the star to become smaller than its thermal equilibrium radius, which for main sequence stars is approximately $R_{d,\rm eq} \propto M_d^{\xi_{\rm eq}}$, where $0 < \xi_{\rm eq} \lesssim 1$.

Thermal Evolution.—In general, the donor star will not be in thermal equilibrium during mass transfer, and its thermal relaxation is an important aspect of binary stellar evolution. The thermal, or Kelvin-Helmholtz, timescale of the whole star is given by

$$\begin{aligned}\tau_{\rm KH} &\sim \frac{GM_d^2}{R_d L_d} \\ &\simeq 3\times 10^7\ {\rm yr}\left(\frac{M_d}{M_\odot}\right)^2\left(\frac{R_d}{R_\odot}\right)^{-1}\left(\frac{L_d}{L_\odot}\right)^{-1} \ ,\end{aligned} \tag{3.17}$$

where L_d is the luminosity of the secondary. If the mass transfer were suddenly turned off, the star would be able to readjust on this timescale to its thermal equilibrium radius. One heuristic prescription for the rate of change of the donor's radius due to thermal relaxation is

$$\left(\frac{\dot{R}_d}{R_d}\right)_{\rm th} \simeq \frac{1}{\tau_{\rm KH}}\left(\frac{R_{d,\rm eq}}{R_d} - 1\right) \ , \tag{3.18}$$

where, just to reiterate, R_d is the *instantaneous* stellar radius. However, in general this prescription is too simplistic. First, the surface layers of the star respond on a shorter, local thermal timescale rather than the bulk thermal relaxation time given in eq. (3.17). Second, when the donor is out of thermal equilibrium, its nuclear luminosity will generally be different than its photospheric luminosity, and $(\dot{R}_d/R_d)_{\rm th}$ should somehow depend on this *luminosity deficit*. We bring these problems to light only to emphasize the need for a more detailed treatment of stellar structure and evolution.

Nuclear Evolution.—The radius of an isolated star changes by virtue of its nuclear evolution. A star spends most of its life on the main sequence, with a timescale given by

$$\tau_{\rm nuc} \sim 10^{10}\ {\rm yr}\left(\frac{M}{M_\odot}\right)^{-3} \ , \tag{3.19}$$

which is a reasonable fit for both low- and intermediate-mass stars of mass M. Following core hydrogen burning, the star expands to giant dimensions. If the donor star in an X-ray

binary fills its Roche lobe during the (sub)giant phase, mass transfer will be driven on the corresponding nuclear expansion timescale. Rapid mass transfer may cause the mass and structure of the donor to change considerably in a time that is comparable to or shorter than the initial thermal timescale. As a result, the nuclear burning processes in the stellar interior may be strongly affected or even interrupted temporarily, although this only occurs for stars that have not yet become giants with degenerate cores. Therefore, as with the thermal evolution of the donor during mass transfer, a self-consistent treatment of the star's nuclear evolution is necessary.

For the purposes of our analytic discussion, we may suppose that the donor star precisely fills its Roche lobe during stable mass transfer, so that $R_{\mathrm{L}d} = R_d$ and $\dot{R}_{\mathrm{L}d} = \dot{R}_d$. With these constraints, eqs. (3.7) and (3.10) can be combined to yield an equation for $\dot{M}_d/M_d$:

$$-\frac{\dot{M}_d}{M_d} = \frac{(\dot{R}_d/R_d)_{\mathrm{th}} + (\dot{R}_d/R_d)_{\mathrm{nuc}} - 2(\dot{J}/J)_{\mathrm{GR}} - 2(\dot{J}/J)_{\mathrm{MB}}}{\xi_{\mathrm{ad}} - \xi_{\mathrm{RL}}} , \tag{3.20}$$

where

$$\xi_{\mathrm{RL}} \equiv \left(\frac{d\ln R_{\mathrm{L}d}}{d\ln M_d}\right)_{\mathrm{MT}} = -2(1-\beta q) + q\left(\frac{1-\beta}{1+q}\right)(1+2\alpha q) + (1+\beta q)\zeta(q) . \tag{3.21}$$

The radius-mass exponent ξ_{RL} gives the change in the Roche-lobe radius due to mass transfer (hence the subscript 'MT') —that is, eq. (3.7) coupled with eq. (3.10), but neglecting $(\dot{J}/J)_{\mathrm{GR}}$ and $(\dot{J}/J)_{\mathrm{MB}}$.

The numerator in eq. (3.20) contains the secular terms (i.e., those terms that do not explicitly depend on mass transfer), while the denominator, $\mathcal{D}(q, \alpha, \beta, \xi_{\mathrm{ad}})$, encapsulates all those effects that give the dynamical response of the star and the orbit to mass transfer alone. Equation (3.20) makes it clear mathematically that the secular effects are responsible for *driving* (stable) mass transfer. The timescale for the dominant driving mechanism (the largest term in the numerator) gives roughly the timescale for mass transfer. We show in the next section that mass transfer is dynamically *unstable* if $\mathcal{D} < 0$, and thus for stable mass transfer it must be that both the numerator and denominator of eq. (3.20) are positive, since $\dot{M}_d < 0$. As q is increased, so is ξ_{RL}, and thus significant mass ratios of $q > 1$ require that ξ_{ad} be sufficiently large in order for the mass tranfser to be stable. It is the large, positive values of ξ_{ad} in radiative stars that allow stable mass transfer when the donor is initially of intermediate mass; this is discussed more quantitatively in the next section.

An intermediate-mass donor star that is not too massive or too evolved will transfer material on its thermal timescale in the early phases of Roche-lobe overflow. This can be seen as follows. When $q \gtrsim 1$, the Roche lobe of the donor shrinks when a small amount of mass is transferred (i.e., $\xi_{\mathrm{RL}} > 0$). The donor likewise shrinks if its envelope is radiative ($\xi_{\mathrm{ad}} \gg 1$), and since $0 < \xi_{\mathrm{eq}} \lesssim 1$, the star will be smaller than its thermal equilibrium radius. Therefore, the tendency for the star to reexpand on its thermal timescale provides the mechanism to drive further mass transfer. In this situation, the $(\dot{R}_d/R_d)_{\mathrm{th}}$ term dominates the numerator in eq. (3.20).

Most of the mass that is transferred on the thermal timescale of the secondary, where $|\dot{M}_d| \gtrsim 10^{-7}\ M_\odot\ \mathrm{yr}^{-1}$, will not be accreted by the NS. It is generally assumed that the NS cannot accrete at rates exceeding the Eddington limit. Assuming spherical symmetry of the surrounding matter and radiation, the Eddington luminosity for a 1.4-$M_\odot$ NS is

$$L_{\rm Edd} \simeq 3.5 \times 10^{38}\ \mathrm{ergs\ s^{-1}}\,(1+X)^{-1}\ , \tag{3.22}$$

where X is the mass fraction of hydrogen in the accretion flow. The accretion luminosity comes at the expense of gravitational potential energy, and thus

$$L_{\rm acc} \sim \frac{GM_a\dot{M}_a}{R_a}\ , \tag{3.23}$$

where $R_a \sim 10\,\mathrm{km}$ is the NS radius. The Eddington mass transfer rate for a NS is then $\dot{M}_{\rm Edd} \sim 10^{-8}\ M_\odot\ \mathrm{yr}^{-1}$. Material that is donated at rates greater than $\dot{M}_{\rm Edd}$ will likely be ejected from the system, possibly as a radiatively driven wind from the accretion disk or in the form of relativistic jets. Evidence for both of these processes is seen in the X-ray binary SS 433 (Blundell et al. 2001), a system known to be in a phase of super-Eddington mass transfer. Thermal-timescale mass transfer is expected to quite *nonconservative*, with a mass capture fraction of $\beta \lesssim 0.1$. One heuristic prescription for β that covers all mass transfer rates is

$$\beta = \begin{cases} b & |\dot{M}_2| < \dot{M}_{\rm Edd} \\ b\,\dot{M}_{\rm Edd}/|\dot{M}_2| & |\dot{M}_2| > \dot{M}_{\rm Edd}\ , \end{cases} \tag{3.24}$$

where $b \leq 1$ is a constant. This formula limits the accretion rate to be $\dot{M}_a < b\,\dot{M}_{\rm Edd}$.

An interesting problem arises if $b \sim 1$, which we now discuss semi-quantitatively. The amount of mass transferred to the NS will generally be some significant fraction of the initial donor mass, $M_{d,i}$. If the mass transfer is sub-Eddington during the X-ray binary phase, then the NS accretes a total mass of $\lesssim b\,M_{d,i}$. Intermediate-mass donors lose most of their mass during the early phase of super-Eddington mass transfer, in which case a more appropriate estimate of the accreted mass is $\sim b\,\dot{M}_{\rm Edd}\,\tau_{\rm nuc}$, where $\tau_{\rm nuc}$ (see eq. [3.19]) is an approximate lifetime of the X-ray binary. For $b \sim 1$ and $\tau_{\rm nuc} \gtrsim 10^8$ yr, we see that the NS may accrete in excess of $\sim$1 $M_\odot$, giving final NS masses of $\gtrsim$2–3 $M_\odot$. However, most modern NS equations of state give maximum masses of $\sim$2–3 $M_\odot$, and thus for $b \sim 1$ it would follow that perhaps a large fraction of the NSs in X-ray binaries collapse into low-mass black holes. No binary with a black hole of mass $\sim$2–3 $M_\odot$ has yet been identified. Such systems would not exhibit X-ray bursts and are not likely show the twin kHz quasi-periodic oscillations seen in LMXBs (van der Klis 2000). The severity of this "black-hole problem" is reduced by using a smaller value of b. Podsiadlowski et al. (2002) utilized $b = 0.5$ and find that in most cases the NS mass remains $\lesssim$2 $M_\odot$ (see § 3.4).

3.3.2 Stability of Mass Transfer

Using the analytic formulae derived above, we now determine under what conditions the mass transfer becomes unstable on the dynamical time scale of the donor. In physical terms, a runaway dynamical instability sets in when further mass transfer will cause the Roche lobe to penetrate more deeply into the star, which results in a larger mass-transfer rate, and so on. At the onset of dynamical mass transfer, one finds that there does not exist a hydrostatic solution for which the secondary precisely fills its Roche lobe. We now derive the algebraic expression that is equivalent to this statement.

Since we are interested in changes that occur on a dynamical timescale, we can neglect orbital angular momentum losses via GR and MB, as well as the thermal and nuclear evolution of the secondary. The dynamical response of the donor radius to mass loss is given the adiabatic relation $(\dot{R}_d/R_d)_{\rm ad} = \xi_{\rm ad}\dot{M}_d/M_d$ (eq. [3.16]), and the response of the Roche lobe radius is $(\dot{R}_{{\rm L}d}/R_{{\rm L}d})_{\rm MT} = \xi_{\rm RL}\dot{M}_d/M_d$ (eq. [3.21]). A necessary and sufficient condition for runaway dynamical mass transfer is that $(\dot{R}_d/R_d)_{\rm ad} > (\dot{R}_{{\rm L}d}/R_{{\rm L}d})_{\rm MT}$, or alternatively $\xi_{\rm MT} < \xi_{\rm ad}$, where have assumed that $R_d \simeq R_{\rm L2}$ at this instant. Three possibilities are admitted by this inequality: (i) when both the star and the Roche lobe grow, but the star grows faster; (ii) when the star grows and the Roche lobe shrinks; (iii) when both the star and Roche lobe shrink, but the Roche lobe shrinks faster. Thus, we see that mass transfer is dynamically unstable if $\mathcal{D}(q,\alpha,\beta,\xi_{\rm ad}) < 0$ in eq. (3.20). In other words, the *onset* of dynamically unstable mass transfer is signified by $\mathcal{D}(q,\alpha,\beta,\xi_{\rm ad}) = 0$.

For given values of α, β, and $\xi_{\rm ad}$, and sufficiently small values of q, we find that $\mathcal{D}(q,\alpha,\beta,\xi_{\rm ad}) > 0$. As q is increased, $\mathcal{D}$ approaches zero and eventually becomes negative. We would like to identify the maximum value of q, and thus the maximum donor mass, for which mass transfer is dynamically stable. For simplicity, we specialize to the case where $\alpha = 1$, so that any ejected matter carries away the specific orbital angular momentum of the NS. Figure 3-1 shows the maximum donor mass as a function of $\xi_{\rm ad}$, for $\beta = 0$ and 1, where the NS mass is taken to be 1.4 $M_\odot$. Secondaries with convective envelopes ($\xi_{\rm ad} < 0$) may be as massive as $\sim$1.6 $M_\odot$. Furthermore, notice that the maximum donor mass increases monotonically with increasing $\xi_{\rm ad}$. However, if an initially large value of $\xi_{\rm ad}$ decreases as mass is removed from the donor, then mass transfer that is initially stable according to Fig. 3-1 may quickly become dynamically unstable.

Unevolved stars of mass $\gtrsim$1 $M_\odot$ have radiative envelopes with $\xi_{\rm ad} \gg 1$ near the surface. This can be seen in the lower panel of Fig. 3-2, where $\xi_{\rm ad}$ and the stellar radius are plotted as a function of the instantaneous mass of a star that is losing material very rapidly, and hence adiabatically. In all cases shown in Fig. 3-2, $\xi_{\rm ad}$ decreases from $\xi_{\rm ad} > 10$ to $\xi_{\rm ad} \sim 1$ as the outer $\sim$10% of the star's mass is removed. Therefore, thermal-timescale mass transfer from an intermediate-mass donor star in an binary system quickly leads to small values of $\xi_{\rm ad}$, which even become negative if rapid mass transfer continues beyond a certain point. Large initial values of $\xi_{\rm ad}$ allow the donor to shrink rapidly and stay within its contracting Roche lobe, at least for a short time. However, as $\xi_{\rm ad}$ decreases, so does the rate at which the star shrinks, and the mass transfer may become dynamically unstable after roughly 10% of the mass of the donor has been removed. While the formal stability criteria displayed in

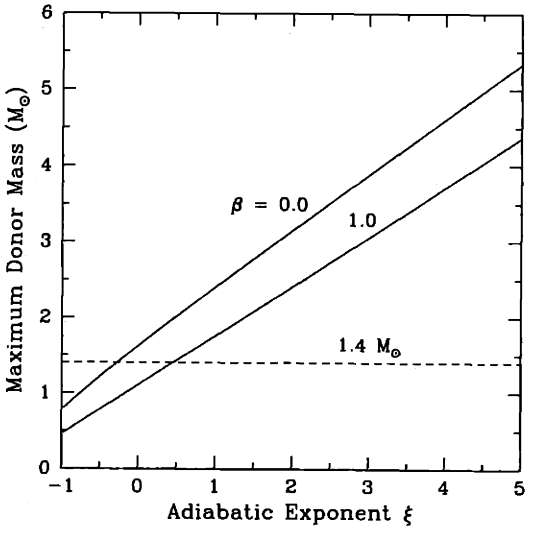

Figure 3-1: Curves showing the maximum donor mass for which the mass transfer is dynamically stable, as a function of the adiabatic index $\xi_{\rm ad}$. The two solid curves are for $\beta = 0$ (totally nonconservative mass transfer) and $\beta = 1$ (conservative mass transfer). The dashed line indicates the conventional NS mass.

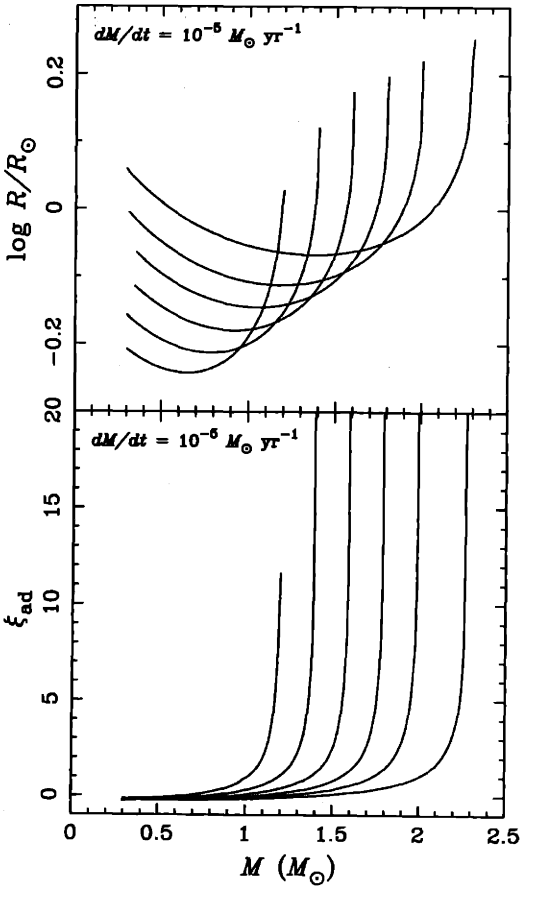

Figure 3-2: Radius (*top panel*) and adiabatic index (*bottom panel*) as a function of mass for unevolved stars of masses 1.2, 1.4, 1.6, 1.8, 2.0, and 2.3 $M_\odot$. These were calculated using a Henyey-type stellar evolution code, assuming a constant mass-loss rate of $10^{-5}\,M_\odot\,{\rm yr}^{-1}$. (This plot was kindly provided by Ph. Podsiadlowski.)

Fig. 3-1 indicate that mass transfer be initially stable for rather massive stars, the dynamical instability is sure to set in very soon thereafter for donors above a certain mass.

It should be clear that it would be very difficult, if not impossible, to correctly estimate the maximum mass for prolonged stable mass transfer using analytic techniques (with, e.g., a polytropic equation of state), since the structure of the donor star must be modeled self-consistently. In fact, most previous analytic calculations (e.g., Rappaport et al. 1983) of the stability criteria utilized characteristic adiabatic exponents of $\xi_{\rm ad} \sim 1$ (see, however, Kalogera & Webbink 1996) for the envelopes of radiative stars of mass $\gtrsim 1\ M_\odot$, which is certainly incorrect in light of Fig. 3-2. Using a complete stellar evolution code, Podsiadlowski et al. (2002) find that all systems with subgiant donors of mass $\lesssim 2\ M_\odot$ are stable *against* dynamical mass transfer throughout their evolutions. Stable mass transfer is possible for donors as massive as $\sim 4\ M_\odot$ if the envelope is radiative. For somewhat higher initial masses, systems experience a *delayed* dynamical instability after a phase of stable, but very rapid, mass transfer that may last $\sim 10^6$ yr. We now discuss selected results and conclusions given in the work of Podsiadlowski et al. (2002).

3.4 Library of L/IMXB Evolutionary Sequences

A complete population synthesis study of L/IMXBs must incorporate both a model for their formation and an adequate numerical treatment of their evolution. Having discussed the basics of binary stellar evolution theory in the last section, we now summarize some of the important results and show a selection of plots from the systematic evolutionary study of Podsiadlowski et al. (2002). We follow this overview with a description of how the library of L/IMXB evolutionary sequences is implemented in our population study.

3.4.1 Overview and Examples

The 100 L/IMXB evolutionary sequences described in Podsiadlowski et al. (2002) cover initial secondary masses of 0.6–7 $M_\odot$ and initial orbital periods of $\sim$4 hours to $\sim$100 days, in order to sample the range of parameters that are likely to be encountered in the population synthesis study. A large variety of evolutionary histories and outcomes is found among the sequences. Of particular interest is that binaries with intermediate-mass donors experience an early phase of thermal-timescale mass transfer. After passing through this rapid phase, some of these systems evolve to resemble LMXBs that we presently observe. We now show a series of plots that illustrate the important characteristics of binary stellar evolution and their dependence on the initial orbital period and donor mass.

Figure 3-3 shows all 100 evolutionary sequences in the $P_{\rm orb}$-M_d plane, where the degree of shading roughly indicates the logarithm of the time spent in a given bin, where darker shading implies longer times. The sequences may be broadly divided into three categories: (1) systems that evolve to shorter orbital periods, (2) systems that evolve to longer orbital periods, and (3) systems with initially more massive donors ($\gtrsim$3–4 $M_\odot$) that eventually undergo dynamically unstable mass transfer. Binaries with initial secondary masses

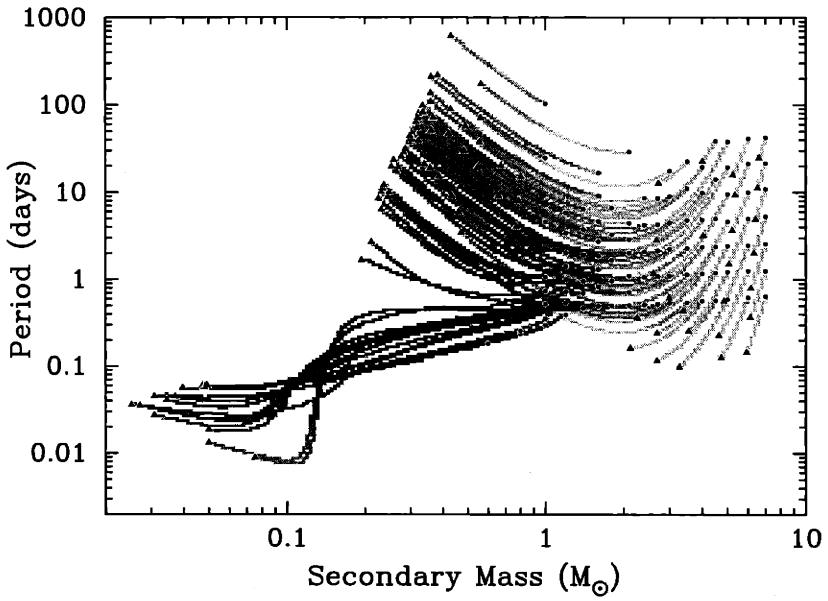

Figure 3-3: Evolutionary tracks of LMXBs and IMXBs in the $P_{\rm orb}$-M_d plane. The degree of shading roughly indicates the logarithm of the time spent in a given pixel, where darker shading implies to longer times. The circle and triangle symbols mark, respectively, the beginning and end of the evolution. Notice the well-defined *bifurcation period* at $P_{\rm orb} \sim 1\,{\rm day}$.

of $\lesssim$1.5 $M_\odot$ and initial orbital periods longer than the well-known *birfurcation period* of $\sim$1 day (e.g., Tutukov et al. 1985; Pylyser & Savonije 1988) expand during mass transfer, while binaries with initial orbital periods $\lesssim$1 day contract. Expanding orbits reflect the tendency for stars to grow by virtue of their nuclear evolution as they evolve off of the main sequence. The contraction of orbits below the bifurcation period is at first driven by angular momentum losses via MB, and then later by GR when the period is sufficiently short. For the contracting systems, minimum orbital periods as short as $\sim$10 min are reached after the hydrogen-depleted stellar core has been exposed. As the mass of the helium core is reduced, the degree of degeneracy grows until degeneracy pressure provides the main support against self-gravity, at which point $\zeta_{\rm ad} < 0$ and the core expands in response to further mass loss. The *ultracompact* X-ray binary 4U 1820–30 ($P_{\rm orb} \simeq 11\,{\rm min}$) in the globular cluster NGC 6624 may have formed in this way (see, however, Rasio et al. 2000).

For the sequences shown in Fig. 3-3, the binary evolution is terminated near the minimum period for the contracting systems, or when the HeCO core is exposed in the expanding systems (see Podsiadlowski et al. 2002 for more details). For the systems that evolve to longer orbital periods, this truly marks the end of the mass transfer phase. The NS is likely to have accreted $\gtrsim$0.1 $M_\odot$ of material and been spun up to millisecond rotation periods. Thus, the binaries with final orbital periods of $\gtrsim$10 day in Fig. 3-3 are expected to ultimately resemble the observed wide binary radio pulsars with low-mass white-dwarf companions (see Rappaport et al. 1995 for a full discussion). X-ray binaries that evolve

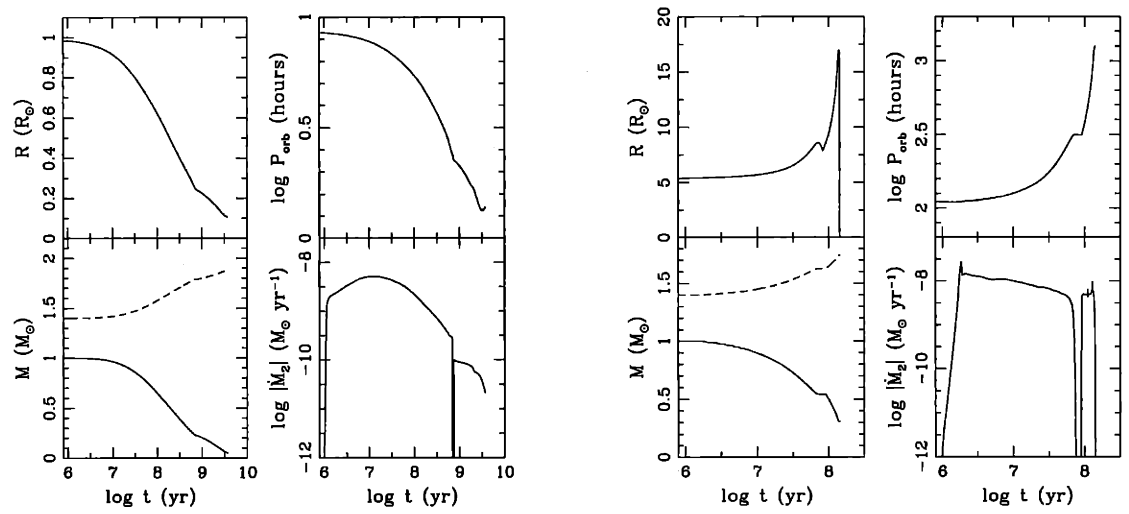

Figure 3-4: LMXB evolution with an initial donor mass of 1 $M_\odot$ and initial orbital periods of $\simeq$9 hr (*left*) and $\simeq$110 hr (*right*). The *solid* and *dashed* curves in the lower left panels indicate the donor mass and the NS mass, respectively.

to short periods of $\lesssim$1 hr will continue mass transfer after the minimum period is reached. Gravitational radiation drives further mass transfer from the degenerate companion, with the result that both the companion and the orbit expand, since $q \ll 1$ and $\xi_{\rm ad} < 0$. Such a system will ultimately consist of a very low-mass (of order 0.01 $M_\odot$) companion in a $\gtrsim$1-hr orbit with a NS rotating at millisecond periods. There are currently three known binary millisecond X-ray pulsars with these characteristics, and a handful of similar binary millisecond *radio* pulsars that have so far only been detected in globular clusters (Camilo et al. 2000).

Data from three specific evolutionary sequences are depicted in Figs. 3-4, 3-5, and 3-6. Each four-panel plot shows the evolution with time of the donor radius, donor mass (*solid curve*), NS mass (*dashed curve*), orbital period, and mass-loss rate from the donor. Figure 3-4 illustrates canonical LMXB evolution above and below the bifurcation period, with initial periods of $\sim$9 hr (main sequence) and $\sim$110 hr (post-main sequence). IMXB sequences are shown in Figs. 3-5 and 3-6, in which the early phase of thermal-timescale mass transfer is clearly evident. Each of the left-hand plots in Figs. 3-5 and 3-6, where the secondary fills its Roche lobe on the main sequence, show very similar evolutionary behavior. The systems evolve at a roughly constant period of $\sim$12 hr for $\sim 3 \times 10^9$ yr, after which MB turns on when $M_d \sim 1.1\ M_\odot$ and causes the orbit to shrink by an order of magnitude before GR drives the mass transfer to a minimum period of $\sim$1 hr.

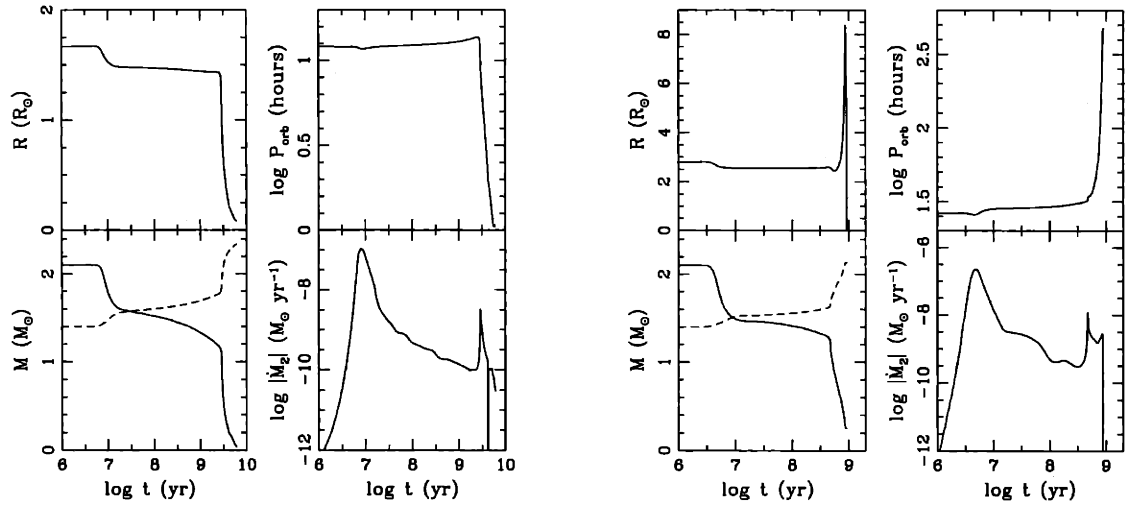

Figure 3-5: IMXB evolution with an initial donor mass of 2.1 $M_\odot$ and initial orbital periods of $\simeq$12 hr (*left*) and $\simeq$48 hr (*right*).

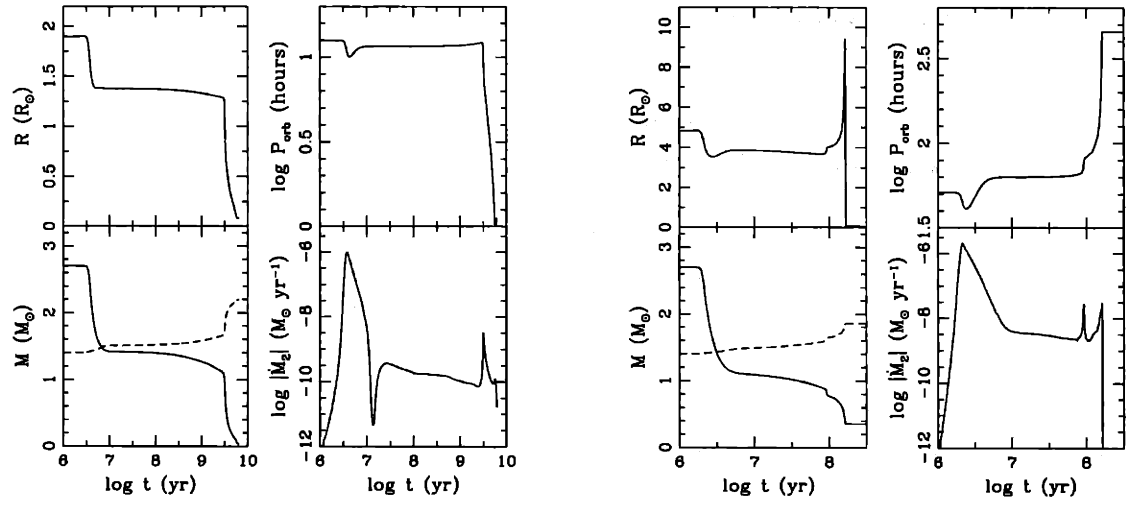

Figure 3-6: IMXB evolution with an initial donor mass of 2.7 $M_\odot$ and initial orbital periods of $\simeq$12 hr (*left*) and $\simeq$51 hr (*right*).

3.4.2 Implementation

Each incipient L/IMXB that emerges from the Monte Carlo population synthesis calculation is characterized by the mass of the secondary and the circularized orbital period at which the star first fills its Roche lobe. For any given initial $P_{\rm orb}$ and M_d, there is a sequence in the library with "nearby" initial parameters, such that the evolution of the synthesized binary would closely resemble the evolutionary sequence selected from the library. In order to make this selection, we first identify a subset of sequences in the library with the closest initial donor mass. We then scan this subset to find the one sequence with the closest initial orbital period. The next task it to use the evolution data for each sequence selected from the library to compute distributions at the current epoch of observable quantities, such as $P_{\rm orb}$, M_d, and $\dot{M}_a$.

First, we define a set of times. Let $t_{\rm ev}$ be the time since the start of mass transfer, $T_{\rm MT}$ be the age of the Galaxy when mass transfer begins ($t_{\rm ev} = 0$), and $T_{\rm now} \simeq 13\,{\rm Gyr}$ be the present age of the Galaxy, so that $t_{\rm ev} = T_{\rm now} - T_{\rm MT}$. An additional time that one generally needs to consider is the time lag between the formation of the massive primordial binary and the onset of mass transfer in its descendant L/IMXB, which might be $\sim 10^9$ yr for low-mass secondaries. However, we assume for simplicity that the formation rate of massive stars and binaries has been constant for the past $\sim 10\,{\rm Gyr}$, in which case we may neglect the evolutionary time lag. Averaged over the Galaxy, the present massive binary formation rate is $\mathcal{R}_{\rm SN} \sim 10^{-2}\ {\rm yr}^{-1}$, or roughly the rate for core-collapse SNe (e.g., Cappellaro et al. 1999). It is straightforward to extend our formalism to include a variable star formation rate.

Suppose, for instance, that we would like to compute the distribution of some quantity Q (e.g., $P_{\rm orb}$, M_d, or $\dot{M}_a$) at the current epoch for all L/IMXBs throughout the Galaxy, unweighted by observational selection effects. For a particular sequence, we have Q as a function of $t_{\rm ev}$, which is generally not monotonic. We imagine an ensemble of identical evolutionary sequences, each of which is parameterized by a different "birth time" $T_{\rm MT}$. An observer at the current epoch would thus have snapshots of the same sequence at different evolutionary times $t_{\rm ev}$. For two snapshots separated by a small time $\delta t_{\rm ev} = \delta T_{\rm MT}$, the quantity Q varies over a small range $(Q_0, Q_0 + \delta Q)$. The probability of observing the system with Q in any finite interval $(Q_1, Q_1 + \Delta Q)$ is then proportional to $\sum \mathcal{R}_{\rm SN} \delta T_{\rm MT}$, where the symbolic sum is over all times during the evolution when $Q \in (Q_1, Q_1 + \Delta Q)$. The total (weighted) time $\sum \mathcal{R}_{\rm SN} \delta T_{\rm MT}$ accumulated in a given interval of Q is proportional to the number of primordial binaries used in the simulation. Therefore, in order to obtain an actual number of systems present in the Galaxy at the current epoch, we must then divide the total time by this number of primordial binaries. After all selected sequences are evolved, the result is a histogram of the number of systems at the current epoch as a function of the quantity Q.

3.5 Preliminary Results

We now discuss some of the important results and conlusions of our study. As this research is still in progress, all of the results presented here are preliminary. In what follows, we will indicate how our calculations could be made more realistic and what additional topics related to L/IMXB formation and evolution we may explore in the future.

3.5.1 Incipient Systems

The first step in our study of LMXBs and IMXBs is to generate a population of incipient X-ray binaries. The output of the population synthesis calculation is a set of binaries with circular orbits, each identified by the orbital period and mass of the donor; we take the initial mass of the NS to be 1.4 $M_\odot$. At present, we neglect the shrinkage of the circularized orbit as a result of MB. However, this is an important effect when $P_{\rm orb} \lesssim 1$ day, since the MB timescale may be shorter than the main-sequence lifetime ($\tau_{\rm nuc} \sim 10^{10}$ yr) of a $\lesssim$1-$M_\odot$ secondary. In fact, for low-mass secondaries it may be impossible for the star to fill its Roche lobe within the age of the Galaxy unless MB is operative. A complete treatment of tidal interactions and MB between the time of the SN and Roche-lobe overflow will be incorporated into future studies.

Figures 3-7, 3-8, 3-9, and 3-10 show distributions of M_d, $P_{\rm orb}$, and the binary CM speed for the inicpient L/IMXBs. For reference, the initial models from our library of evolutionary sequences have been overlayed on each scatter plot. We have chosen to vary only two free parameters of our population study, the CE structure parameter $\lambda = \{0.1, 0.3, 0.5\}$ (see eqs. [2.11] and [3.1]) and the parameter $\sigma({\rm km\,s^{-1}}) = \{0, 50, 100, 200\}$ in the kick distribution (eq. [3.4]). The values of these parameters are shown to the left of each pair of plots. Also given in Figs. 3-7 through 3-10 is the fomation efficiency, $\mathcal{F}_{\rm FE}$, for each parameter set, which we define to be the number of incipient L/IMXBs with initial secondary masses of $\lesssim$4 $M_\odot$ that are produced in the simulation, divided by the chosen number of massive primordial binaries.

Notice that for all parameter sets shown, the distribution of initial secondary masses has an overall increasing trend. This trend is, of course, modified if we adopt a somewhat different distribution of mass ratios for the components of the primordial binaries. Nonetheless, the general statistical importance of initally intermediate-mass secondaries is clear. Also apparent in Figs. 3-7 through 3-10 is the tendency for the initial orbital periods to decrease as λ is decreased, as explained in § 3.2.1. What is most striking, however, is that $\mathcal{F}_{\rm FE}$ drops precipitously as λ goes from 0.3 to 0.1 (i.e., as the absolute value of the envelope binding energy is increased). The reason for this is that the maximum orbital period of the incipient L/IMXBs grows with increasing secondary mass, largely as a result of the depence of the post-CE separation on the primordial mass ratio (see § 3.2). Therefore, decreasing λ below a certain value leads to the merger of most of the systems with primordial secondary masses of $M_2 \lesssim 3$ $M_\odot$. The fact that so few incipient L/IMXBs with $M_d \lesssim 3$ $M_\odot$ are produced when $\lambda = 0.1$ is a very interesting sensitivity, since Dewi & Tauris (2001) calculate $\lambda \sim 0.1$–0.2 for the primary masses of 8–20 $M_\odot$ that we are considering. With more refined

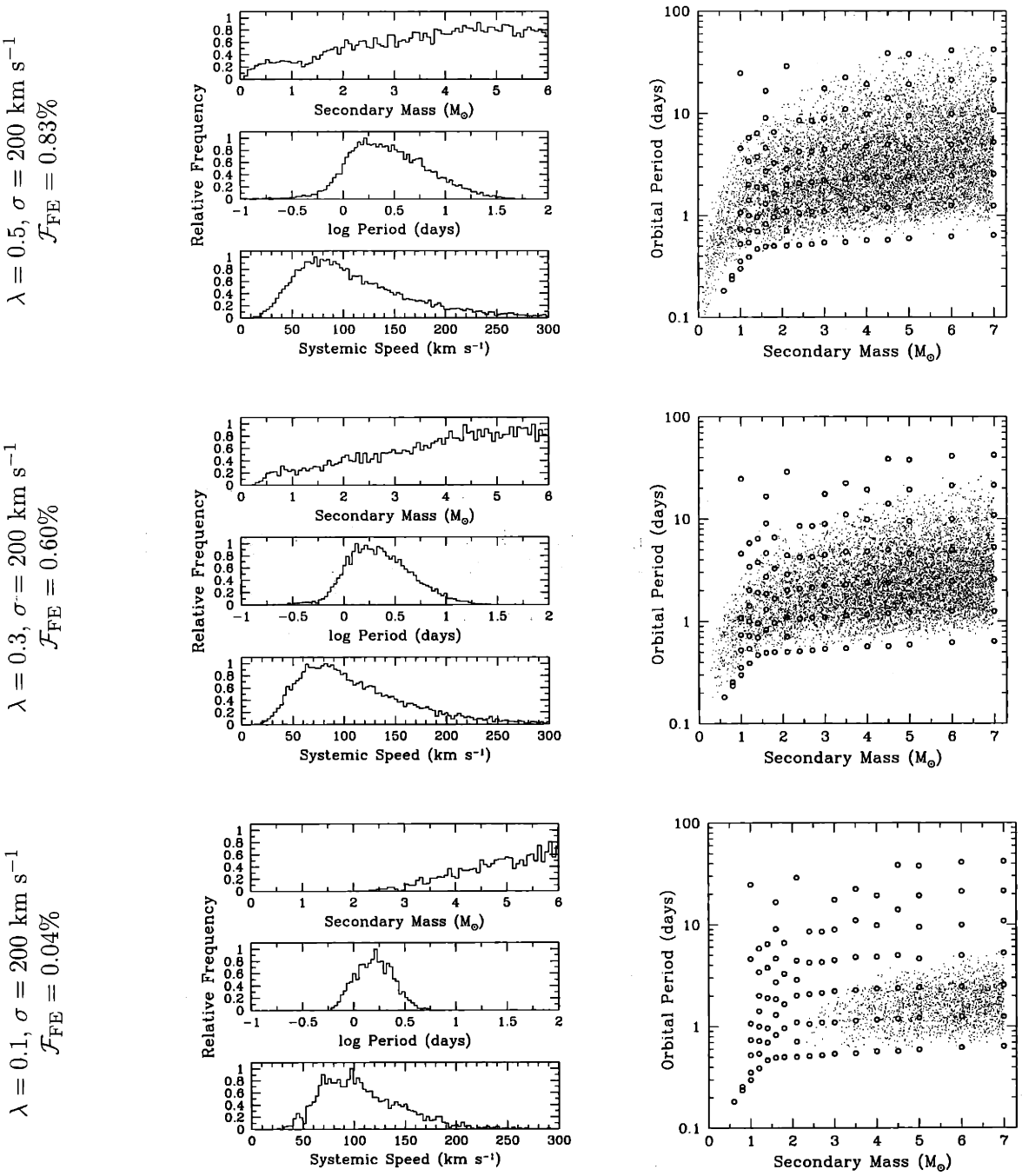

Figure 3-7: On the left are the distribution of binary parameters and systemic speeds for the incipient L/IMXBs, which we assume have circularized prior to mass transfer. The scatter plots on the right show how the orbital periods and secondary masses are correlated. For reference, we have overlayed the initial parameters from the library of evolutionary sequences described in Podsiadlowski et al. (2002). The model parameters that we have varied are shown on the left. In each simulation, we started with 500,000 massive primordial binaries.

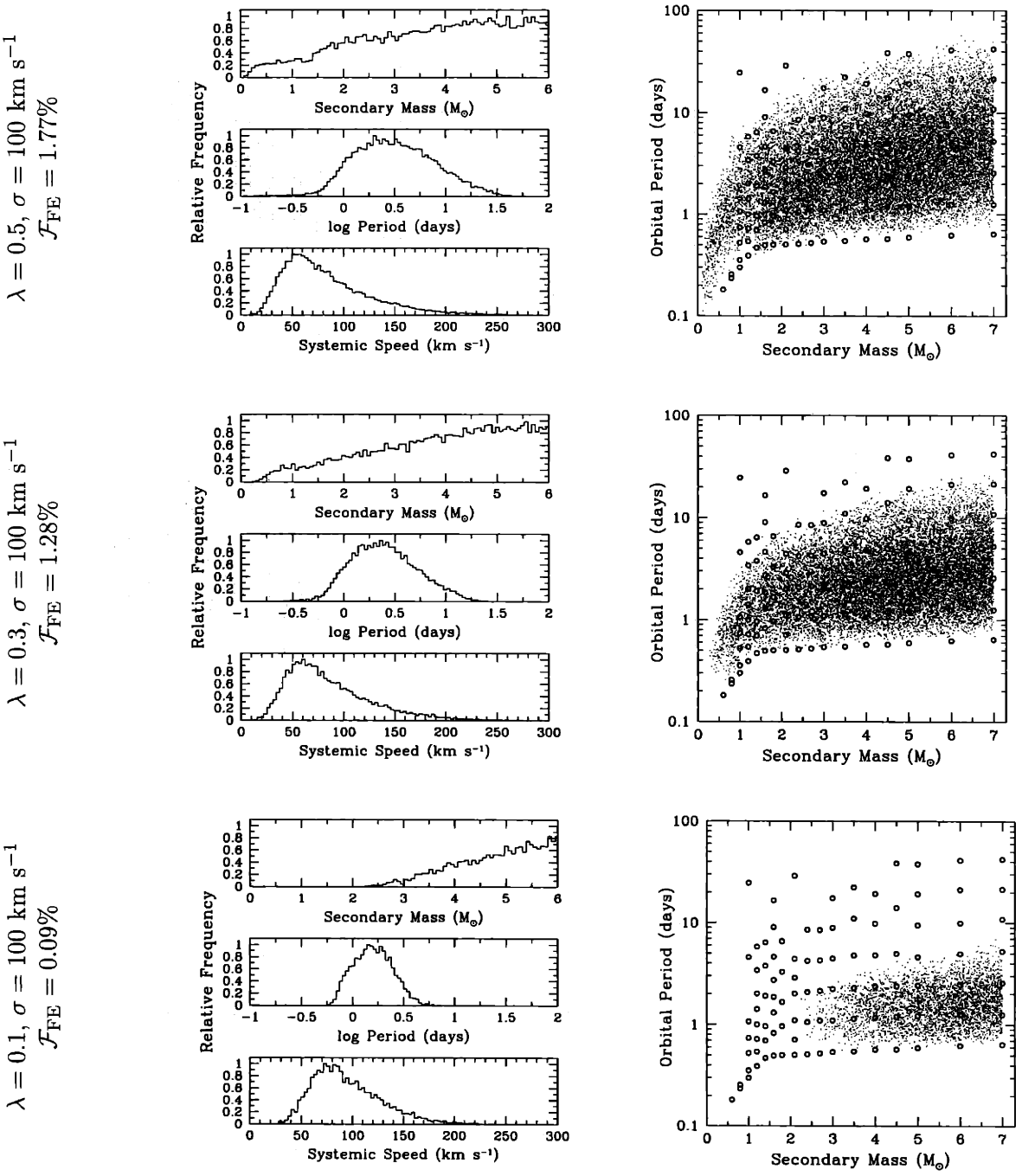

Figure 3-8: Similar to Fig. 3-7, but with $\sigma = 100$ km s^{-1}.

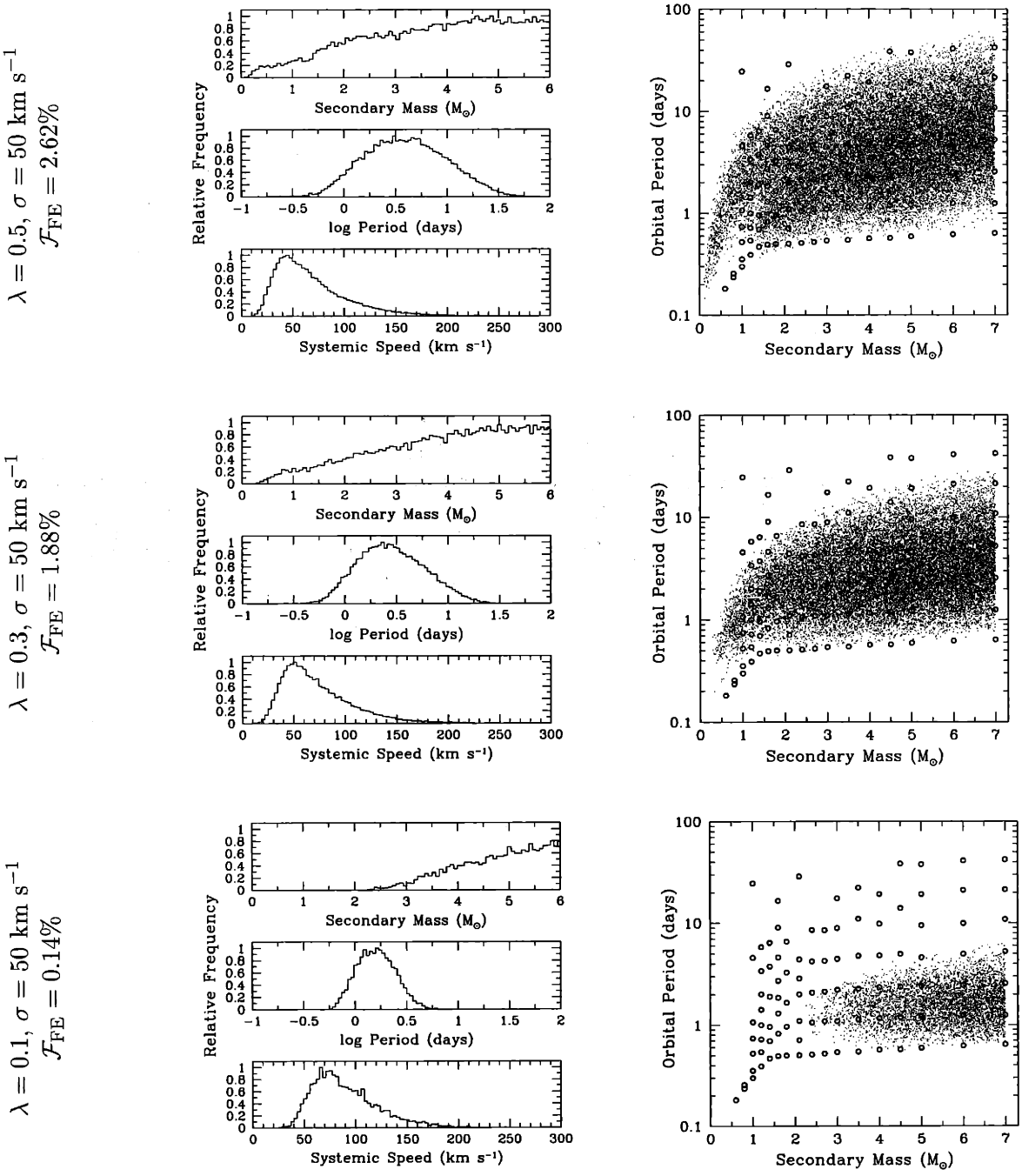

Figure 3-9: Similar to Fig. 3-7, but with $\sigma = 50$ km s^{-1}.

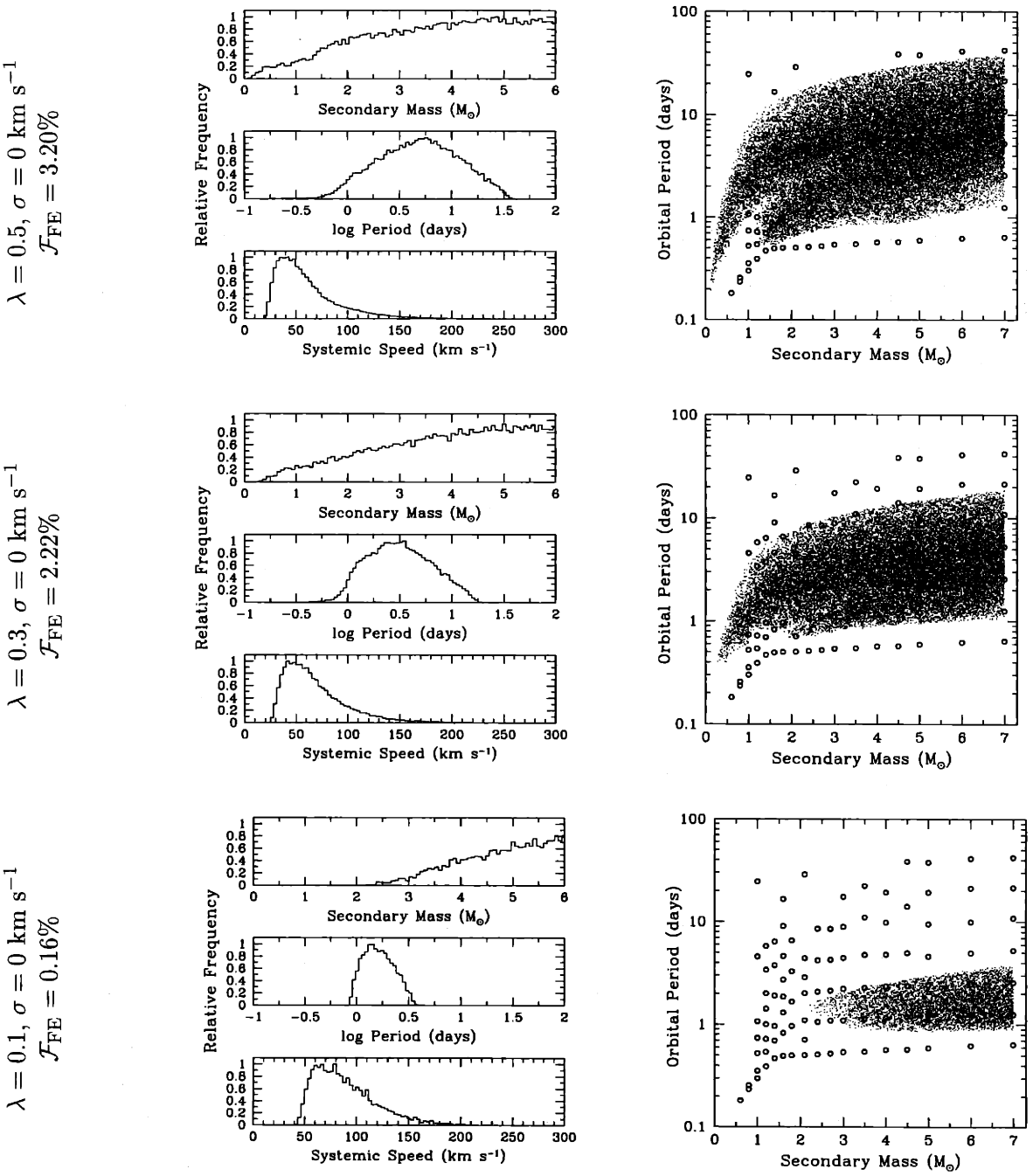

Figure 3-10: Similar to Fig. 3-7, but with $\sigma = 0$ km s^{-1}.

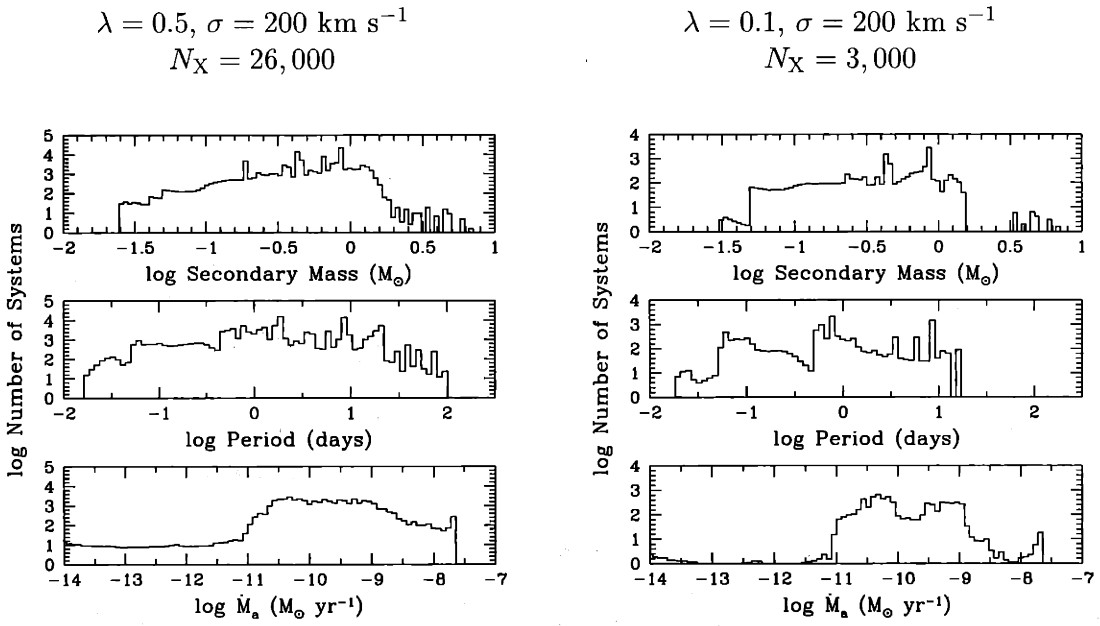

Figure 3-11: Distributions at the *current epoch* of system parameters and mass accretion rate onto the NS. Plotted is the logarithm of the actual number of X-ray binaries that are presently active in the Galaxy. The model parameters for the population synthesis calculation are indicated above, along with the number N_X of systems with with $-10 < \log \dot{M}_a(M_\odot\,\mathrm{yr}^{-1}) < -8$, rounded to the nearest thousand.

population studies, we may be able to indirectly set limits on the possible values of λ.

3.5.2 Distributions at the Current Epoch

Using the time-weighting scheme outlined in § 3.4.2, we have computed theoretical distributions at the current epoch of the orbital periods, secondary masses, and mass accretion rates of LMXBs and IMXBs. From Figs. 3-7 through 3-10, we see that the shapes and ranges the of distributions of *initial* orbital periods and secondary masses appear to be rather insensitive to the value of σ, although larger kick speeds cause the distributions to broaden somewhat. The most important effect of the kicks is to reduce the overall normalization given by $\mathcal{F}_{\rm FE}$. We have therefore chosen to show in Fig. 3-11 two representative examples of the current-epoch distributions, both for $\sigma = 200$ km s^{-1}, but with $\lambda = 0.1$ (*right*) and $\lambda = 0.5$ (*left*). The sharp features in these distributions are not a result of poor statistical resolution per se, but are a consequence of having a fairly coarse grid of evolutionary sequences in our library. As more sequences are added, these distributions will become smoother.

In Fig. 3-11, we show the actual number of systems present in the Galaxy with the parameters indicated. Also shown above each plot is the estimated present number, N_X, of

luminous X-ray sources, with $-10 < \log \dot{M}_a(M_\odot\,\mathrm{yr}^{-1}) < -8$. For both $\lambda = 0.1$ ($N_\mathrm{X} = 2600$) and $\lambda = 0.5$ ($N_\mathrm{X} = 25700$), our calculated numbers strongly disagree with the total observed number of $\sim$100 LMXBs, since such luminous sources are detectable over a large Galactic volume. It thus appears that LMXBs are far too easily produced with our current model assumptions. Kalogera & Webbink (1998) used $\lambda = 0.5$ and $\sigma \sim 200$, but obtained numbers of potentially observable X-ray binaries that are roughly consistent with observations. However, her study included only systems with initial donor masses $\lesssim$1.5 $M_\odot$. Possible resolutions to this overproduction problem will be investigated in the future. Perhaps λ is actually smaller than Dewi & Tauris (2001) suggest, or some of our assumptions regarding the formation and evolution of massive primordial binaries require significant modification. Another possibility is that a large fraction of LMXBs are transient X-ray sources for reasons that we do not yet understand.

3.6 Conclusions

Although our results are preliminary, we have discussed a number of important new ideas in the preceding sections, which we now briefly review.

(1) In general, we find that incipient IMXBs are more easily produced than LMXBs; there are two main reasons for this. First, for a given primary mass in the primordial binary, less orbital shrinkage is required to unbind the CE as the secondary mass is increased (see § 3.2.1 and eq.[3.2]), and thus merger of the primordial binary components is less likely if the secondary is of intermediate mass than if it is a low-mass star. Second, fewer systems with intermediate-mass secondaries are disrupted at the time of the SN, which is primarily a result of the reduced fractional mass loss in the explosion (see § 3.2.2).

(2) The number of L/IMXBs that are produced in the population synthesis calculation depends very sensitively on the value of the envelope binding energy parameter λ. Smaller values of λ (i.e., more tightly bound common envelopes) lead to a larger fraction of systems that merge during the CE phase, and thus fewer incipient X-ray binaries are produced. Furthermore, decreasing λ has the effect of increasing the relative proportion of binaries with intermediate-mass secondaries, since the low-mass systems are more likely to merge in any case.

(3) We find that with our current range of model assumptions, potentially observable LMXBs are greatly overproduced in comparison to the observed number. This is largely a result of our allowing for IMXBs in the combined population syntehsis and evolutionary study. After evolving through a short ($\lesssim 10^7$ yr) phase of thermal-timescale mass transfer, where most of the transferred matter is ejected from the system, many of the IMXBs eventually evolve to resemble standard LMXBs. In fact, once the mass of an initially intermediate-mass donor is reduced to $\lesssim$1 $M_\odot$ in the early, rapid phase of mass transfer, the evolutionary lifetime of the X-ray binary may increase to of order 1 Gyr (see Figs. 3-4 through 3-6). Therefore, many systems that begin as IMXBs actually resemble LMXBs for most of the X-ray binary phase.

(4) Recall that the mass capture fraction $\beta < 1$ is defined by $\dot{M}_a = -\beta \dot{M}_d$. We take $\beta = b$ for sub-Eddington mass transfer ($|\dot{M}_d| < \dot{M}_{\rm Edd}$) and $\beta = b\dot{M}_{\rm Edd}/|\dot{M}_d|$ for super-Eddington mass transfer ($|\dot{M}_d| > \dot{M}_{\rm Edd}$), so that the accretion rate is always less than $b\dot{M}_{\rm Edd}$. For $b = 0.5$, we find that in most cases the NS accretes $\gtrsim 0.5\ M_\odot$ after $\lesssim 1$ Gyr of mass transfer, and thus the NSs in most LMXBs at the current epoch would have masses of $\sim 2\ M_\odot$. Values of b closer to unity would imply final NS masses of $\gtrsim 2$–$3\ M_\odot$, possibly in excess of the NS maximum mass, in which case the majority of NSs would collapse to low-mass black holes. No such system has yet been detected, and so perhaps $b \lesssim 0.5$ is the general rule, for reasons that are not understood.

Chapter 4

A New Class of High-Mass X-ray Binaries

This chapter is adapted from the paper, "A New Class of High-Mass X-ray Binaries: Implications for Core Collapse and Neutron-Star Recoil," by Eric Pfahl, Saul Rappaport, Philipp Podsiadlowski, & Henrik Spruit, to appear in *The Astrophysical Journal.*

4.1 Introduction

It has become fashionable in recent years to suppose that the majority of neutron stars (NSs) are born with speeds in excess of $\sim$ 100–200 km s^{-1}, presumably as a result of some asymmetry in the core collapse or the subsequent supernova (SN) explosion of the NS progenitor. The strongest support for this notion comes from the high speeds inferred for the $\sim$ 100 Galactic pulsars with well-measured interferometric proper motions (Harrison, Lyne, & Anderson 1993). Mean speeds for these pulsars of $\gtrsim$ 300 km s^{-1} have been estimated by a number of authors (e.g., Lyne & Lorimer 1994; Hansen & Phinney 1997; Cordes & Chernoff 1998; Arzoumanian et al. 2002). Various classes of binary systems containing NSs also show strong evidence for substantial natal "kick" velocities, based upon their present orbital parameters, their systemic speeds, and/or their heights above the Galactic plane (e.g., Brandt & Podsiadlowski 1995; Verbunt & van den Heuvel 1995; Johnston 1996; van den Heuvel et al. 2000).

Very large uncertainties, both observational and theoretical, still pervade studies of the underlying distribution in NS natal kick speeds. Complications include the fairly small sample of pulsars with proper-motion measurements, questionable dispersion-measure distances, serious observational selection effects, and uncertainties regarding the formation of NSs and their dynamical evolution in the Galaxy. Fortunately, the sample of pulsars with reliable proper motions is growing (see McGary et al. 2001), as is the number of pulsars with accurate parallax distances (e.g., Toscano et al. 1999; Brisken et al. 2000).

The most popular models for NS kicks involve a momentum impulse delivered around

the time of the core collapse that produced the NS. Mechanisms in this class include purely hydrodynamical processes, as well as primarily neutrino-driven kicks (see Lai 2001 for a review). In either case, some process must be responsible for breaking spherical symmetry during core collapse, such as a combination of Rayleigh-Taylor instabilities and neutrino-induced convection (e.g., Janka & Mueller 1994; Fryer & Heger 2000). A fundamentally different mechanism for producing significant NS velocities was proposed by Harrison & Tademaru (1975), whereby the NS is accelerated *after* the core-collapse event as a result of asymmetric electromagnetic (EM) dipole radiation — the so-called EM "rocket" effect, which is distinctly non-impulsive.

A theoretical determination of the emergent velocity distribution associated with each kick mechanism is extremely difficult and would require an ensemble of detailed three-dimensional hydrodynamical simulations (with the exception of the EM "rocket" mechanism). Furthermore, it is unlikely that a single process accounts for the full range of NS velocities. For instance, it is plausible that the dominant kick mechanism and the magnitude of the kick depend at least somewhat on the evolutionary history of the NS progenitor. In this paper, we explore a possible linkage between the kick magnitude and the evolution of the NS progenitor in a binary system. This work was inspired by a new observed sub-class of high-mass X-ray binaries (HMXBs).

Previously, significant eccentricities of $e \sim 0.3$–0.5 seemed to be the general rule among HMXBs with $P_{\rm orb} \sim 20$–100 d (see Bildsten et al. 1997), which presumably result from substantial NS kicks (e.g., Brandt & Podsiadlowski 1995; Verbunt & van den Heuvel 1995; van den Heuvel et al. 2000). By contrast, the members of the new class of HMXBs are clearly distinguished by their low eccentricities of $e \lesssim 0.2$ and long orbital periods of $P_{\rm orb} \sim 30$–250 d, which indicate that tidal circularization should not have played a significant role if the massive stellar component is not very evolved. Eccentricities of this magnitude are roughly consistent with the dynamical effect of mass loss alone in the SN explosion, although relatively small kick speeds of $\lesssim 50$ km s^{-1} cannot be ruled out on statistical grounds.

There are currently six candidates for the new class of HMXBs. This is a substantial number, given the difficulties associated with detecting these binaries and measuring their orbits, and the fact that there are only ~ 20 HMXBs with measured orbital parameters. We suggest that the observed wide, nearly circular HMXBs are representative of a much larger intrinsic population, and that the NSs in these systems received only a small kick ($\lesssim 50$ km s^{-1}). We further speculate that the magnitude of the kick is correlated with the evolutionary history of the binary system, before the formation of the NS. Specifically, we propose that the kick speed depends on the rotation rate of the core of the NS progenitor following a phase of mass transfer, wherein the hydrogen-rich envelope of the star is removed. The sense of the proposed effect is that slowly rotating cores produce NSs with the conventional large kicks, while the collapse of rapidly rotating cores are accompanied by relatively small natal kicks. If our basic picture is correct, there may be important implications for magnetic field evolution and core collapse in massive stars, the retention of NSs in globular clusters, and the birthrate of double NS binaries in the Galaxy.

Table 4.1. Orbital Parameters for Nearly Circular High-mass X-ray Binaries.

Object	$P_{\rm orb}$(days)	e	$f_{\rm X}(M)(M_\odot)$[a]	References
X Per/4U 0352+30	249.90 ± 0.50	0.111 ± 0.018	1.61 ± 0.06	1
γ Cas/MX 0053+604[b].....	203.59 ± 0.29	0.260 ± 0.035	...	2
GS 0834–430	105.80 ± 0.40	< 0.17	0.2 ± 0.3	3
XTE J1543–568	75.56 ± 0.25	< 0.03	8.2 ± 0.5	4
KS 1947+30	41 ± 1	< 0.15	∼ 1.8	5,6
2S 1553–542	30.60 ± 2.20	< 0.09	5.0 ± 2.1	7

[a]Mass function from X-ray timing.

[b]Orbital parameters determined from the optical light curve.

References. — (1) Delgado-Martí et al. 2001; (2) Harmanec et al. 2000; (3) Wilson et al. 1997; (4) in 't Zand, Corbet, & Marshall 2001; (5) Chakrabarty et al. 1995; (6) Galloway et al. 2001, in preparation; (7) Kelley, Rappaport, & Ayasli 1983

4.2 The New Class of Long-Period, Low-Eccentricity HMXBs

A HMXB consists of a NS, which often appears as an X-ray pulsar, and a massive stellar companion. Of the ∼ 130 known HMXBs (see Liu et al. 2000), ∼ 20 have reasonably well-measured orbital elements (see Bildsten et al. 1997 for a somewhat dated list). In all but one case (γ Cas; Harmanec et al. 2000), the parameters were determined from the timing of the X-ray pulsar.

Two classes of HMXBs, distinguished by their orbital parameters, are apparent in Table 3 of Bildsten et al. (1997): (i) systems with $P_{\rm orb} \lesssim 10$ d and $e \lesssim 0.1$, and (ii) moderately wide, eccentric binaries with $P_{\rm orb} \sim 20$–100 d and $e \sim 0.3$–0.5. A new third class of HMXBs has recently emerged. These systems are distinguished from the well-known HMXBs by their wide orbits (all have $P_{\rm orb} > 30$ d) and fairly low eccentricities ($e \lesssim 0.2$). Table 4.1 lists the names and orbital parameters of these interesting binaries, and below we give a brief synopsis of relevant observational information for each system. For two of the binary X-ray pulsars discussed below (XTE J1543–569 and 2S 1553–542), the optical counterpart has not been identified. In these cases, we should remain open to the possibility that the companion may have evolved beyond the main sequence and is filling a significant fraction of its Roche lobe, thus possibly explaining the low eccentricities as being due to tidal circularization.

4.2.1 X Per/4U 0352+309

The X-ray counterpart to the classical O/Be star X Per, 4U 0352+309, exhibits pulsations with a period of ∼ 837 s. Variations in the pulse period strongly suggest that the X-ray source is an accreting NS. The X-ray pulsar was observed by Delgado-Martí et al. (2001) over an interval of nearly 600 days with the *Rossi X-ray Timing Explorer* (*RXTE*). These

observations have revealed the orbital period of the system, $P_{\rm orb} = 250.3 \pm 0.6$ d, and the orbital eccentricity, $e = 0.111 \pm 0.018$.

Estimates of the distance to X Per range from 700 ± 300 pc to 1.3 ± 0.4 pc (see Delgado-Martí et al. 2001 and references therein). It is then especially interesting to note that X Per lies at a Galactic latitude of approximately $-17°$. For an assumed distance of ~ 1 kpc, this latitude places X Per at a height of ~ 300 pc above the Galactic plane, which is considerably larger than the scaleheight of massive stars in the Galactic disk. This large height may be explained by the systemic impulse received due to the mass loss and kick associated with the formation of the NS. However, the magnitude of the kick would have to be quite large, and the near circularity of the orbit would make the X Per system a very unlikely object. A far simpler and more reasonable hypothesis is that the binary was, in fact, born in an OB association within the Gould Belt (e.g., Torra et al. 2000), a disk-like structure with a radial extent of $\gtrsim 500$ pc, inclined by $\sim 20°$ to the Galactic plane. It is thought that the associations comprising the Gould Belt account for roughly 60% of the O and B stars within ~ 500 pc from the Sun.

4.2.2 γ Cas/MX 0053+604

It has long been suspected that γ Cas, the first-known Be star (Secchi 1867), is a member of a binary system; however, the orbit has defied detection at both X-ray and optical wavelengths until very recently. Harmanec et al. (2000) have measured the orbit of the γ Cas system using optical spectroscopy. Periodic shifts in Hα and He I line features were attributed to the orbital motion of the Be star. The Hα measurements yielded the orbital parameters $P_{\rm orb} = 203.59 \pm 0.29$ d and $e = 0.26 \pm 0.035$. The optical mass function implies that the unseen companion has a mass of $\sim 1\ M_\odot$, consistent with a massive white dwarf or a NS.

There is still debate regarding the nature of the X-ray counterpart to γ Cas/MX 0053+60. If the companion is indeed a compact object, it is not clear from the X-ray emission whether it is a NS or a white dwarf. For instance, no significant X-ray pulsations have ever been confirmed (see Smith et al. 1998). If the system presently contains a white dwarf, we would expect the orbit to be circular as a result of an earlier episode of mass transfer. On these grounds, the NS hypothesis is compelling, since the SN that accompanied the formation of the NS could have easily perturbed the orbit to yield the observed eccentricity. Smith, Robinson, & Corbet (1998; see also Robinson & Smith 2000) argue against the hypothesis that the X-rays emanate from a compact object and favor a model where the X-ray emission is the result of magnetic activity on the stellar surface. Further observations are required to determine the origin of the X-rays and the nature of the companion to γ Cas.

4.2.3 GS 0834–430

Wilson et al. (1997) analyzed the data from seven outbursts of the transient X-ray pulsar GS 0834–430, observed with the BATSE instrument on board the *Compton Gamma Ray*

Observatory (*CGRO*). Timing analysis of the 12.3-s X-ray pulsar revealed an orbital period of $P_{\rm orb} = 105.8 \pm 0.4$ d, but did not place very tight constraints on the eccentricity. According to Wilson et al. (1997), a likely value for the eccentricity is $e \lesssim 0.2$; larger values are permitted, but require a very small binary inclination. From the spin-up behavior of the X-ray pulsar, the estimated distance of the binary is $\gtrsim 4.5$ kpc. The optical counterpart to GS 0834–430 has been identified as a Be star by Israel et al. (2000).

4.2.4 XTE J1543–569

After a year-long monitoring campaign with *RXTE*, In't Zand et al. (2001) have determined the orbital parameters of the transient X-ray pulsar XTE J1543–569. The system has an orbital period of $P_{\rm orb} = 75.56 \pm 0.25$ d and an eccentricity of $e < 0.03$ at the 2σ level. This eccentricity is surprisingly small if the massive companion to the NS is near the main sequence and thus is greatly underfilling its Roche lobe, even if we assume that the NS did not receive a kick. However, an optical counterpart has yet to be discovered, although the orbital and pulse periods place XTE J1543–569 amongst the confirmed Be/X-ray transients in the "Corbet" diagram (Corbet 1986; see also Bildsten et al. 1997).

It is interesting to note that the present eccentricity of XTE J1543–569 is not likely to be consistent with a vanishing NS kick. If we consider only mass loss in the SN explosion, the induced eccentricity for an initially circular orbit is $e = \Delta M/(M_b - \Delta M)$, where ΔM is the mass lost and M_b is the pre-SN mass of the binary (e.g., Blaauw 1961; Dewey & Cordes 1987). An eccentricity of ~ 0.03 is obtained if $\Delta M = 0.6\ M_\odot$, for a low pre-collapse core mass of $2\ M_\odot$, and a somewhat high binary mass of $M_b = 20\ M_\odot$. However, more typical values of ΔM and M_b are $\sim 1.6\ M_\odot$ and $\sim 15\ M_\odot$, respectively, which yield $e \sim 0.11$. In this case, a kick is required to "correct" the eccentricity to produce the smaller observed value, but the magnitude and direction of the kick must be somewhat finely tuned. We suggest that either the stellar companion to the X-ray source XTE J1543–569 is very massive or that the companion has evolved well beyond the main sequence and is filling a sizable fraction of its Roche lobe, so that tidal circularization accounts for the low eccentricity.

4.2.5 KS 1947+30

The transient X-ray source KS 1947+30 was first detected by the Kvant instrument on board the *Mir* space station (Borozdin et al. 1990). In 1994, 18.7-s X-ray pulsations were detected by BATSE during an outburst that lasted 33 d (Chakrabarty 1995 and references therein). However, the $\sim 10\,{\rm deg}^2$ position resolution of BATSE was not sufficient to identify the X-ray pulsar as the Kvant source, and the pulsar was given the designation GRO J1948+32. Modulation of the pulse frequency during the 33 d outburst was suggestive of a binary orbit, but with less than one full orbital cycle of coverage. Preliminary estimates placed the orbital parameters in the ranges $P_{\rm orb} = 35$–70 d and $e < 0.25$

A recent outburst has allowed KS 1947+30 to be "rediscovered" by the All Sky Monitor (ASM) on board *RXTE* (Galloway et al. 2001, in preparation). It was quickly realized that GRO J1948+32 and the old Kvant source are the same, and so the earlier designation, KS

1947+30, has been adopted. The X-ray pulsar has now been timed for ~ 5 orbits, and a more precise orbital solution has been determined, with $P_{\rm orb} = 41.12 \pm 0.65$ d and $e < 0.15$. Furthermore, the accurate position has led to the identification of an optical counterpart, probably an O/Be star (Negueruela et al. 2000).

4.2.6 2S 1553–542

The transient X-ray pulsar 2S 1553–542 was first detected with the *SAS 3* satellite during the only known outburst of the source in 1975 (Apparao et al. 1978). Kelley et al. (1983) analyzed data that spanned 20 d of the outburst and discovered regular variations in the 9.27-s pulse period that they attributed to a binary orbit. They determined that the system has an orbital period of $P_{\rm orb} = 30.6 \pm 2.2$ d and an eccentricity of $e < 0.09$. The orbital parameters were not well constrained because the observations did not cover a full orbital cycle. Although no optical counterpart to 2S 1553–542 has been identified, the transient nature of the source is suggestive of an unevolved Be star companion (see Kelley, Rappaport, & Ayasli 1983 and references therein).

4.3 The Statistical Significance of the New Class of HMXBs

Before we begin to explore alternative models to explain the new class of HMXBs with wide orbits and small or moderate eccentricities, it is important that we provide some reasonable confirmation that this class is really a distinct population and does not fit within the conventional framework of massive binary population synthesis. It is, of course, possible that these systems are not dynamically significant (e.g., that their low eccentricities are the result of tidal circularization), or that they represent the tail of a distribution and that some observational bias favors their detection.

4.3.1 Tidal Circularization

The high, persistent X-ray luminosities of the short-period HMXBs ($P_{\rm orb} \lesssim 10$ d) are maintained by the strong stellar winds from secondaries that are nearly filling their Roche lobes. This hypothesis is supported by the ellipsoidal variations of the optical lightcurves for a number of these sources, which indicate that the stellar companions are tidally distorted. Therefore, strong tidal interactions can easily explain the low eccentricities seen among the short-period HMXBs. However, it is extremely unlikely that tidal circularization has played a significant role in modifying the orbits of the new class of wide, nearly circular HMXBs.

Efficient tidal circularization requires that the star almost fills its Roche lobe and that there be an effective mechanism for damping the tide. These conditions are encapsulated by the cicularization timescale,

$$\tau_{\rm cir} = \tau_{\rm dis} \left(\frac{a}{R} \right)^8 , \tag{4.1}$$

in the limit of weak tidal friction (e.g., Zahn 1977; Rieutord & Zahn 1997), where a is the semimajor axis of the orbit, R is the radius of the star, and $\tau_{\rm dis}$ is the timescale associated

with viscous dissipation in the star. Radiative dissipation of the tidal luminosity is enormously inefficient in comparison to turbulent dissipation in a convection zone. As a result, the tidal coupling to the radiative envelope of a massive main-sequence star is much weaker than the coupling to the convective core (Zahn 1977). However, since the core comprises only $\sim 20\%$ of the radius of the star, the resulting circularization timescale is comparable to, or shorter than, the star's nuclear lifetime only when the star is very nearly filling its Roche lobe. This statement is supported by the near circularity ($e \lesssim 3 \times 10^{-3}$) of the orbits of SMC X-1, LMC X-4, and Cen X-3, which have orbital periods shorter < 4 d (Bildsten et al. 1997; Levine et al. 2000). However, tidal torques should have little effect on the orbit of a HMXB with $P_{\rm orb} \gtrsim 10$ d, as long as the secondary is not too evolved and the eccentricity is not so large that the tidal interaction is enhanced dramatically at periastron.

4.3.2 Observational Selection Effects

There are currently six candidates for the class of wide, low-eccentricity HMXBs (Table 4.1), four of which have identified O or B optical counterparts. If we count all six candidates, then the new class of binaries accounts for roughly 30% of the HMXBs with measured orbital parameters. This fairly large fraction suggests that either these systems are preferentially selected for purely observational reasons or that their intrinsic population is actually quite large.

We should expect that an X-ray pulsar in a wide orbit with a low eccentricity is more difficult to detect and measure than if the orbital period is relatively short. There are two primary reasons for this. First, Bondi-Hoyle accretion theory (Bondi & Hoyle 1944) predicts that the persistent luminosity of a wind-fed X-ray pulsar decreases with increasing orbital period, for a given rate of mass loss from the stellar companion. Therefore, very wide binaries have a small effective Galactic volume in which their orbits are readily measurable; e.g., for low-luminosity sources that resemble X Per/4U 0352+309, it would currently be difficult to determine orbits if the systems lie much beyond 1 kpc. Second, an accurate determination of the orbit from X-ray timing requires a series of observations that cover at least one full orbital cycle. If the orbital period is very long, this may not be feasible, especially given the transient behavior of many sources and the limited amounts of observing time. Transient sources, of which there are four in Table 4.1, may be very conspicuous during outburst, but because of their transient nature and possibly large pulse-period variations (due to accretion torque noise), it can be difficult to measure their orbits very precisely. For all these reasons, we conclude that, if anything, observational selection effects should be biased against long-period HMXBs with low eccentricities, and in fact such systems may dominate the Galactic population of HMXBs.

4.3.3 The Case for Small Kicks: Preliminary Arguments

The most important factor in determining from model calculations the number of wide, low-eccentricity HMXBs in the Galaxy is the distribution in NS natal kick speeds. A kick speed that is comparable to the relative orbital speed prior to the SN is likely to yield a

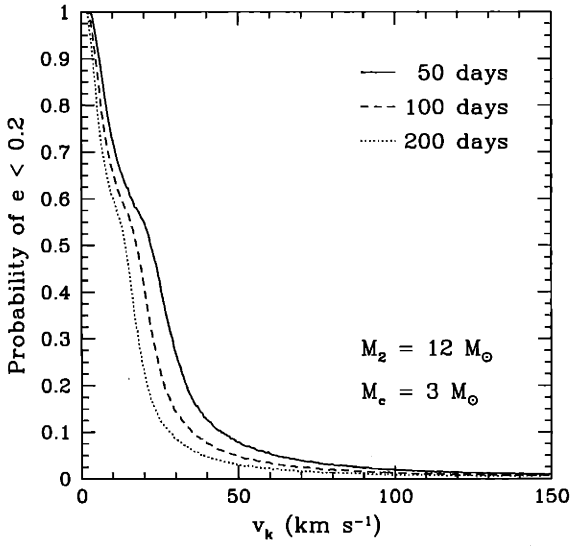

Figure 4-1: Probability that the post-SN eccentricity is < 0.2 for a helium star of mass 3 $M_\odot$ and a secondary of mass 12 $M_\odot$, for three different pre-SN orbital periods, as a function of the kick speed. The directions of the kicks are distributed isotropically.

highly eccentric binary following the explosion, including the probable event that the binary is disrupted ($e > 1$). This statement is illustrated more quantitatively in Fig. 4-1, where we plot the probability that the post-SN eccentricity is < 0.2 for a 3-$M_\odot$ helium-star primary (NS progenitor) and a 12-$M_\odot$ secondary (typical pre-SN masses) with one of three pre-SN orbital periods, as a function of the kick speed, v_k. The distribution in kick directions was assumed to be isotropic. For all three initial orbital periods, the probability is $< 5\%$ when $v_k > 0.5\, v_{\rm orb}$, and the probability is $< 10\%$ when $v_k > 50$ km s^{-1}.

Hansen & Phinney (1997) found that a Maxwellian distribution in kick speeds, given by

$$p(v_k) = \sqrt{\frac{2}{\pi}} \frac{v_k^2}{\sigma^3} e^{-v_k^2/2\sigma^2} \ , \tag{4.2}$$

is consistent with the data on pulsar proper motions, where the best fit was obtained with $\sigma \simeq 190$ km s^{-1}. A recent study by Arzoumanian et al. (2002) utilized a two-component Maxwellian distribution, and found that 40% of their model pulsars were contained in the low-speed component with $\sigma \sim 90$ km s^{-1}, while the remaining pulsars populated the high-speed component with $\sigma \sim 500$ km s^{-1}. A single-component Maxwellian kick distribution predicts that $\sim 3\%$ of NSs are born with speeds < 50 km s^{-1} for $\sigma = 100$ km s^{-1}, and $\sim 0.4\%$ for $\sigma = 200$ km s^{-1}. This information, combined with the results displayed in Fig. 4-1, illustrates that the conventional wisdom regarding NS kicks does not lead to the favorable production of wide binaries with low eccentricities. In order to quantitatively demonstrate the statistical significance of the new class of HMXBs, we must combine a complete binary population synthesis study with observational considerations regarding the discoverability of these systems.

4.3.4 The Case for Small Kicks: Population Study

Our population synthesis study yields the fraction, F_0, of massive, primordial binaries that evolve into incipient HMXBs with orbital parameters in the range $P_{\rm orb} > 30$ d and $e < 0.2$. An upper limit to the expected present total number of HMXBs in the Galaxy with properties similar to those in Table 4.1 is obtained if we multiply F_0 by the Galactic formation rate of massive stars, $\sim 10^{-2}$ yr^{-1} (the approximate Galactic rate of core-collapse supernovae; Cappellaro et al. 1999), and the maximum lifetime of the HMXB phase, $\sim 10^7$ yr (the approximate evolutionary timescale of the massive secondary). Therefore, the current total number of wide, low-eccentricity HMXBs in the Galaxy is expected to be $N_{\rm tot} < F_0 \times 10^5$.

Of course, only a fraction, $F_{\rm dis} = N_{\rm dis}/N_{\rm tot}$, of the $N_{\rm tot}$ HMXBs could have been discovered by X-ray satellites that have scanned and/or monitored the X-ray sky (e.g., *Uhuru*, *HEAO-1*, *RXTE*, *CGRO*). A simple way to estimate $F_{\rm dis}$ is to apply a flux limit, $S_{\rm min}$, that is appropriate for a particular satellite instrument. For a given X-ray luminosity, $L_{\rm X}$, the maximum distance at which the source could be detected is $d_{\rm max} = (L_{\rm X}/4\pi S_{\rm min})^{1/2}$. An estimate of $F_{\rm dis}$ for a population of HMXBs with luminosity $L_{\rm X}$ is the probability that an O or B star is formed in a cylinder of radius $d_{\rm max}$ about the position of the Sun, perpendicular to the Galactic plane. Following Paczyński (1990) and Brandt & Podsiadlowski (1995), we adopt a disk distribution of stars given by

$$p(R) \propto R \exp(-R/R_0) \ , \tag{4.3}$$

where R is the Galactocentric radius and R_0 is the radial scalelength, taken to be 4.5 kpc (van der Kruit 1987).

The sensitivity with which the 2–10 keV X-ray sky has been probed for weak and transient HMXB is difficult to estimate. Some early scanning detectors aboard *Uhuru* and *HEAO-1* surveyed the sky for relatively brief periods (e.g., ~ 1 yr) with detection sensitivities as low as $S_{\rm min} \simeq 6 \times 10^{-11}$ergs s^{-1} cm^{-2}. In more recent times, the *Ginga* and *RXTE* satellites have been used to conduct limited pointed surveys of small regions of the sky, searching for X-ray pulsations from HMXBs; such studies were sensitive down to $S_{\rm min} \simeq 3 \times 10^{-11}$ergs s^{-1} cm^{-2}. However, the most sustained survey of the sky, with reasonable sensitivity, is that being conducted by the ASM aboard the *RXTE* satellite, which has been operating successfully for the past 6 years. It has sensitivities of $S_{\rm min} \simeq 3 \times 10^{-10}$ergs s^{-1} cm^{-2} for X-ray sources of known position, and $S_{\rm min} \simeq 2 \times 10^{-9}$ergs s^{-1} cm^{-2} for the detection of new sources (e.g., transients).

Sources with persistent luminosities comparable to that of X Per and/or γ Cas (i.e., $\sim 10^{35}$ ergs s^{-1}) would likely have been detected in previous surveys of the sky out to distances of ~ 3 kpc. However, objects that are transient in nature, with only infrequent "on" states at these low luminosities, might be detected with the ASM only out to distances of ~ 600 pc. Thus, the fractional effective volume of our Galaxy (from eq. [4.3]) that has been well studied for wide, low-luminosity HMXBs probably lies in the range of $\sim 10^{-4}$–5×10^{-3}. This is the range of values that we then consider for our parameter $F_{\rm dis}$. However, if

transient X-ray sources flare up to much higher luminosities, then the discovery probability at larger distances can go up dramatically.

Some results of our population synthesis study are shown in Figs. 4-2 and 4-3, where we have adopted a Maxwellian kick distribution with $\sigma = 200$ km s^{-1} and our standard-model parameters that describe the distribution of primordial binaries and mass transfer (see Chap. 2). It is apparent from Figs. 4-2 and 4-3 that binaries containing a massive secondary and that have low eccentricities and long periods are not produced favorably. These simulations yield a production fraction $F_0 \sim 4 \times 10^{-4}$, which corresponds to at most ~ 40 wide, nearly circular HMXBs in the Galaxy. Using $F_{\rm dis} = 10^{-3}$, the number of such systems that could have been discovered with *RXTE* is $N_{\rm dis} \sim 0.04$, or effectively zero. For a reduced value of $\sigma = 100$ km s^{-1}, we find that F_0 is increased by roughly a factor of five, and so perhaps as many as 200 such objects are present in the Galaxy, which is again probably much too small a number. If we adopt $F_{\rm dis} = 10^{-3}$ as a standard value for the discovery probability, and we assume that all 6 objects in Table 4.1 rightfully belong to the new class of HMXBs, then a simple likelihood estimate suggests that $N_{\rm tot} = N_{\rm dis}/F_{\rm dis} \sim 6000$ wide, low-eccentricity HMXBs may be present in the Galaxy.

A Maxwellian kick distribution with $\sigma \sim 100$ km s^{-1}, applied uniformly to *all* NSs, may be consistent with the speeds of a large fraction of isolated pulsars with measured proper motions (Arzoumanian et al. 2002), but conflicts arise when we consider significantly smaller values. The kinematics of the populations of single pulsars and LMXBs do suggest a large mean kick speed (e.g., Hansen & Phinney 1997; Brandt & Podsiadlowski 1995; Johnston 1996), and a Maxwellian distribution with $\sigma \gtrsim 100$ km s^{-1} seems to reproduce the properties of these populations reasonably well. However, based upon our discussion above, we suggest that there are many wide, nearly circular HMXBs in the Galaxy (possibly several thousand), and that the NSs in these systems require fairly small kicks ($v_k \lesssim 50$ km s^{-1}) on average[1]. The apparent conflict with the other known NS populations is resolved if the mean kick speed depends on the evolutionary history of the NS progenitor in a binary system. We now go on to describe this scenario in the next two sections.

4.4 An Evolutionary Model

With some perspective, we can motivate a phenomenological picture that accounts for the new population of long-period, low-eccentricity HMXBs, and which is consistent with what we know about other Galactic NS populations. There are four basic constraints that our model must satisfy. First, the orbits of the systems listed in Table 4.1 suggest that they did not experience a dynamical spiral-in phase prior to the first SN (see § 2.4), and that the NSs in these binaries did not receive a very large kick. We propose that a significant fraction of those NSs whose progenitors underwent case B_e or C_e mass transfer (see § 2.3) received natal kick speeds of $\lesssim 50$ km s^{-1}. Second, the orbits of all other binaries containing a NS and a

[1]Note that the mean of a Maxwellian distribution is given by $(8/\pi)^{1/2}\sigma$.

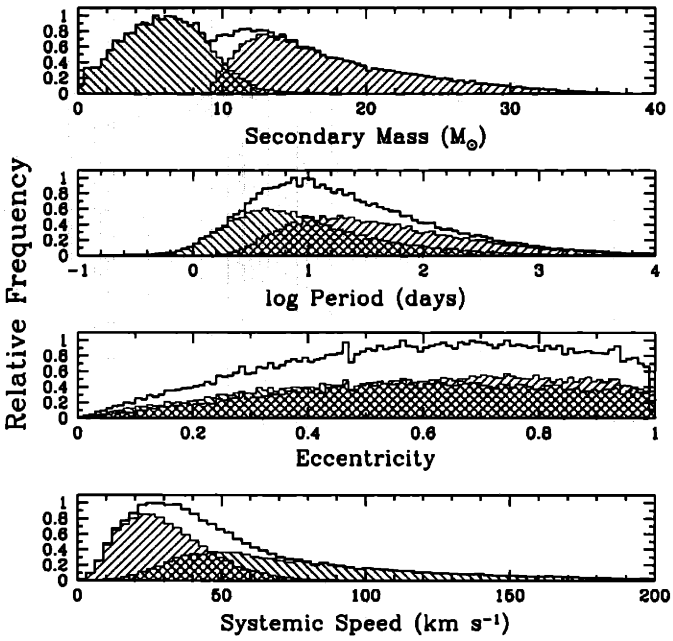

Figure 4-2: Distributions of binary parameters of systems that have undergone case B or C mass transfer from the original primary star to the secondary, have been left bound following the subsequent supernova explosion, and have not merged to form a TŻO (see text). Hatched regions indicate systems that have undergone stable mass transfer (+45°) and dynamically unstable mass transfer (–45°). The histogram that encloses the hatched region is the sum of the distributions for stable and unstable systems. A single Maxwellian kick distribution with $\sigma = 200$ km s^{-1} has been applied to all NSs.

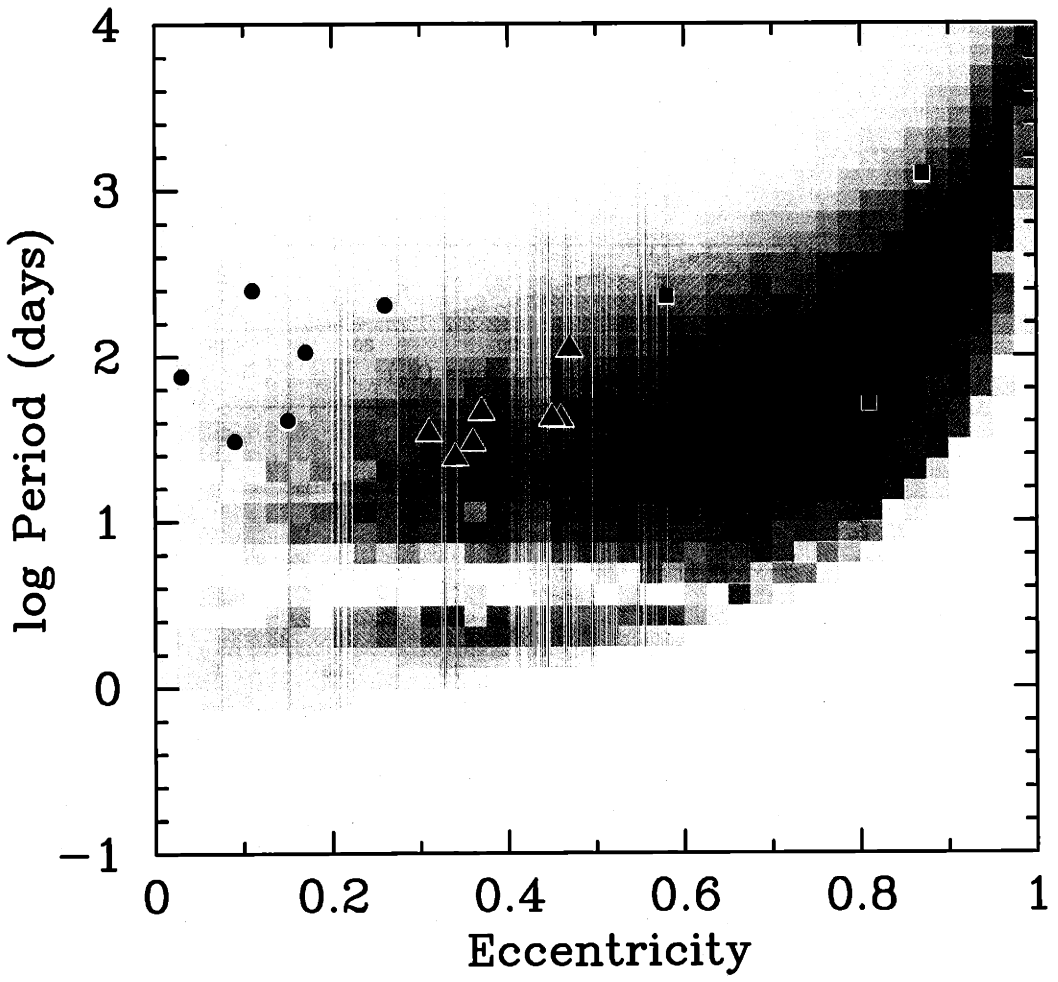

Figure 4-3: Two-dimensional distribution of orbital period and eccentricity for the systems in Fig. 4-2 with secondary masses $> 8\ M_{\odot}$. The intensity and color of a given square "pixel" indicate the total number of binaries and the stability of mass transfer, respectively. Pure red indicates only stable mass transfer, while pure blue indicates only dynamically unstable mass transfer. Colors that are not blue or red represent a mixture of stable and unstable systems; pure green indicates equal numbers. The intensity scale is linear and the lightest pixels represent $\sim 1\%$ of the number contained in the most intense pixel in the figure. Overlayed on the plot are markers that show the period and eccentricity (or upper limit) for the wide, low-eccentricity HMXBs (circles), the better-known eccentric HMXBs (triangles), and the long-period binary radio pulsars with massive companions (squares). The short-period, nearly circular HMXBs have not been plotted. (If this figure does not appear in color, see astro-ph/0109521.)

massive stellar companion should be naturally accounted for. Such binaries include short-period HMXBs and moderately wide, eccentric HMXBs (see § 4.2), as well as the three long-period binary radio pulsars with massive companions (PSR B1259–63, PSR J1740–3052, and J0045–7319; Johnston et al. 1992; Kaspi et al. 1994; Manchester et al. 1995; Kaspi et al. 1996; Stairs et al. 2001). Third, the model should be able to approximately reproduce the numbers and properties of luminous low-mass X-ray binaries in the Galaxy. Fourth, our basic picture should also be consistent with the observed kinematical distribution of isolated pulsars in the Galaxy, on which the NS kick distributions are based.

The third and fourth semi-empirical constraints on our model are satisfied if we suppose that a NS receives the usual large kick if its progenitor is allowed to evolve into a red supergiant (i.e., a single progenitor or case B_l, C_l, or D for a binary system). Within this framework, isolated, fast-moving pulsars are likely to have come from single progenitors or wide binaries that were disrupted by the SN explosion. Also, by our hypothesis, the NSs born in LMXBs would receive kicks drawn from a conventional distribution, since their standard formation channel involves a common-envelope phase in the case B_l or C_l scenario (e.g., Bhattacharya & van den Heuvel 1991; Kalogera & Webbink 1998).

The orbits of the observed short-period HMXBs have been affected by tidal interactions (see § 4.3), and so tell us very little about the NS kick. HMXBs with orbital parameters of $P_{\rm orb} \sim 20$–100 d and $e \sim 0.3$–0.5, in addition to the long-period binary radio pulsars are somewhat difficult to interpret individually, since they are consistent a priori with being the products of either stable or dynamically unstable mass transfer. If these binaries have experienced a dynamical spiral-in, then their survival (as opposed to merger) essentially requires that the mass transfer was case B_l or C_l (see § 2.3), and we suggest that the NSs received the conventional large kicks. If the mass transfer was stable (case B_e or C_e), then a significant eccentricity is still possible as long as the magnitude of the kick is an appreciable fraction of the pre-SN orbital speed. This point is important, and it is worthwhile to discuss a particular example.

Consider the very long-period, highly eccentric binary pulsar PSR B1259–63 with $P_{\rm orb} = 1236.72$ d and $e = 0.87$. The orbital separation at periastron is $\sim 140\ R_\odot$, for an assumed mass of $10\ M_\odot$ for the secondary. This is the smallest circular pre-SN orbit that is permitted (e.g., Flannery & van den Heuvel 1975), and so the largest pre-SN relative orbital speed is $v_{\rm orb} \sim 130$–170 km s^{-1}, for a reasonable range in pre-collapse core masses. If the fractional mass lost in the SN explosion is small, then a post-SN eccentricity of order unity is possible for a kick speed that is $\sim 40\%$ of the orbital speed, or ~ 70 km s^{-1} for PSR B1259–63 (e.g., Brandt & Podsiadlowki 1995); in an absolute sense, this is not a very large kick.

We have redone our population synthesis calculation with the following simple modification. If the mass transfer is case B_e or C_e, the NS kick is chosen from a Maxwellian distribution with $\sigma = 20$ km s^{-1}, a small but otherwise arbitrary value. On the other hand, if the mass transfer begins while the primary is a red supergiant (case B_l or C_l), or there is no mass transfer (case D), we adopt a more conventional kick distribution, with $\sigma = 200$ km s^{-1}. Rather than applying the same kick distribution to *all* case B_e and C_e systems, we could have focused our attention on only the stable case B_e and C_e systems,

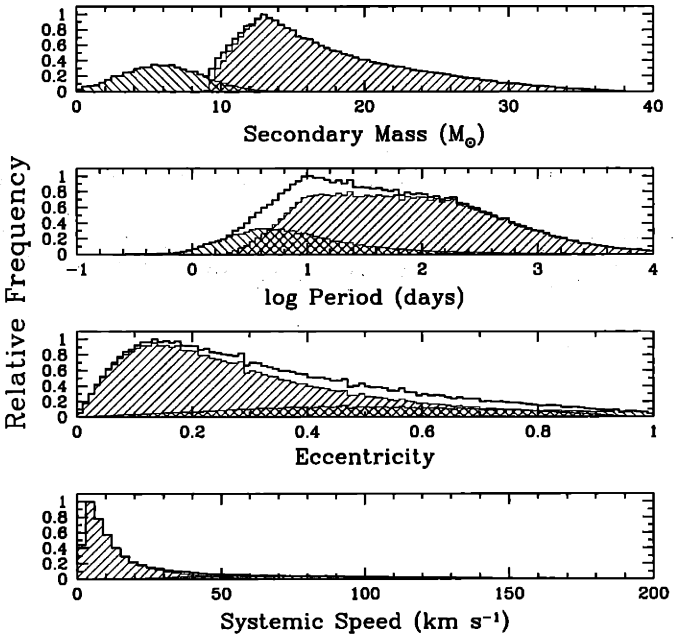

Figure 4-4: Same as Fig. 4-2, but with $\sigma = 20$ km s^{-1} applied to the NSs born in all case B_e and C_e binaries, and $\sigma = 200$ km s^{-1} was applied to all other NSs. Note that the eccentricity distribution for the stable systems has a distinct peak at $e \sim 0.15$.

since these are the alleged progenitors of the new class of HMXBs. However, our choice of treating all case B_e and C_e binaries on an equal footing is partly motivated by a theoretical model, which we discuss in the next section.

Figures 4-4 and 4-5 should be compared to Figs. 4-2 and 4-3, respectively. Many more systems with long periods and low eccentricities are produced when $\sigma = 20$ km s^{-1} is adopted for the case B_e and C_e systems. This simulation yields $F_0 \sim 2.6 \times 10^{-2}$ and a present Galactic population of $\lesssim 2600$ wide, low-eccentricity HMXBs, a factor of 65 more than in the case where $\sigma = 200$ km s^{-1} is applied to all NSs. For $F_{\rm dis} = 10^{-3}$, we see that $N_{\rm dis} \sim 3$, which is completely consistent with the 6 observed systems.

We have also calculated the production efficiency for systems that may evolve to resemble the HMXBs with moderate-to-long periods and significant eccentricities (triangles in Figs. 4-3 and 4-5), as well as for systems similar to the massive, long-period, highly eccentric, binary radio pulsars (squares in Figs. 4-3 and 4-5). In our code, we simply defined the eccentric HMXBs by the parameter ranges of $P_{\rm orb} = 20$–100 d and $e = 0.3$–0.5, and the binary radio pulsars by $P_{\rm orb} = 100$ d–1000 d and $e = 0.5$–0.9. Furthermore, we define the formation efficiency as the fraction of primordial binaries that ultimately evolve into the systems of interest (analagous to the parameter F_0 for the new class of HMXBs). If we apply the conventional kick scenario, with $\sigma = 200$ km s^{-1} for all NSs, the formation efficiencies are $\sim 0.4\%$ for both the eccentric HMXBs and massive binary radio pulsars. On the other hand, in our modified kick scenario described above, the formation efficiencies are $\sim 1.5\%$ for both of classes of binaries. The increase in the number of systems is certainly substantial, but not nearly as dramatic as the increase in the number of long-period, low-eccentricity HMXBs.

4.5 A Physical Model

The simple scenario we have outlined above is purely phenomenological. If the picture is essentially correct, then we should ask: What physical process(es) may account for the dependence of the NS kick on the evolutionary history of its progenitor in a binary system? We suggest that the rotation of the collapsing core plays a crucial role in determining the magnitude of the NS kick, and that there is a natural reason to expect a possibly sharp break in the distribution of rotation rates of stellar cores exposed following mass transfer.

Many young, isolated, massive stars are observed to rotate at ~ 20–50% of their breakup rates (e.g., Fukuda 1982; Howarth et al. 1997). For a main-sequence star of mass 10 $M_\odot$, the breakup angular frequency is $\Omega_b \sim 10^{-4}$ rad s^{-1}. If the stellar core initially has the same angular velocity, and the core retains a constant angular momentum as it evolves, then the NS that is produced is expected to rotate close to its breakup rate (i.e., with a period of $\lesssim 1$ ms). However, the question of exactly how such rapid rotation on the main sequence translates to the rotation of the pre-collapse iron core, immediately prior to NS formation, is difficult to answer, owing to the large number and complexity of hydrodynamical and magnetohydrodynamical angular momentum transport processes. Heger, Langer, & Woosley (2000; hereafter, HLW) have conducted the most sophisticated and detailed study to-date of isolated, rotating, massive stars, which included treatments of various hydrodynamical

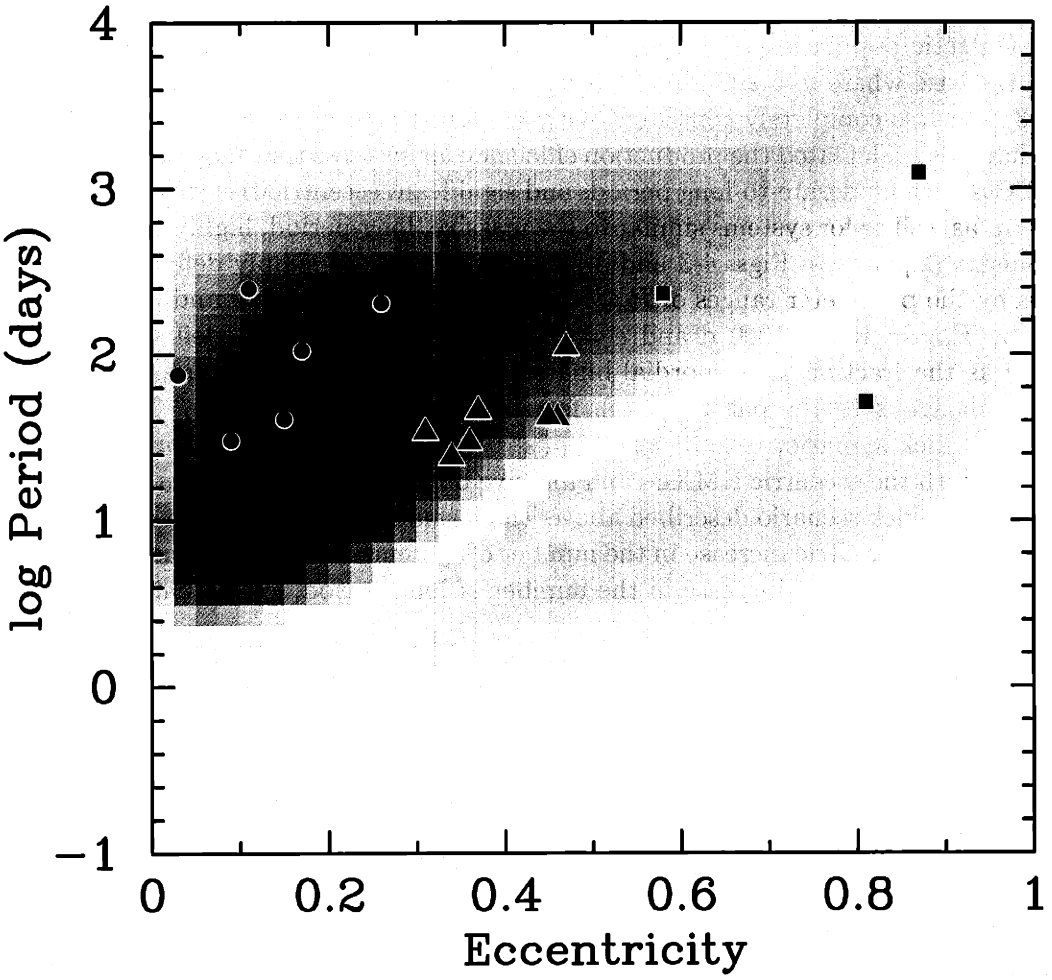

Figure 4-5: Distribution of orbital period and eccentricity for the systems in Fig. 4-4 with secondary masses $> 8\ M_\odot$. A value of $\sigma = 20$ km s^{-1} applied to the NSs born in all case B_e and C_e binaries, and $\sigma = 200$ km s^{-1} applied to all other NSs. The colors, intensities, and symbols have the same meaning as in 4-3. (If this figure does not appear in color, see astro-ph/0109521.)

instabilities, but *neglected the influence of magnetic fields.* Interestingly, they found that the angular momentum of the pre-collapse core was quite insensitive to the initial rotation rate of the star, and that the nascent NS remnant would perhaps spin at close to its breakup rate, although their simulations could not follow the evolution beyond the start of core collapse.

In the binary systems we are considering, the first phase of mass transfer is expected to strip the hydrogen-rich envelope from the primary (see § 2.4), thus exposing its core. The results of HLW suggest that this core will be a fairly rapid rotator if the primary was initially rapidly rotating. Furthermore, the results of HLW indicate that the angular momentum of the exposed core should not depend strongly on the evolutionary state of the primary at the onset of mass transfer, if only hydrodynamical angular momentum transport processes are considered. However, magnetic fields may introduce just such a dependence.

In the presence of differential rotation, an initially poloidal magnetic field will be wound up into a predominantly azimuthal field, where the magnitude of the azimuthal component is proportional to the number of differential turns (for a review of this and related magnetohydrodynamic processes in stars, see Spruit 1999). If this generation and amplification of the magnetic field occurs between the surface of the convective core and the outlying stellar envelope of a massive star, then the resulting magnetic torque will cause the core to spin down. The torque is transmitted by the r-ϕ component, $B_r B_\phi/4\pi$, of the Maxwell stress tensor. Suppose that the core of mass M_c is initially rotating with an angular velocity, Ω_c, and that the stellar envelope is nonrotating. The timescale for the core to spin down, τ_s, is approximately (see Spruit 1998)

$$\tau_s \sim \frac{I_c \Omega_c}{r_c^3 \bar{B}^2} \sim 10 \text{ Gyr} \left(\frac{k}{0.1}\right) \left(\frac{M_c}{M_\odot}\right) \left(\frac{\Omega_c}{10^{-4}\,\text{s}^{-1}}\right) \left(\frac{\bar{B}}{1\,\text{G}}\right)^{-2}, \tag{4.4}$$

where $I_c = k M_c R_c^2$ is the moment of inertia of the core and $\bar{B} = (B_r B_\phi)^{1/2}$. The geometric mean field, $\bar{B}$, appearing in eq. (4.4) increases with time due to the winding-up of the B_r component. The 1-G field used for scaling in eq. (4.4) is quite small as compared with field strengths that can, in principle, be reached as a result of the amplification process. It is thus possible for the coupling timescale, τ_s, to be shorter than the evolutionary timescale of the star.

Immediately following the depletion of hydrogen in the core, a massive star expands to giant dimensions on a thermal timescale ($\sim 10^4$–10^5 yr). Significant differential rotation between the core and the envelope will only be established after the star crosses the Hertzsprung gap and develops a deep convective envelope. It is thus reasonable to suggest that magnetic torques should *not* be very effective in spinning down the core during this short-lived evolutionary phase, and that a helium star should still be rapidly rotating if it is uncovered following case B_e or C_e mass transfer.

If mass transfer takes place at a later stage of evolution (i.e., during the first giant branch or asymptotic giant branch), the stellar core may rotate millions of times with respect to the very slowly rotating convective envelope. One might take the view (Spruit & Phinney 1998)

that under these circumstances there is sufficient time for a strong toroidal magnetic field to build up. The consequence of this would be that the cores of evolved stars would approach corotation with their envelopes, and their angular momentum would then be so small that the NSs formed will have spin periods of hundreds of seconds. This is problematic, since the spin periods of observed young NS are tens of milliseconds in several cases (e.g., the Crab pulsar has a period of 33 ms). Spruit & Phinney (1998) resolved this dilemma by attributing the current, short spin periods to off-center kicks, which give both rotational and translational impluses.

In reality, the magnitude of the geometric mean field $\bar{B}$ that can actually be obtained in a differentially rotating star is not just a matter of the simple winding-up of field lines. The approximately azimuthal fields that develop from differential rotation are known to be prone to instabilities (Tayler 1973; Acheson 1978). These instabilities may limit the attainable field strengths (for a discussion, see Spruit 1999). On the other hand, the unstable fluid displacements would create new poloidal field components which in turn would be wound up to generate more azimuthal field. It is thus possible that an unstable azimuthal field will develop into a *dynamo process* operating on the differential rotation. In Spruit (2002), an estimate is developed for the behavior of such a dynamo process and the $\bar{B}$ it produces. Preliminary calculations of the evolution of rotating stars that incorporate this formalism (Heger, Woosley, & Spruit, in preparation) indicate that the coupling between cores and envelopes could be less efficient than assumed in Spruit & Phinney (1998).

Based upon the physical arguments presented above, and the phenomenological picture discussed in § 4.4, we suggest that rapidly rotating stellar cores exposed following stable case B_e or C_e mass transfer produce NSs with small natal kicks, while NSs formed at a later stage of evolution (case B_l, C_l, or D), where the pre-collapse cores may be spinning quite slowly, receive the conventional large kicks. The collapse of a rapidly rotating core is certainly more dynamically complex than the collapse of a core that is initially nonrotating. However, it is not obvious a priori whether a rapidly or slowly spinning pre-collapse core should ultimately yield a larger average natal kick to the NS, since the physical mechanisms that may be responsible for the kick are poorly understood. One possibility is that rapid rotation has the effect of averaging out the asymmetries that give rise to large NS kicks (Spruit & Phinney 1998).

4.6 Further Implications of the Model

4.6.1 Neutron Star Retention in Globular Clusters

It is apparent that globular clusters must contain appreciable numbers of NSs. For example, 22 millisecond radio pulsars have been detected in the massive globular cluster 47 Tuc, and many more are thought to be present (Camilo et al. 2000; see also Chap. 5 and references therein). This abundance of NSs raises an interesting question. If NSs are born with speeds that are typically in excess of 100–200 km s^{-1}, how is it that even a very dense globular cluster, with a central escape speed of $\sim$ 50 km s^{-1}, can retain so many? A conventional

Maxwellian kick distribution, with $\sigma = 200$ km s^{-1} applied to all NSs, predicts that only $\sim 0.4\%$ of NSs are born with speeds < 50 km s^{-1}, and $\sim 3\%$ with speeds < 100 km s^{-1}. In Chap. 5, we consider the influence of massive binary systems on the NS retention fraction. Our standard-model calculation shows that $\lesssim 5\%$ of NSs born in binary systems can be retained in a typical cluster.

This long-standing *retention problem* is clearly alleviated if there exists a population of NSs that are born with kick speeds $\lesssim 50$ km s^{-1}, which is seemingly at odds with the large speeds inferred for isolated pulsars in the Galactic disk. The scenario that we have proposed in § 4.4 to account for the long orbital periods and low eccentricities of the HMXBs listed in Table 4.1 is not in conflict with the speeds of the isolated pulsars, by construction. Our hypothesis is that low-kick NSs are preferentially born in certain binary systems, and thus these NSs are much more likely to remain bound to their companions following the SN. If the secondary is massive, possibly as a result of accretion, the effect of the impulsive kick on a bound post-SN binary is diluted considerably, thereby allowing the binary to be retained in the cluster. The simulations in Chap. 5 indicate that the NS retention fraction may be increased by more than a factor of four (to $\gtrsim 20\%$) if we adopt the phenomenological picture outlined in § 4.4.

4.6.2 Formation of Double Neutron Star Binaries

A double NS (DNS) — a binary comprised of two NSs — seems like an improbable object; however, five proposed DNSs have been detected in the Galaxy. In all cases, only one of the components of the DNS is detected as a radio pulsar, and the other component is inferred to be a NS based on high-precision timing measurements and their interpretation in the framework of general relativity. The DNS in the globular cluster M15, PSR 2127+11C, probably formed dynamically (e.g., Phinney & Sigurdsson 1991), rather than from a massive primordial binary. The present discussion is restricted to the formation of DNSs in the Galactic disk, where the dynamical formation of binaries does not occur with any significant probability.

In § 2.6, we very briefly described the standard formation scenario for DNSs in the Galactic disk (see, e.g., Bhattacharya & van den Heuvel 1991 for a more detailed discussion). We stated that the envelope of the secondary can only be successfully ejected by the first-formed NS if the orbit is sufficiently wide ($P_{\rm orb} \gtrsim 100$ d; case B_l or C_l) at the time the secondary fills its Roche lobe. Therefore, the episode of mass transfer before the first SN must have been stable for the majority of binaries that ultimately evolve into DNSs in order to accomodate a red supergiant secondary. Our phenomenological picture for the formation of wide, low-eccentricity HMXBs involves relatively low kick speeds applied to NSs born in binary systems that have undergone case B_e or C_e mass transfer. For about half of the case B_e and C_e binaries (for $q_c = 0.5$; see § 2.3) the mass transfer is stable. Thus, our model may result in a dramatically increased formation efficiency for DNS progenitors, since many more wide binaries remain bound following the first SN than if the conventional large kicks are applied to all NSs.

We investigated the formation of DNSs with the following straightforward extensions to our population synthesis code. If the binary survives the first episode of mass transfer and the first SN without merging and without being disrupted, then we consider the eccentric post-SN orbit of the first-formed NS and the secondary. We suppose that once the secondary evolves to fill its Roche lobe, the orbit quickly circularizes. Because of the extreme mass ratio, the subsequent phase of mass transfer is guaranteed to be dynamically unstable, and the orbital separation following the spiral-in is computed using eq. (2.11). If the new separation indicates that the radius of the hydrogen-exhausted core of the secondary exceeds its Roche lobe radius, then we assume a coalescence is the result. Finally, the new orbital parameters are computed following the SN explosion of the secondary's core.

It is interesting to note that, for the preferred progenitors of DNSs, the first episode of mass transfer is stable (case B_e or C_e mass transfer), in which case the the secondary accretes a considerable amount of mass and angular momentum and first-formed NS most likely receives a small kick by hypothesis (see § 4.4). As a result, the secondaries in these systems should be rotating rapidly following mass transfer. This seems to be borne out by observations of HMXBs, where many systems contain a Be optical counterpart; the Be phenomenon is likely a consequence of rapid rotation (e.g., Slettebak 1988). Given that stable mass transfer produces massive, rapidly rotating secondaries, we apply a kick to the second NS in precisely the same way as for the first, with a value of σ that depends on the evolutionary state of the secondary when it fills its Roche lobe. The value of σ in this case turns out *not* to be very important, however, since the mass loss from the exploding core of the secondary typically has a more disruptive influence on the orbit than the kick.

As a point of reference, we applied the more-or-less standard Maxwellian kick distribution, with $\sigma = 200$ km s^{-1}, to all NSs, both first- and second-formed. We find that the fraction of massive primordial binaries that successfully evolve into DNSs is $\sim 10^{-3}$. For a core-collapse SN rate of 10^{-2} yr^{-1}, this fraction corresponds to an approximate DNS birthrate of $\sim 10^{-5}$ yr^{-1}, consistent with other recent theoretical calculations that used similar methods and assumptions (e.g., Lipunov et al. 1997; Portegies Zwart & Yungelson 1998).

If, by contrast with the above calculation, we assume that NSs born following case B_e or C_e mass transfer receive kicks drawn from a Maxwellian with $\sigma = 20$ km s^{-1}, we find that the DNS birthrate is increased by roughly a factor of twenty, to $\sim 2 \times 10^{-4}$ yr^{-1}, which is high, but not alarmingly so. This order-of-magnitude increase is almost entirely accounted for by the increase in the number of viable DNS progenitors — systems where the common-envelope is successfully ejected during the dynamical mass transfer episode from the secondary to the first-formed NS.

4.7 Summary

Using a combination of observational and theoretical arguments, we have considered the significance of a new observed class of HMXBs, with orbits that are distinguished by relatively long periods ($P_{\rm orb} \sim 30$–250 d) and low eccentricities ($e \lesssim 0.2$). Our analysis indicates that

the conventional wisdom regarding NS kicks does not adequately account for the number of these systems known at present, which comprise roughly 30% of HMXBs with measured orbital parameters. Members of this new class of HMXBs contain NSs that almost certainly received a fairly small kick ($\lesssim 50$ km s^{-1}) at the time of formation. The prevalence of such low-kick NSs is simply incompatible with the large mean natal kick speeds ($\gtrsim 200$–300 km s^{-1}) inferred for isolated radio pulsars in the Galaxy. However, we have developed a phenomenological model that simultaneously accounts for the long-period, low-eccentricity HMXBs and which does not violate any previous notions regarding the numbers and kinematics of other NS populations (i.e., radio pulsars, LMXBs, and other HMXBs).

Specifically, we propose that a NS receives a relatively small kick if its progenitor star experienced case B_e or C_e mass transfer in a binary system. In operational terms, we utilized a Maxwellian distribution in kick speeds, but with a somewhat arbitrarily selected low value of $\sigma = 20$ km s^{-1} applied to NSs born in case B_e or C_e binaries, and for all other NSs (case B_l, C_l, or D binaries, as well as isolated progenitors) we adopted a much higher value of $\sigma = 200$ km s^{-1}. This scenario results in sufficient numbers for the new class of HMXBs, and, by construction, is consistent with the numbers and properties of other NS populations in the Galaxy.

If this phenomenological picture is basically correct, then there must be some physical explanation for why the magnitude of the kick depends on the evolutionary history of the NS progenitor. We suggest that the rotation of the pre-collapse core of a massive star introduces just such a dependence. If the hydrogen-exhausted core of an initially rapidly rotating massive star is exposed following case B_e or C_e mass transfer in a binary, then the core is also likely to be a rapid rotator. On the other hand, if the NS progenitor is allowed to evolve into a red supergiant (case B_l, C_l, D, or a single star), then significant magnetic torques, amplified by the strong differential rotation between the core and the deep convective envelope (Spruit & Phinney 1998; Spruit 1999), may cause the core to spin down dramatically. Thus, for whatever reason, the dynamics of core collapse may be such that low kick speeds result for rapidly rotating pre-collapse cores, and cores that are spinning slowly preferentially yield the conventional large kick speeds.

Our model to explain the new class of HMXBs requires that a significant fraction of all NSs born in binary systems receive only a small recoil speed following core collapse and the SN explosion. This simple requirement has important implications for at least two very different problems. First, the problem of retaining NSs in globular clusters is alleviated if not solved if our hypothesis is correct. Second, our scenario predicts an order of magnitude larger birthrate of double NS binaries than if the conventional kick distributions are applied.

Chapter 5

Neutron-Star Retention in Globular Clusters

This chapter is adapted from the paper, "A Comprehensive Study of Neutron-Star Retention in Globular Clusters," by Eric Pfahl, Saul Rappaport, & Philipp Podsiadlowski, to appear in *The Astrophysical Journal.*

5.1 Neutron-Star Kicks and the Retention Problem

A growing body of observational and theoretical evidence suggests that some massive globular clusters may contain more than ~ 1000 neutron stars (NSs). However, the presence of even as few as ~ 100 NSs is difficult to reconcile with the large NS "kicks" inferred from proper motion studies of single, young radio pulsars in the Galactic disk. The problem is that globular clusters presently have central escape speeds $\lesssim 50$ km s^{-1}, while it is widely thought that most NSs are born with speeds $\gtrsim 200$ km s^{-1}. This is the essence of the NS *retention problem* in globular clusters.

If one accepts the conventional wisdom regarding NS kicks, then only a very small fraction of NSs that are remnants of isolated progenitors should be retained in a globular cluster. Hansen & Phinney (1997) found that a Maxwellian distribution in kick speeds, with a mean of ~ 300 km s^{-1}, is consistent with data on pulsar proper motions. This distribution predicts that only $\sim 0.4\%$ of NSs are born with speeds < 50 km s^{-1}, and $\sim 3\%$ with speeds < 100 km s^{-1}. If one adopts an initial mass function derived from stars in the solar neighborhood (e.g., Kroupa et al. 1993), it can be shown that $\lesssim 5000$ NSs will be formed in a cluster that initially contains 10^6 stars. A retention probability of 1% predicts that $\lesssim 50$ NSs should be present in a massive globular cluster such as 47 Tuc, where we have assumed that the cluster has not lost a significant fraction of its mass. Such a small number of NSs in 47 Tuc is incompatible with the observational sample of more than 20 millisecond radio pulsars (Camilo et al. 2000) when selection effects are taken into account.

Using the NS kick distribution determined by Lyne & Lorimer (1994), in which they estimated the mean kick speed to be ~ 450 km s^{-1}, Drukier (1996) calculated that $< 1\%$

of NSs with *single* progenitors would be retained in a typical globular cluster. However, if a NS is formed with a massive *binary* companion, then there is a significant probability that the NS will remain bound to its companion following the supernova (SN) explosion, and that the recoil speed of the system could be sufficiently small to allow it to be retained in the cluster. Applying the results of Brandt & Podsiadlowski (1995), Drukier (1996) demonstrated quantitatively that the retained fraction of NSs born in binary systems may be several times larger than for the case of single stars. Davies & Hansen (1998) also emphasized the importance of binaries for retaining NSs. While these studies provide a useful verification of the potential importance of massive binaries, they did not involve a systematic population study to determine a quantitatively realistic NS retention fraction.

Our primary goal in this paper is to make a detailed quantitative assessment of the role of massive binaries in retaining NSs in globular clusters. This calls for a realistic description of the population of primordial binaries, as well as a sufficiently detailed consideration of the relevant stellar evolution processes that precede the first SN explosion. To this end, we have developed a Monte Carlo population synthesis code that follows each of an ensemble of massive, primordial binaries from the main-sequence phase, through any important episodes of mass transfer, up to and immediately beyond the time of the first SN.

We estimate a maximum NS retention fraction for a given cluster by applying the same nominal *central* escape speed to all stars and binaries. A more realistic calculation of the cluster structure (e.g., the Fokker-Planck method used by Drukier 1996) will generally yield a smaller retention fraction when the mean NS kick speed is large. With this highly simplified, yet entirely adequate, treatment of the model globular clusters, we are able to focus our attention on the stellar evolution issues relevant to the retention problem.

5.2 Neutron Stars in Globular Clusters

Several tens of millisecond pulsars (MSPs), a dozen bright X-ray sources, and numerous low-luminosity X-ray sources have been detected in the Galactic globular cluster system. See Table 5.1 for a list of clusters that may contain large numbers of NSs. The nature of the pulsars is clear: these are rapidly spinning NSs, many of which have binary companions. The luminous cluster X-ray sources are all low-mass X-ray binaries (LMXBs) powered by accretion onto a NS. An accepted familial relationship exists between LMXBs and the majority of MSPs, the former being the evolutionary progenitors of the latter. Recent observations (Grindlay et al. 2001b) provide tantalizing evidence that many of the low-luminosity X-ray sources may be MSPs for which radio pulsations have not yet been detected (see, however, Pfahl & Rappaport 2001).

More refined pulsar searches, deeper X-ray observations, and thorough theoretical population studies will advance our understanding of the cluster populations of NSs, and in turn may provide powerful new insights into the formation and evolution of globular clusters. We now briefly review what is known and what is speculated regarding NSs in globular clusters.

Table 5.1. Neutron Stars in Globular Clusters

Cluster	Luminous[a] X-ray Sources	Low-luminosity[b] X-ray Sources	Radio Pulsars	Distance[c] (kpc)	[Fe/H][c]	$\log \rho_0$[c] ($M_\odot$ pc^{-3})
Liller 1	1	0	0	10.5	0.22	5.9
NGC 104/47 Tuc	0	108[d]	>20[e]	4.5	-0.76	5.3
NGC 1851	1	0	0	12.1	-1.22	5.8
NGC 5904/M5	0	9	2[f]	7.5	-1.29	4.4
NGC 6205/M13	0	12	2[g]	7.7	-1.54	3.8
NGC 6397	0	20[h]	1[i]	2.3	-1.95	6.2
NGC 6440	1	24[j]	1[k]	8.4	-0.34	5.8
NGC 6441	1	0	1[l]	11.2	-0.53	5.7
NGC 6624	1	0	2[m]	8.0	-0.42	5.7
NGC 6652	1	0	0	9.6	-0.96	5.0
NGC 6712	1	0	0	6.9	-1.01	3.6
NGC 6752	0	19[n]	5[l]	4.0	-1.56	5.4
NGC 7078/M15	2[o]	0	8[g]	10.3	-2.25	5.9
Terzan 1	1	0	0	6.2	-0.35	4.0
Terzan 2	1	0	0	8.7	-0.40	5.1
Terzan 5	1	0	2[p]	7.6	-0.28	5.9
Terzan 6	1	0	0	9.5	-0.50	5.9

References. — (a) Deutsch, Margon, & Anderson 2000, unless otherwise noted; (b) Verbunt 2001, unless otherwise noted; (c) Harris 1996; (d) Grindlay et al. 2001a; (e) Camilo et al. 2000; (f) Anderson et al. 1997; (g) Anderson 1993; (h) Grindlay et al. 2001b; (i) D'Amico et al. 2001b; (j) Pooley et al. 2001b; (k) Lyne, Manchester, & D'Amico 1996; (l) Possenti et al. 2001; (m) Biggs et al. 1994; (n) Pooley et al. 2001a; (o) White & Angelini 2001; (p) Lyne et al. 2000

5.2.1 Millisecond Radio Pulsars

The last several years have seen a dramatic increase in the number of known single and binary MSPs in globular clusters. The vast majority of these new pulsars have been detected with the Parkes radio telescope (see Camilo et al. 2000; D'Amico et al. 2001b). Most notable among these discoveries is the doubling of the known MSP population in 47 Tuc, bringing the current total to over 20 (Camilo et al. 2000; see also Freire et al. 2000). With a cursory analysis of the selection effects and a reasonable pulsar luminosity function, Camilo et al. (2000) estimated that 47 Tuc may contain ~ 200 potentially observable MSPs, and therefore the total number of NSs in 47 Tuc is expected to be even larger. It seems likely that other clusters, with properties similar to those of 47 Tuc, have comparable numbers of MSPs.

5.2.2 LMXBs

Many of the members of the well-known class of bright X-ray sources in globular clusters, with X-ray luminosities $L_{\rm X} \sim 10^{36}$–10^{38} ergs s^{-1} (see Deutsch et al. 2000 and references therein), exhibit type I X-ray bursts (Lewin et al. 1993) and are therefore accreting NSs in binary systems. Each of these objects resides in a different globular cluster (Table 5.1). While this sample of X-ray binaries does not constitute a large number of NSs in itself, the existence and properties of these systems may have important implications regarding the evolution of the NS population in their respective host clusters (see § 5.2.4 below).

5.2.3 Low-Luminosity X-ray Sources

Not as well known, and certainly not as well understood, is the class of low-luminosity cluster X-ray sources (e.g., Johnston & Verbunt 1996; Verbunt 2001), with $L_{\rm X} \sim 10^{31}$–10^{34} ergs s^{-1}, where the lower limit is set by detection sensitivities. Prior to the launch of the *Chandra X-ray Observatory*, fewer than 50 of these faint sources had been discovered in the entire Galactic globular cluster system (see Verbunt 2001 for a recent analysis of the *ROSAT* database), primarily with the *ROSAT* and *Einstein* satellites. However, recent deep *Chandra* observations of 47 Tuc have revealed $\gtrsim 100$ faint sources in this cluster alone (Grindlay et al. 2001b), whereas only 9 had been confirmed previously (Verbunt & Hasinger 1998). There is compelling evidence that the majority of the faint X-ray sources in 47 Tuc may be NSs, perhaps MSPs that have not yet been detected at radio wavelengths. All of the 15 MSPs in 47 Tuc with well-measured radio timing positions (Freire et al. 2000) have counterparts in the *Chandra* images (Grindlay et al. 2001b).

5.2.4 Theoretical Considerations for Neutron-Star Binary Formation

Variations in the number of detected radio pulsars and X-ray sources from cluster to cluster may be attributed to the distances of the clusters, selection effects inherent in the observations, as well as differences between the intrinsic NS populations. Predictions of the total number of potentially observable NSs — in the form of MSPs or accretion-powered

X-ray sources — present in a globular cluster are difficult. Empirical likelihood estimates based on the observational sample are hindered by small-number statistics and uncertainties regarding selection effects. Theoretical studies aimed at accounting for the numbers and properties of the detected pulsars involve models that utilize various uncertain stellar evolution and dynamical processes.

Large-scale population studies of the formation and evolution of X-ray binaries and MSPs in globular clusters have only recently been undertaken (see Davies 1995; Sigurdsson & Phinney 1995; Rasio et al. 2000; Rappaport et al. 2001). The dense stellar environment in a globular cluster allows for dynamical binary formation channels not accessible in the Galactic disk, such as three- and four-body exchange processes (e.g., Hills 1976; Hut et al. 1991; Sigurdsson & Phinney 1993; Bacon et al. 1996; Rasio et al. 2000), and possibly two-body tidal capture (e.g., Fabian et al. 1975; Rasio & Shapiro 1991; Di Stefano & Rappaport 1992). The absolute probabilities of dynamical encounters depend on the local stellar environment and thus implicitly on the dynamical evolution of the cluster. This nonlinear linkage between *local* dynamical processes and the *global* cluster evolution poses significant computational problems, but the potential rewards are far-reaching. Such population studies promise to be a powerful tool that relates the current NS population to the formation and evolution of globular clusters.

Preliminary calculations (Rasio et al. 2000; Rappaport et al. 2001) indicate that a large initial pool of single NSs ($\sim 10^4$) may be required to explain the handful of very short-period binary radio pulsars in 47 Tuc; i.e., the formation efficiency is quite low. Short-period binary MSPs and LMXBs in other clusters may be good indicators of an initially large number of NSs in those clusters as well. The purpose of the present paper is to investigate the conditions that favor the retention of such a large NS population.

5.3 Semi-Analytic Study of Neutron-Star Retention

We now present a semi-analytic population study of massive binaries and NS formation that involves the use of *characteristic* binary component masses and orbital separations, rather than the full distributions of binary parameters. With this more simplistic approach, we are able to clearly discern how different assumptions influence the net NS retention fraction, and highlight the most profitable binary channels for retaining NSs in globular clusters. The method of calculation described in this section is in the same spirit as the preliminary estimates by Drukier (1996) of the retained fraction of NSs born in binary systems. With such approximate techniques, the estimated retention fractions may vary by factors of ~ 2–3 depending on the very subjective choice of characteristic masses. The use of a complete binary population synthesis calculation (see § 5.4) is necessary, since it eliminates much of this subjectivity, and the uncertainty in the retention fraction then reflects mainly the uncertainties in binary formation and evolution. We begin our semi-analytic study by providing some reasonably quantitative characterizations of the population of primordial binaries and the effects of mass transfer.

We recall from Chap. 2 that cases A, B, C, and D comprise roughly 5%, 25%, 25%,

and 45%, respectively, of the primordial binary population. The 25% of case B systems are divided into $\sim$ 20% case B_e and $\sim$ 5% case B_l. Likewise, case C is comprised of $\sim$ 15% case C_e and $\sim$ 10% case C_l. Depending on various assumptions, these percentages are found to increase or decrease by at most one-half of the values given above. It is expected that $\sim$ 35% of the primordial binaries evolve according to the case B_e or C_e scenario; this has important implications for the retention problem.

Stable and quasi-conservative mass transfer, which is expected in a significant fraction of the case B_e and case C_e systems (depending on the value of q_c), has two notable consequences: (i) the secondary accretes much of the hydrogen-rich envelope of the primary, and (ii) the final orbital separation is typically within a factor of a few of the initial separation (see Fig. 2-3). The increased mass of the secondary provides a deeper gravitational potential well for the hydrogen-exhausted core of the primary, which raises the likelihood that the orbit will remain bound following the SN and hence that the NS will be retained in the cluster. The modest change in orbital separation during stable mass transfer is in sharp contrast to the dramatic shrinkage that accompanies CE evolution (see Fig. 2-4). For the case of small natal NS kicks, there is a clear dynamical distinction between stable and unstable mass transfer with regard to the subsequent SN explosion. As a general rule, a NS kick can be considered "small" if it is appreciably less than the relative orbital speed of the components (see Brandt & Podsiadlowski 1995).

First, consider the case of circular pre-SN orbits and *vanishing kicks*. If the binary is intact after the SN, retention in the cluster is determined by the new center-of-mass speed, $v'_{\rm CM}$ (e.g., Blaauw 1961; Dewey & Cordes 1987):

$$v'_{\rm CM} = \frac{\Delta M_1}{M_b - \Delta M_1} v_1 \ , \tag{5.1}$$

where ΔM_1 is the mass lost in the explosion (envelope of the primary) and v_1 is the pre-SN orbital speed of the primary (hydrogen-exhausted stellar core) about the CM. The mass M_b and the orbital speed v_1 used above correspond to the conditions immediately before the explosion. The factor that multiplies v_1 can be identified as the post-SN orbital eccentricity, e', which gives the memorable result, $v'_{\rm CM} = e' v_1$. Disruption of the binary must occur if the mass lost in the explosion is more than one-half of the initial systemic mass. In this case it can be shown that the speed at infinity of the liberated NS is simply equal to v_1. Therefore, regardless of whether or not the binary is unbound following the SN, the relevant speed that determines if the NS is retained in a globular cluster is proportional to the pre-SN orbital speed of the primary.

These arguments are made more quantitative by considering a prototypical binary with a range of initial separations. Suppose this model primordial binary consists of a 10 $M_\odot$ primary and a 6 $M_\odot$ secondary. A typical initial orbital separation for case B_e systems is $\sim$ 0.5 AU. Immediately after a phase of stable mass transfer, the binary will consist of the $\sim$ 2.2 $M_\odot$ core of the primary and the $\sim$ 10–14 $M_\odot$ secondary, for $\beta \gtrsim 0.6$. The binary separation at this point is likely to be in the range $\sim$ 0.2–1.5 AU (see Fig. 2-3), in which case the core has an orbital speed of $\lesssim$ 200 km s^{-1}. A spherically symmetric SN will leave

the system bound, with $e' \sim 0.06$ and $v'_{\rm CM} \lesssim 15$ km s^{-1}. There is then a good chance that such a binary would be retained in a globular cluster. For the case of CE systems that avoid a merger (most case B_l and C_l binaries), a typical initial separation is ~ 5 AU. Following the expulsion of the CE, the essentially unaltered secondary orbits the core of the primary with a separation of $\lesssim 0.05$ AU (assuming hundred-fold decrease; see Fig. 2-4), giving the core an orbital speed of ~ 280 km s^{-1}. For a 6 $M_\odot$ secondary, the binary remains bound after a symmetric SN, but acquires a larger recoil speed of ~ 30 km s^{-1}. Thus, even in the case of small kicks, it is expected that a significant fraction of the post-CE binaries would be ejected from a typical globular cluster.

We now extend this discussion and allow for a distribution in NS kick speeds. The semi-analytic formalism that we employ is described in Appendix B, and the main results are displayed in Figure 5-1. Figure 5-1 is a plot of the retained percentage of *bound* NS binaries as a function of the orbital separation immediately prior to the SN, where the escape speed is taken to be $v_{\rm esc} = 50$ km s^{-1} and kick speeds are distributed as a Maxwellian with $\sigma = 200$ km s^{-1}. The results are displayed for two different secondary masses, $M_2 = 6$ and 12 $M_\odot$, which are representative values for systems that have undergone dynamically unstable mass transfer and stable mass transfer, respectively. A range of core masses, $M_c = 2$–6 $M_\odot$, is also considered.

There are a number of notable features in Fig. 5-1. First, the retention fractions are clearly larger for $M_2 = 12$ $M_\odot$ and a given core mass, as expected. Also, for a given M_2 and M_c, there is a maximum retention fraction located at some value of the initial orbital separation. The fall-off at large separations results from the high characteristic kick speed relative to the comparatively low orbital speeds; many of these systems are left unbound following the SN. At sufficiently small orbital separations, which correspond to high orbital speeds, the mean CM speed of the bound post-SN binaries exceeds the cluster escape speed, and thus accounts for the decreased retention fraction at small separations. The location and height of the peak depend on the core mass. In light of the discussion above regarding vanishing kicks, it is clear that a more massive core will result in a larger dynamical perturbation to the system at the time of the SN, simply by virtue of the increased mass loss. More mass loss results in a larger fraction of the orbital speed being transformed into CM speed for a bound post-SN binary (see eq. [5.1]), and also raises the likelihood that the system will be disrupted if the characteristic kick speed is large. The combination of these effects explains the trends in Fig. 5-1, namely that, for a larger core mass, the height of the peak is reduced and its location shifts to larger separations (i.e., smaller orbital speeds).

If we know the typical pre-SN component masses and orbital separations among the systems that undergo stable or dynamically unstable mass transfer, Fig. 5-1 can be used to estimate the fraction of NSs that both remain bound to their companions following the SN and are retained in the cluster. The secondary masses used for Fig. 5-1 have already been appropriately chosen for this purpose. A typical core mass is likely to be $M_c \sim 3$ $M_\odot$. For the characteristic orbital separations, we chose 0.5 AU for the stable systems and 0.05 AU for the unstable systems (see the discussion above). Restricting ourselves to the case B and C binaries, we should expect the ratio of stable to unstable systems to be roughly 2 : 3. Now,

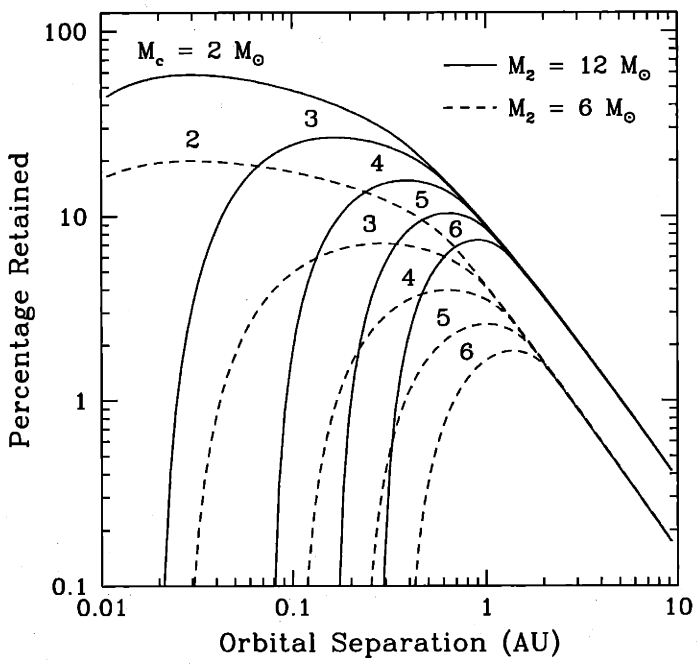

Figure 5-1: Retention probability as a function of the pre-SN orbital separation using the semianalytic formalism outlined in Appendix B. Curves are shown for secondary masses $M_2 = 12\ M_\odot$ (*solid*) and $M_2 = 6\ M_\odot$ (*dashed*) and five different masses, $M_c(M_\odot) = \{2, 3, 4, 5, 6\}$, of the primary's core prior to the supernova explosion. We have assumed an escape speed of 50 km s^{-1} and Maxwellian kicks with $\sigma = 200$ km s^{-1}.

reading numbers from Fig. 5-1, we estimate the percentage of NS binaries retained following case B or C mass transfer to be $\sim 8\%$, with $\sim 7\%$ being systems where the mass transfer was stable and the remaining $\sim 1\%$ corresponding to the unstable systems. Of course, since case B and C systems comprise only $\sim 50\%$ of the primordial binary population, the net NS retention fraction is $\sim 4\%$. This estimate is in accord with the results of the "standard model" discussed in the next section, where we calculate a net retention fraction of $\sim 5\%$ from all binary channels (that is, unweighted by the binary fraction among stars in the cluster). If we had used a characteristic pre-SN core mass of 5 $M_\odot$, as in Brandt & Podsiadlowski (1995), and our favored secondary mass of 12 $M_\odot$ to represent the systems that underwent stable mass transfer, the contributed retention fraction from the stable systems (using Fig. 5-1 with $a = 0.5$ AU) is $\sim 4\%$. If, on the other hand, we had chosen a typical secondary mass of 17 $M_\odot$ for the stable systems, as in Brandt & Podsiadlowski (1995), and our favored core mass of 3 $M_\odot$, we find that the contributed retention fraction is $\sim 12\%$. We thus see that quite a large variation in the retention fraction is possible given a modest range of "characteristic" pre-SN component masses.

5.4 Detailed Population Study

5.4.1 Computational Procedure

We have written two versions of our population synthesis code, each with same basic engine. One version applies a given distribution in kick speeds (e.g., a Maxwellian) and a single central escape speed. With this version of the code we are able to discern which individual evolutionary pathways contribute most to the net NS retention fraction, and we can assess in a very detailed manner the influence of varying certain parameters. Only $\lesssim 10^5$ primordial binaries are sufficient to obtain reliable statistics for the ~ 70 distinct evolutionary channels followed in our code.

The second version of our code is more global; here we are interested only in the net retention fraction. A large regular grid of kick speeds and escape speeds is established. We consider a range in escape speeds from 0 to 200 km s^{-1} and a range in kick speeds from 0 to 1000 km s^{-1}. At each position in the grid, an ensemble of binaries (typically 2×10^4) is generated and evolved. The output of the calculation is an array of retention fractions. It is then trivial to convolve the results with any tabulated kick distribution. For each escape speed and a given kick distribution, we compute a net NS retention fraction. Examples of these retention curves are shown in Figure 5-8. Additionally, we may also convolve the grid with a distribution of escape speeds in order to gauge the influence of a realistic cluster potential (§ 5.4.3).

5.4.2 Primary Results

We begin the discussion of our detailed population synthesis calculations by considering the Maxwellian kick distribution. Our *standard model* utilizes the Maxwellian kick distribution with $\sigma = 200$ km s^{-1} and $v_{\rm esc} = 50$ km s^{-1}, a central escape speed characteristic of present-day clusters. The parameters that describe the primordial binary population and mass transfer for the standard model are listed in Table 5.3, model 5.

Distributions of the primordial binary parameters for systems that undergo case B or C mass transfer are shown in Figure 5-2. We have not included systems that merge following mass transfer, and hence the distribution in $\log a$ is not flat over the range shown, as would be expected from eq. (2.3). Furthermore, case A binaries are not included due to the small number of systems as well as the large uncertainties regarding their evolution. Figure 5-3 illustrates the correlation between the orbital separation and secondary mass for the systems in Fig. 5-2. The binaries that undergo dynamically unstable mass transfer and avoid a merger have a low mean secondary mass ($\sim 5\ M_\odot$) and a large mean initial separation (~ 5 AU).

Figure 5-4 shows histograms of the binary parameters following mass transfer for precisely the same systems in Fig. 5-2. The distribution of secondary masses (sum of stable and unstable systems) shows a clear bimodality, with peaks around 5 and 13 $M_\odot$. This is simply a consequence of the distinction between stable and dynamically unstable mass transfer. If the mass transfer is stable, a secondary of mass $\gtrsim 4\ M_\odot$ (assuming $q_c \sim 0.5$)

Table 5.2. Branching Percentages for Maxwellian Kicks

Outcome	A	B_e	B_l	C_e	C_l	D
Total	5.40	21.51	3.11	15.03	6.69	48.27
Stable MT[a]	2.73	10.83	0.00	7.56	0.00	0.00
Unstable MT (CE[b])	2.68	10.67	3.11	7.47	6.69	0.00
Merger Following MT	3.19	10.64	2.08	5.82	0.30	0.00
$\sigma = 200$ km s^{-1}						
Unbound following SN	0.78	7.52	0.47	7.42	3.96	48.26
Bound following SN	1.43	3.34	0.56	1.78	2.44	0.01
Merger following SN	0.53	0.81	0.24	0.46	0.93	0.00
Retained single NS	0.01	0.10	0.00	0.08	0.04	0.22
Retained binary NS	0.93	2.60	0.19	0.96	0.67	0.01
Total retained	0.94	2.70	0.19	1.03	0.71	0.23
$\sigma = 100$ km s^{-1}						
Unbound following SN	0.18	4.50	0.17	5.30	2.05	48.22
Bound following SN	2.03	6.36	0.86	3.91	4.34	0.05
Merger following SN	0.33	0.56	0.19	0.38	0.92	0.00
Retained single NS	0.01	0.27	0.01	0.31	0.09	1.54
Retained binary NS	1.52	5.71	0.63	2.90	2.46	0.05
Total retained	1.53	5.98	0.64	3.21	2.55	1.60
$\sigma = 50$ km s^{-1}						
Unbound following SN	0.00	1.73	0.01	2.76	0.63	47.91
Bound following SN	2.20	9.13	1.02	6.45	5.77	0.36
Merger following SN	0.07	0.13	0.07	0.10	0.46	0.00
Retained single NS	0.00	0.31	0.00	0.55	0.08	9.90
Retained binary NS	1.69	8.49	0.94	5.35	4.41	0.36
Total retained	1.69	8.80	0.94	5.90	4.49	10.26

[a]MT $\equiv$ Mass Transfer.

[b]CE $\equiv$ Common-Envelope.

accretes a substantial amount of material, while the secondary mass is assumed to be unchanged if the system evolves through a CE phase. Therefore, the peak in the distribution of secondary masses for the stable systems is shifted to a higher value, and the distribution as a whole is broadened, thus reducing the height of the peak relative to the secondary mass distribution for the unstable systems. Also noteworthy is the broad peak in orbital separations (summed distribution) centered at ~ 0.1 AU, which results from the overlap of the stable and unstable systems.

A scatter plot of the secondary mass and orbital separation following mass transfer is shown in Figure 5-5. There is a clearly-defined boundary that marks the Roche lobe radius of the secondary for a given M_2 and M_c. Systems below this boundary have merged following mass transfer, where the majority of merged binaries result from dynamically unstable case

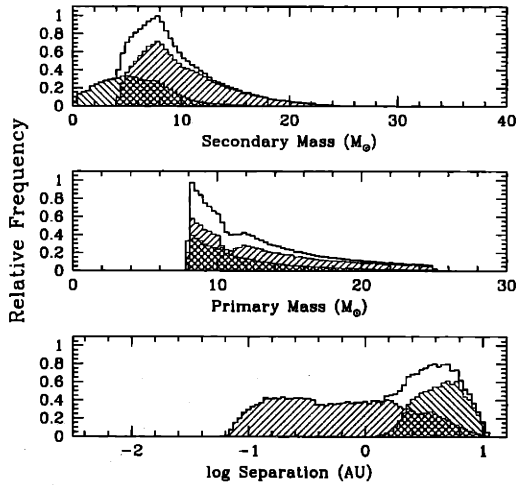

Figure 5-2: Distributions of masses and orbital separations of *primordial binaries* that undergo case B or case C mass transfer and do not merge. Hatched regions indicate systems that undergo stable mass transfer (+45°) and dynamically unstable mass transfer (−45°).

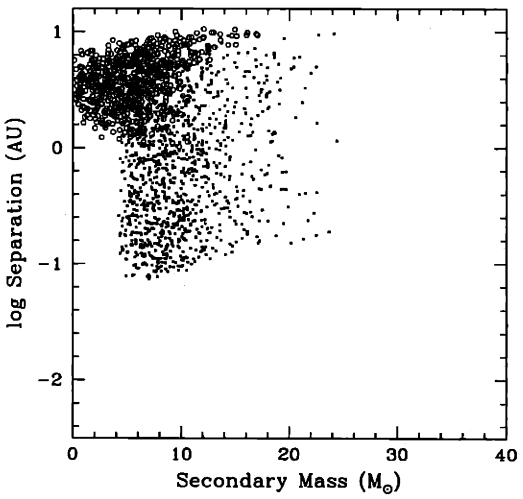

Figure 5-3: Scatter plot of circularized orbital separation versus secondary mass for the *primordial binaries* shown in Fig. 5-2. Filled and unfilled circles indicate systems that undergo stable and dynamically unstable mass transfer, respectively.

B_e and C_e mass transfer. From Table 5.2 we see that roughly one-half of the case B_e and C_e systems are expected to merge following mass transfer. This factor of one-half is a direct consequence of our somewhat arbitrary choice of $q_c = 0.5$. Nearly 50% more stable systems result if we set $q_c = 0.25$, but additional dilution factors lead to a net retention fraction that is only ~ 1.3 times as large when $v_{\rm esc} = 50$ km s^{-1} and $\sigma = 200$ km s^{-1} (see Table 5.3).

Figures 5-6 and 5-7 show distributions relevant to the bound and retained binaries immediately following the SN that underwent case B or C mass transfer (a subset of the binaries in Figs. 5-2 and 5-4). Small periastron separations ($\lesssim 1$ AU) among the retained NS binaries indicate that the secondaries in most of these systems, the majority of which have a mass $> 10\ M_\odot$, will transfer material to the NS at some stage. In fact, in some cases ($\log(a/{\rm AU}) \lesssim -1.3$) the radius of the secondary is larger than the periastron separation immediately after the SN, indicating an immediate coalescence (these points are discussed in § 5.5). Also, note that the speed distribution of the retained binaries has significant values all the way up to the standard-model escape speed of 50 km s^{-1}. A more realistic cluster potential and spatial distribution of stars may therefore result in a somewhat reduced net retention fraction, since the fastest of the binaries in Fig. 5-6 would be preferentially removed removed from the retained population (see § 5.4.3).

Table 5.2 and Figure 5-8 show the main quantitative results of our retention study. The importance of case B_e and C_e systems, which contribute a large number of bound and retained binaries (see § 5.3), is clear in Table 5.2. Figure 5-8 shows the percentage of NSs retained in a cluster as a function of the central escape speed (applied to all stars and binaries); the curves are not weighted by the binary fraction. The range in central escape speeds we consider extends to 200 km s^{-1}, since the clusters we see today may have been significantly more massive when the massive stars were present, although a central escape speed of 200 km s^{-1} may be a bit extreme unless the clusters were extremely massive — perhaps $> 10^7\ M_\odot$ (see § 5.7.4). For $\sigma = 200$ km s^{-1}, the retention fraction is $\sim 3\%$ for single stars and $\sim 10\%$ for binaries when $v_{\rm esc} = 100$ km s^{-1}. We also note that our results for single stars with $\sigma = 200$ km s^{-1} are in excellent agreement with the retention fractions calculated by Drukier (1996), who used a somewhat different kick distribution (that of Lyne & Lorimer 1994) and a much more sophisticated treatment of the cluster structure. It is evident from Table 5.2 and Fig. 5-8 that the retention problem is eliminated for $\sigma = 50$ km s^{-1}, where the retained fraction of NSs with isolated progenitors is $\sim 10\%$, roughly one-half of the binary contribution. However, such a low value of σ does not appear to be consistent with the speeds of isolated pulsars.

Finally, in order to gauge how the net retention fraction changes when the free parameters of our study are modified, we have tabulated the retention fraction for a rather comprehensive set of parameters associated with the selection of primordial binaries and the behavior of mass transfer (Table 5.3). For Table 5.3, we have fixed the escape speed at $v_{\rm esc} = 50$ km s^{-1} and we have utilized the Maxwellian kick distribution with $\sigma = 200$ km s^{-1}. The largest net retention fraction shown in Table 5.3 ($\sim 8.3\%$; model 9) is only a factor ~ 1.5 times larger than the retention fraction computed for the standard model (model 5). Thus, we can be secure that, for reasonable variations in the parameters listed in Table 5.3, the

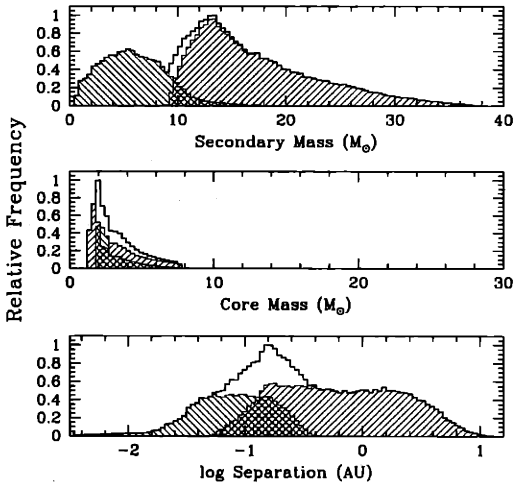

Figure 5-4: Distributions of masses and orbital parameters of systems that have undergone case B or case C mass transfer and have not merged. The hatchings have the same meaning as in Fig. 5-2. These parameters indicate the state *immediately prior to the SN* of the core of the primary.

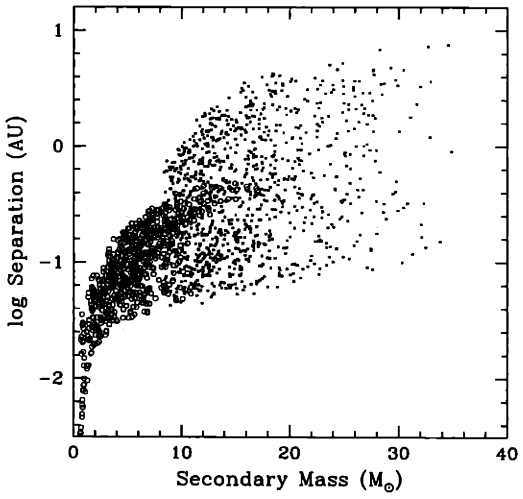

Figure 5-5: Scatter plot of separation versus secondary mass for the *post-mass transfer* binaries shown in Fig. 5-4. Filled and unfilled circles indicate systems that have undergone stable and dynamically unstable mass transfer, respectively.

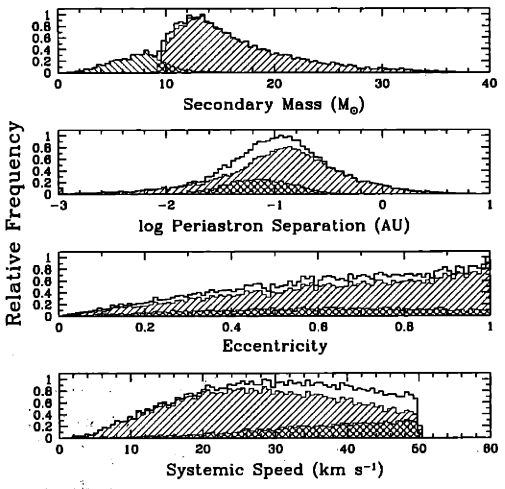

Figure 5-6: Distributions of binary parameters of systems that have undergone case B or C mass transfer, have been left *bound following the supernova explosion*, and have been retained in the cluster. Note that many of the systems with $\log(a/\mathrm{AU}) \lesssim -1.3$ will coalescence immediately following the SN.

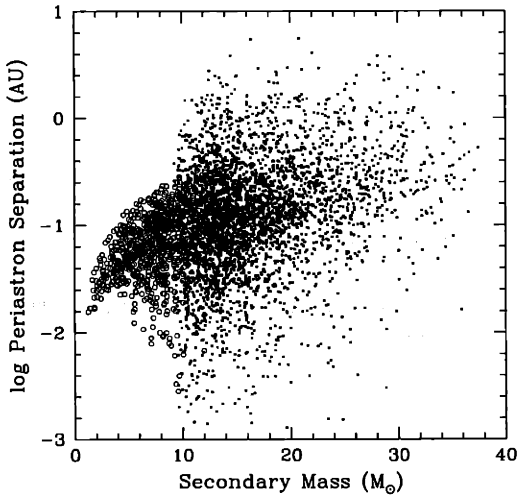

Figure 5-7: Scatter plot of periastron separation versus secondary mass for the same post-SN systems as in Fig. 5-6. The open and filled circles have the same meaning as in Figs. 5-3 and 5-5.

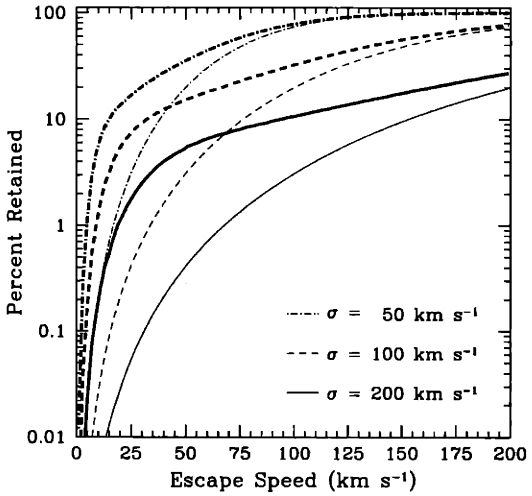

Figure 5-8: Percentage of NSs retained as a function of the cluster escape speed, for a Maxwellian distribution of kick speeds. Heavy curves correspond to binary channels, while the lighter curves are for single stars only.

retained fraction of NSs born in binary systems is not likely to exceed $\sim$ 10%, a number that probably overestimates the true net retention fraction, and which still seems only marginally consistent with the inferred large number of NSs in certain globular clusters.

5.4.3 Influence of the Cluster Potential

Up to this point, we have discussed those calculations where the nominal central escape speed has been applied to all stars and binaries in question. The combination of competitive gas accretion processes, stellar collisions, and dynamical mass segregation in the early phases of cluster development and star formation may lead to a centrally concentrated population of massive stars (e.g., Bonnell et al. 1998). However, the spatial distribution would certainly have been finite and the same escape speed would not have applied to all stars. We investigate the possibility that massive stars and binaries are born within a finite spherical volume, with a gravitational potential that is appropriate for a young globular cluster. The calculation presented in this section is meant to be illustrative, but is nonetheless reasonably quantitative.

For simplicity, we suppose that all massive single stars and binaries are distributed uniformly within a spherical volume of radius R about the center of the cluster. Thus, the probability that an object is located within a spherical shell of radius r and thickness dr is simply

$$p(r)\,dr = \frac{3r^2 dr}{R^3}\ . \tag{5.2}$$

At the time of the SN explosion, we assume that the single star or binary is at rest. This is reasonable when the mean NS kick speed is large, since it is expected that the velocity dispersion of these massive objects is < 10 km s^{-1}.

We adopt a Plummer model (e.g., Binney & Tremaine 1987) for the background gravi-

Table 5.3. Retention Fractions for Various Parameter Sets

Model Number	x[a]	y[b]	α[c]	β[d]	η_{CE}[e]	q_{crit}[f]	Percent Retained
1	2.0	-0.5	1.5	0.75	1.0	0.50	3.23
2	2.0	0.0	1.5	0.75	1.0	0.50	5.39
3	2.0	1.0	1.5	0.75	1.0	0.50	7.87
4	2.5	-0.5	1.5	0.75	1.0	0.50	3.28
5*.....	2.5	0.0	1.5	0.75	1.0	0.50	5.79
6	2.5	1.0	1.5	0.75	1.0	0.50	8.03
7	3.0	-0.5	1.5	0.75	1.0	0.50	3.41
8	3.0	0.0	1.5	0.75	1.0	0.50	5.71
9	3.0	1.0	1.5	0.75	1.0	0.50	8.27
10	2.5	0.0	1.0	0.25	0.3	0.50	3.70
11	2.5	0.0	1.0	0.25	1.0	0.50	4.12
12	2.5	0.0	1.0	0.75	0.3	0.50	4.20
13	2.5	0.0	1.0	0.75	1.0	0.50	3.70
14	2.5	0.0	1.0	1.00	0.3	0.50	2.94
15	2.5	0.0	1.0	1.00	1.0	0.50	3.32
16	2.5	0.0	1.5	0.25	0.3	0.50	2.23
17	2.5	0.0	1.5	0.25	1.0	0.50	2.63
18	2.5	0.0	1.5	0.75	0.3	0.50	5.15
19	2.5	0.0	1.5	1.00	0.3	0.50	2.94
20	2.5	0.0	1.5	1.00	1.0	0.50	3.32
21	2.5	0.0	2.0	0.25	0.3	0.50	0.72
22	2.5	0.0	2.0	0.25	1.0	0.50	1.15
23	2.5	0.0	2.0	0.75	0.3	0.50	5.54
24	2.5	0.0	2.0	0.75	1.0	0.50	5.93
25	2.5	0.0	2.0	1.00	0.3	0.50	2.94
26	2.5	0.0	2.0	1.00	1.0	0.50	3.32
27	2.5	0.0	1.5	0.75	1.0	0.25	7.06
28	2.5	0.0	1.5	0.75	1.0	0.75	3.38

*Standard model.

[a]IMF exponent.

[b]Exponent for mass ratio distribution.

[c]Angular momentum-loss parameter.

[d]Mass capture fraction.

[e]Common-envelope efficiency.

[f]Critical mass ratio that separates stable and unstable mass transfer when the secondary is radiative.

tational potential, given by

$$\Phi(r) = -\frac{GM_*}{(r^2 + b^2)^{1/2}} , \tag{5.3}$$

where M_* is the total mass in stars, r is the distance from the cluster center, and b is the "core" radius of the model. Furthermore, we assume that the potential is static during the $\lesssim 10^8$ yr when massive stars are present. This is not very realistic, but is probably adequate for the present discussion.

In dynamical models of globular cluster evolution that include of the effects of tidal mass loss, it is often assumed that any star that crosses a sphere of radius r_t (the tidal radius) is lost from the cluster (e.g., Joshi et al. 2001 and references therein). The tidal radius is a function of position in the Galaxy; at a few kiloparsecs from the Galactic center, r_t is of order 100 pc for a 10^6 $M_\odot$ cluster. The escape speed, $v_{\rm esc}(r)$, at a radius r is obtained from the energy relation

$$\frac{1}{2} v_{\rm esc}^2(r) = \Phi(r_t) - \Phi(r) . \tag{5.4}$$

However, for the purposes of this investigation we assume that r_t is sufficiently large in comparison to any relevant radius in the cluster that we may drop $\Phi(r_t)$, so that $v_{\rm esc}^2(r) = -2\Phi(r)$. In this case, the core radius, b, is a simple function of the central escape speed, $v_{\rm esc}(0)$:

$$b = \frac{2GM_*}{v_{\rm esc}^2(0)} . \tag{5.5}$$

The output of our population synthesis code is a two-dimensional grid of retention fractions as a function of the escape speed and the kick speed (see § 5.4.1). Combining eqs. (5.2), (5.3), and (5.4), with $\Phi(r_t) = 0$, we obtain a distribution of escape speeds for the uniform spherical distribution of massive stars:

$$p(u_{\rm esc})\, du_{\rm esc} = 6 \left(\frac{b}{R}\right)^3 u_{\rm esc}^{-7} (1 - u_{\rm esc}^4)^{1/2}\, du_{\rm esc} , \tag{5.6}$$

where $u_{\rm esc} \equiv v_{\rm esc}/v_{\rm esc}(0)$ is a dimensionless escape speed.

It is a simple matter to convolve the grid of retention fractions with both the distribution of kick speeds and the distribution of escape speeds to obtain a net retention fraction, as a function of $v_{\rm esc}(0)$ and R. Table 5.4 shows the net retention fraction for different values of $v_{\rm esc}(0)$ and R, where we have used a Maxwellian kick distribution with $\sigma =$ 200 km s^{-1} and a cluster mass of $M_* = 10^6$. For $v_{\rm esc}(0) = 50$ km s^{-1} and $R = 10$ pc, the percentage of NSs retained in the cluster is reduced by a factor of ~ 2 below the standard-model value of $\sim 5.6\%$ (see Table 5.3). Thus, a realistic cluster potential and finite spatial distribution of stars may significantly *reduce* the NS retention fraction below our earlier quoted values. Although, it does seem likely that the massive stars will be more initially centrally concentrated than a uniform 10-pc sphere, as a consequence of both the star formation process and dynamical mass segregation. Therefore, the reduction factors listed in Table 5.4 are probably smaller than one would obtain with a more self-consistent

Table 5.4. Modified Retention Fractions for a Finite Spatial Distribution of Stars

$v_{esc}(0)$ (km s^{-1})	R (pc)	b (pc)	Percent Retained	Reduction Factor*
30	5	9.88	2.44	0.94
30	10	9.88	2.10	0.81
30	20	9.88	1.47	0.56
50	5	3.56	4.44	0.79
50	10	3.56	3.12	0.55
50	20	3.56	1.81	0.32
70	5	1.81	5.19	0.64
70	10	1.81	3.38	0.42
70	20	1.81	1.87	0.23

*Factor by which retention fraction is reduced below value obtained with $R = 0$ pc.

calculation of the cluster structure. However, this just emphasizes that our highly simplified treatment of the cluster structure, where all objects have the same central escape speed, is entirely adequate for addressing the NS retention problem.

5.5 Binary Evolution After the First Supernova

The standard model (§ 5.4.2) has a very striking feature: massive secondaries ($M_2 \gtrsim 10\ M_\odot$) are prevalent among the retained binaries following the first SN (see Figs. 5-6 and 5-7). The majority of these massive systems have periastron separations $\lesssim 1$ AU, which implies that most of the secondaries will begin to transfer material to the NS at some point. Furthermore, the extreme mass ratios suggest that the mass transfer will be dynamically unstable, resulting in a spiral-in of the NS into the envelope of the secondary. It should be noted that the evolution of the secondary following mass transfer may not precisely resemble the evolution of an isolated star of the same mass (e.g., Braun & Langer 1995; Wellstein et al. 2001); in fact, the evolution may be qualitatively different.

Before we discuss the possible outcomes of the spiral-in, we mention an important caveat. Extreme accretion rates ($> 10^{-4}\ M_\odot\ \mathrm{yr}^{-1}$) onto the NS — rates far exceeding the standard, radiative Eddington limit of $\sim 10^{-8}\ M_\odot\ \mathrm{yr}^{-1}$ — may be possible if the gravitational energy is lost to neutrinos (e.g., Chevalier 1993, 1996; Fryer et al. 1996; Brown et al. 2000). If this "hypercritical accretion" occurs while the NS spirals into the envelope of a massive secondary, it is likely that the NS will collapse into a black hole, although the three-dimensional nature of the hydrodynamical problem implies that this process is very uncertain. Obviously, this outcome is not desirable in regard to the retention problem, since a NS is lost if it is transformed into a black hole. We now proceed under the assumption that the NS does not undergo hypercritical accretion during the spiral-in phase; however, the NS may

still collapse to a black hole at a later stage.

The envelope of the massive secondary may be successfully ejected if the circularized orbital separation is $\gtrsim 1$ AU (see Taam et al. 1978). This applies to only a few percent of the systems in Figs. 5-6 and 5-7. If the envelope is ejected, and the core of the secondary is exposed, the formation of a second NS is possible. However, because the orbital speed following the spiral-in is large (> 200 km s^{-1}), as is the fractional mass lost in the SN ($\gtrsim 30\%$), both the first- and second-formed NSs are likely to be ejected from the cluster, even if the kick to the second NS is small and the binary remains bound after the explosion (see § 5.3).

The much more likely outcome among the retained NS binaries is a complete coalescence of the NS and the massive secondary, resulting in the formation of a Thorne-Żytkow object (TŻO; Thorne & Żytkow 1975, 1977; Biehle 1991; Cannon 1993; Podsiadlowski, Cannon, & Rees 1995), where hydrostatic support is provided by gravitational energy release or exotic nuclear burning processes near the surface of the NS. The ultimate fate of the NS is unclear. If the NS survives, it will probably emerge as a rapidly rotating object with the slow speed of the retained post-SN binary. However, it is possible, and perhaps likely, that the NS will collapse into a black hole during the late stage of massive TŻO evolution (Podsiadlowski et al. 1995; Fryer et al. 1996).

In addition to the high-mass systems in Figs. 5-6 and 5-7, roughly 10% of the retained binaries have low- to intermediate-mass secondaries ($M_2 \lesssim 8\ M_\odot$), all of which are the product of dynamically unstable mass transfer prior to the SN. Mass transfer onto the NS in the circularized binary is likely to be dynamically unstable for $M_2 \gtrsim 4\ M_\odot$ (Podsiadlowski et al. 2002), while for secondaries of lower mass the system will exist for some time as a low- or intermediate-mass X-ray binary, which may ultimately yield a millisecond radio pulsar with a very low-mass companion.

5.6 Conclusions

The NS retention fraction calculated within our standard model is $\sim 5\%$ for NSs born in binary systems. Reasonable variations of the parameters that describe the primordial binary population and binary evolution during mass transfer give a retained percentage as low as ~ 1, but not much larger than $\sim 8\%$ (Table 5.3). If we distribute the massive binaries within a sphere of some finite radius and embed the population in a realistic background gravitational potential, the retention fraction may be reduced by a factor of $\lesssim 2$ (Table 5.4). If we suppose that one-half of the massive stars in a young cluster are in binaries, then the retention fraction is further reduced by a factor of two. Furthermore, since many of the retained NSs are in close, massive binaries after the first SN, a TŻO is likely to form, which may cause the NS to collapse to a black hole. Therefore, it would seem that a more realistic net retention fraction is probably no larger than several percent, when we apply the Maxwellian kick distribution with $\sigma = 200$ km s^{-1} and a central escape speed of 50 km s^{-1}.

As compared to the contribution from single stars, binary systems do provide a much more efficient channel for retaining NSs when the characteristic kick speed is large. However,

it appears the net NS retention fraction still may not be sufficient to explain the abundance of NSs in globular clusters. In fact, even if as many as 10^4 NSs are formed out of 10^6 stars, our standard model, combined with the binary fraction and realistic cluster potential, predicts that only $\sim$ 100 NSs may have been retained. It is unlikely that $\sim$ 100 retained NSs is compatible with what is observed in certain clusters (e.g., 47 Tuc). We therefore suggest that binaries alone may not provide a robust solution to the retention problem, and we now discuss alternative hypotheses.

5.7 Discussion

Our standard model for the formation and retention of NS in globular clusters predicts a retention fraction of $\sim 5\%$. Consideration of a finite spatial distribution of stars embedded in a background cluster potential, the binary fraction of massive stars, and the uncertain fate of TZOs implies that the net retention fraction may be significantly smaller. We suggest that our standard model requires significant modification in order for the results to be consistent with observations. Here, we briefly speculate on possible alternative solutions to the retention problem.

5.7.1 The Kick Distribution

Even with a substantial fraction of NS kicks in a Maxwellian component with $\sigma \sim 100$ km s^{-1}, as suggested by Arzoumanian et al. (2002), the retention fraction due to *single stars* is at most several percent (see Fig. 5-8) for a cluster central escape speed of 50 km s^{-1}. The retained fraction of NSs born in *binaries* is increased to $\sim 15\%$ (see Fig. 5-8), but given the additional considerations mentioned above, even this fraction may not be sufficient. A very simple and robust "fix" to the retention problem is to assume that the true underlying distribution in NS kicks has a much lower mean speed than the Galactic pulsars suggest. Such a distribution would require a substantial number of slowly-moving isolated pulsars, which, for some reason, have not yet been detected. Maybe the pulsar sample is too small, or perhaps some systematic effect is unaccounted for in studies of pulsar kinematics, or both. A complete consistency check is difficult, if not impossible, and must incorporate all of the uncertain theory of single star and binary stellar evolution. In addition, we require some rudimentary understanding of the physical mechanism that produces the largest NS kicks. One possibility is that small kicks preferentially occur in binary systems, in which case the associated NS is likely to remain bound to its companion following the SN and thus will not appear as an isolated pulsar.

5.7.2 Implications of Long-Period, Low-Eccentricity HMXBs

Recently, a new class of high-mass X-ray binaries (HMXBs) has emerged. These systems exhibit relatively low eccentricities ($e \lesssim 0.2$) and orbital periods sufficiently long ($P_{\rm orb} \gtrsim$ 100 d) that tidal circularization should not have played a significant role *if* the massive

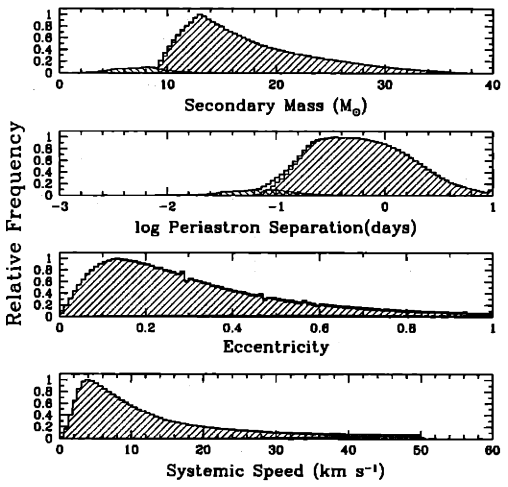

Figure 5-9: Distributions of binary parameters of systems that have undergone case B or C mass transfer, have been left bound following the supernova explosion, and have been retained in the cluster, where we have assumed that case B_e and C_e receive kicks drawn from a Maxwellian with σ = 20 km s^{-1}.

stellar component is not very evolved. A detailed analysis of one such system (X Per/4U 0352+30; Delgado-Martí et al. 2001) revealed that the observed orbit is entirely consistent with the NS having been born with no kick whatsoever. Table 4.1 lists names and orbital parameters of systems that belong to the class of long-period, low-eccentricity HMXBs. See Chap. 4 for a full discussion of these systems.

In § 4.5, we presented a model that appears consistent with the numbers and kinematical properties of bright low-mass X-ray binaries in the Galaxy, all known HMXBs, including the members of the new class, as well as isolated radio pulsars in the Galaxy, on which the inferred NS kick distributions are based. To account for the statistically significant population of HMXBs with long orbital periods and low eccentricities, we propose that a significant fraction of those NSs whose progenitors underwent case B_e or C_e mass transfer received a relatively small kick speed (e.g., $\lesssim$ 50 km s^{-1}). On the other hand, the requirement of consistency with the other NS populations suggests that a NS received the usual large kick if its progenitor was allowed to evolve into a red supergiant (i.e., a single progenitor or case B_l, C_l, or D for a binary system).

There is a plausible physical scenario that may support the empirically-motivated phenomenological hypothesis outlined above. Young, isolated, massive stars are observed to rotate at $\sim 20-50\%$ of their breakup rates (e.g., Fukuda 1982; Howarth et al. 1997). During the hydrogen-burning main sequence, the structure of the star changes sufficiently slowly that various hydrodynamical and magnetohydrodynamical processes should be effective in enforcing nearly uniform rotation throughout much of the star (Spruit & Phinney 1998; Heger et al. 2000). Immediately following the depletion of hydrogen in the core, the structure of the star changes dramatically; the envelope expands to giant dimensions on a thermal timescale ($\sim 10^3$–10^4 yr) and the core contracts while conserving angular momentum. If the stellar core is exposed during this rapid expansion phase as a result of mass transfer in a binary system (case B_e or possibly C_e; see Figs. 2-1 and 2-2), it is likely to be rapidly

rotating. On the other hand, if the star is allowed to evolve into a red supergiant, Maxwell stresses may strongly couple the mostly convective and very slowly rotating envelope to the core, causing the core to spin down to the angular velocity of the envelope (Spruit & Phinney 1998; Spruit 1998).

These arguments suggests a possible dichotomy in core-collapse dynamics between isolated stars and some stars born in close binary systems. It may be that a stellar core exposed following case B_e or C_e mass transfer is rotating much faster than the core of an isolated star at a late stage of its evolution. Dynamically, the collapse of a rapidly rotating core is certainly more phenomenologically complex than the collapse of an initially static core. However, it is not obvious a priori whether a rapidly rotating or slowly rotating pre-collapse core should ultimately yield a larger average natal kick to the NS. Perhaps the rapid rotation stalls the collapse somewhat (e.g., Fryer & Heger 2000), allowing many rotations before the NS is formed. A large number of rotations of the collapsing core may have the effect of averaging out the asymmetries that give rise to large NS kicks (Spruit & Phinney 1998). These speculations aside, we are motivated by empirical evidence to suggest that hydrogen-exhausted cores exposed following case B_e or (possibly) C_e mass transfer produce NSs with small natal kicks, while NSs formed following mass transfer at a later stage of evolution may receive the conventional large kicks.

We repeated the retention study with the following assumptions regarding NS kicks. If the orbit of the primordial binary is sufficiently wide that mass transfer begins when the star is a red supergiant (i.e., case B_l, C_l, or D), the NS kick is chosen from a Maxwellian distribution with $\sigma = 200$ km s^{-1}, as in the standard model (see § 5.4.2). However, if the mass transfer is stable and case B_e or C_e, we utilize a Maxwellian kick distribution with $\sigma = 20$ km s^{-1}. Using the standard-model parameters given in Table 5.3, model 5, we calculate a net retention fraction contributed by binary channels of $\sim 20\%$. Therefore, we see that the above scenario greatly reduces the severity of the retention problem. Figure 5-9 shows the distributions in orbital parameters and speeds for the retained NS binaries. On average, the systems in Fig. 5-9 are wider, more circular, and are moving more slowly than the systems in Fig. 5-6, which shows the same distributions, but for the standard model.

5.7.3 Accretion-Induced Collapse

Thus far, we have considered only massive stellar progenitors of NSs. However, if the mass of a white dwarf (WD) can be increased to the critical Chandrasekhar value ($\simeq 1.4\ M_\odot$), the WD may collapse to form a NS. This *accretion-induced collapse* (AIC) scenario was proposed by Grindlay (1987; see also Bailyn & Grindlay 1990) in the context of globular clusters to explain a number of things regarding cluster NS populations, the retention problem among them. Two fundamentally different scenarios have been proposed for the formation of a NS via AIC, which we now review briefly.

A WD may be "grown" to the Chandrasekhar mass by the slow accumulation of material accreted from a stellar companion. In this scenario, if the WD has a C/O composition it is more likely to explode in a Type Ia SN, than to collapse to form a neutron star (e.g.,

Nomoto 1987; Rappaport et al. 1994). More favorable candidates for AIC are relatively rare WDs of mass $\gtrsim 1.2\ M_\odot$ and an O/Ne/Mg composition (e.g., Nomoto 1987; Nomoto & Kondo 1991). However, growth of the WD to the Chandrasekhar mass requires that the mass transfer rate lie in the narrow range of $\sim 3\text{–}7 \times 10^{-7}\ M_\odot\ \mathrm{yr}^{-1}$ (Iben 1982; Nomoto 1982; Rappaport et al. 1994). For lower accretion rates, the accreted material may be lost in hydrodynamical nova explosions, while larger accretion rates cause the WD atmosphere to expand to giant dimensions and overflow its Roche lobe. Perhaps the most promising cases for obtaining mass transfer rates within the above narrow range occur for thermal timescale mass transfer in binaries with relatively unevolved companions in the mass range $1.5\text{–}2.5 M_\odot$ (e.g., supersoft X-ray sources; van den Heuvel et al. 1992; Rappaport et al. 1994).

A second possible AIC channel involves the coalescence of two WDs (e.g., Nomoto 1987; Chen & Leonard 1993; Rasio & Shapiro 1995), whereby the orbit shrinks as gravitational radiation removes orbital angular momentum. Like the standard AIC scenario discussed above, the double WD merger model has been proposed as an evolutionary pathway to the formation of Type Ia SNe (e.g., Iben & Tutukov 1984; Webbink 1984; Saffer, Livio, & Yungelson 1998, and references therein); however, it is now considered more likely that this will lead to disruption of the lighter WD (see Nomoto & Iben 1985). Under the assumption that the merger does not produce a Type Ia SN, in order for the double WD system to ultimately yield a NS, the sum of the masses must exceed the Chandrasekhar mass. In the Galactic plane, $\sim 0.1\%$ of primordial binaries should produce such a massive double WD close enough to merge within a Hubble time (e.g., Han 1998; Nelemans et al. 2001). If a sizable fraction of these systems can collapse to form a NS, rather than explode as a Type Ia SN, then perhaps as many as 1000 NSs can be formed in this way in a globular cluster. However, the situation is much more complex in a globular cluster, owing to the dynamical interactions among binaries and single stars.

We have not attempted to follow any of these channels in this work. This would certainly be a worthwhile future study to help quantify the formation rates of NSs via AIC in both globular clusters and in the Galactic plane. Finally, we note that even if a significant number of NSs are formed via AIC in a globular cluster, it seems plausible that these NSs would be subject to the same kicks as those formed from collapsed cores of massive stars, especially if the NS velocities are acquired as a result of asymmetric neutrino emission or the post-natal electromagnetic rocket mechanism (Harrison & Tademaru 1975; see also Lai, Chernoff, & Cordes 2001).

5.7.4 Supermassive Globular Clusters

Tidal stripping of globular clusters is a theoretically well-studied phenomenon (e.g., Chernoff & Weinberg 1990; Takahashi & Portegies Zwart 2000; Joshi et al. 2001). It has been shown (see Joshi, Nave, & Rasio for a recent discussion) that, for a range in parameters that describe the initial cluster equilibrium model, a cluster may disrupt in the tidal field of the Galaxy in less than 10^{10} yr, owing to the combined effects of mass loss during stellar evolution and the diffusion of stars across the cluster's tidal boundary. The survivability

of a cluster depends on its orbit through the Galaxy, its initial central concentration, and on the slope of the cluster IMF. Clusters with a high central concentration and a small proportion of massive stars are more likely to survive to core collapse, although as much as 90% of the initial mass of the cluster may be lost before this phase is reached (Joshi et al. 2001).

The idea that a cluster may lose a very significant fraction of its mass, but still "survive" in some sense, brings to light the interesting and very real possibility that some of the globular clusters that presently have a mass of $\sim 10^6\ M_\odot$ are, in fact, remnants of clusters with an initial mass in stars of $\gtrsim 10^7\ M_\odot$. At least one such supermassive cluster has been discovered in the Andromeda galaxy (Meylan et al. 2001), and it has been speculated that this cluster is actually the core of a dwarf elliptical galaxy. For a cluster of initial mass $10^7\ M_\odot$, a net NS retention fraction of a few percent, along with a standard IMF, implies possibly a thousand NSs at the current epoch, which may be sufficient to explain the present pulsar and X-ray binary populations in globular clusters. In this regard, we suggest that a large inferred number of NSs in a present-day globular cluster may indicate that the cluster was initially supermassive. It can be argued (see § 5.2) that $> 10\%$ of the globular clusters in the Milky Way may fall into this category.

We are not the first to consider this rather extreme possibility. Motivated by the hundred-fold overabundance (per unit mass) of bright X-ray sources in globular clusters relative to the Galactic disk, Katz (1983) suggested that some clusters may lose all but $\sim 1\%$ of their mass through evaporative processes. Although it is now believed that 3- and 4-body dynamical scenarios (e.g., Rasio et al. 2000), and perhaps tidal capture (e.g., Fabian et al. 1975; Di Stefano & Rappaport 1992; Podsiadlowski et al. 2002), can explain the overabundance of X-ray binaries, excessive mass loss from initially supermassive globular clusters is still an interesting possibility for explaining the large numbers of NSs found in clusters today.

Chapter 6

Wind-Accreting Neutron Stars

This chapter is adapted from the paper, "On the Population of Wind-Accreting Neutron Stars in the Galaxy," by Eric Pfahl, Saul Rappaport, & Philipp Podsiadlowski, published in *The Astrophysical Journal*, 2002, Vol. 571, p. L37–L40.

6.1 Introduction

Of all the binary X-ray sources in the Galaxy that contain a neutron star (NS), the most abundant, though typically not the most luminous, are systems in which the NS accretes from the wind of a main-sequence stellar companion. Immediately following the supernova (SN) explosion that accompanies the formation of the NS, the companion is, in most cases, relatively unevolved. Stellar masses ranging from a few to several tens of solar masses are likely, with corresponding lifetimes of $\sim 10^7$–10^8 yr. The long phase of wind accretion onto the NS is a fairly quiet prelude to the more dramatic Roche-lobe overflow that follows, where the NS may appear as a low/intermediate-mass X-ray binary (L/IMXB), or, more commonly, as a short-lived high-mass X-ray binary (HMXB) before being engulfed by its companion.

Well known examples of wind-accreting NSs (WNSs) are present in HMXBs, which are typically assumed to contain $\gtrsim$10-$M_\odot$ stars. It has long been suggested (e.g., Rappaport & van den Heuvel 1982) that there is a large unobserved Galactic population of HMXBs with steady X-ray luminosities of $L_{\rm X} \lesssim 10^{35}$ ergs s^{-1}. Most importantly for the present work, WNSs in HMXBs have been proposed (e.g., Ögelman & Swank 1974; Koyama et al. 1989) to account for much of the so-called "Galactic ridge" of previously unresolved, hard ($\sim$1–10 keV) X-ray emission.

The nature and contributions of diffuse and discrete X-ray sources to the X-ray spectrum and total X-ray luminosity of the Galactic ridge has been a point of debate for decades. Prior to *Chandra*, X-ray satellites that have surveyed the Galactic plane (e.g., *ASCA*, *RXTE*) lacked the angular resolution and/or sensitivity to identify point sources near the Galactic center. Wang, Gotthelf, & Lang (2002; hereafter, WGL02) recently reported on a high-

resolution survey of a $0.8° \times 2°$ field about Sgr A*, carried out with *Chandra*/ACIS-I in the energy range of 1–8 keV. Throughout most of the observed field, the sensitivity for detecting discrete sources is $S_{\rm X,min} \sim 10^{-13}\,{\rm ergs\,s^{-1}\,cm^{-2}}$, corresponding to $L_{\rm X} \sim 10^{33}$ ergs s^{-1} at the distance ($\sim$8.5 kpc) of the Galactic center.

WGL02 estimate $\gtrsim$500 previously undetected point sources in the *Chandra* survey, the nature of which are unknown. Sources with X-ray emission in the 1–3 keV band are probably within several kiloparsecs of the Sun. Many of the sources with energies $\gtrsim$3 keV, for which the softer X-rays have been absorbed by the interstellar medium, are nearer to or beyond the Galactic center. WGL02 suggest that as many as $\sim$50% of the hard point sources may be background active galactic nuclei (AGN), although the true fraction may be closer to $\sim$10–20%, as estimated from the $\log N$-$\log S$ curve for sources in the Chandra Deep Field (Brandt et al. 2001). This leaves $\gtrsim$100 Galactic objects that are most likely a population of binary X-ray sources, including black-hole binaries (BHBs), LMXBs, cataclysmic variables (CVs), and WNSs. In the next section, we devote a short discussion to each candidate class of X-ray binary, and we support the case that most of the hard (>3 keV) Galactic point sources detected by *Chandra* are WNSs.

As we argue below, the field surveyed by *Chandra* encompasses roughly 1% of the stars in the Galactic disk. This nontrivial fraction may translate to $\gtrsim$100 WNSs (see § 6.3), and thus the survey may provide an important partial census of these objects. However, even if future observations reveal that few of the hard sources detected by *Chandra* are WNSs, the main ideas of this paper provide a foundation for constraining their numbers and properties.

6.2 The Nature of the Point Sources

The total numbers for each class of X-ray binary in the solid angle of 1.6 deg^2 observed by *Chandra* may be estimated as follows. We suppose that the space density of stars in the Galactic disk is given by $n(R,z) \propto \exp(-R/R_0)\exp(-|z|/z_0)$, where R is the galactocentric radius, and z is the displacement from the Galactic midplane. The scale radius, R_0, is taken to be 4 kpc (van der Kruit 1987), and the vertical scale height is $z_0 \gtrsim 100$ pc. Upon integrating $n(R,z)$ over 1.6 deg^2 through the Galactic center, we find that the field contains $\lesssim$1% of the Galactic population of hypothetical X-ray sources. Thus, the detection by *Chandra* of $\gtrsim$100 Galactic sources implies a total number of $\gtrsim 10^4$ in the entire Galaxy. We now consider each of the candidate X-ray binaries in turn.

Various semi-empirical and theoretical estimates give total numbers of LMXBs and BHBs (quiescent and active) in the Galaxy at $\sim 10^3$ each (e.g., Verbunt & van den Heuvel 1995; Romani 1998). Therefore, it seems that at most of order 10 LMXBs and BHBs could have been detected in the WGL02 survey. This estimate is consistent with the $\lesssim$20 LMXBs and one BHB already known in the surveyed field (see Liu et al. 2001).

There are probably $\sim 10^6$ CVs in the Galaxy (e.g., Howell et al. 2001), and therefore $\sim 10^4$ CVs in the field surveyed by WGL02. Most observed CVs have $L_{\rm X} \lesssim 10^{32}$ ergs s^{-1} in the bandpass of 0.1–2.5 keV, and decreasing power toward higher energies. Luminous CVs, with $L_{\rm X} \sim 10^{33}$–10^{34} ergs s^{-1}, which should comprise only $\sim$1% of the intrinsic population

(e.g., Howell et al. 2001), likewise have relatively soft X-ray spectra. Therefore, we expect that few CVs are detectable beyond several kiloparsecs for $S_{\rm X,min} = 10^{-13}\,{\rm ergs\,s^{-1}\,cm^{-2}}$ (1–8 keV), because of their low total $L_{\rm X}$, as well as the heavy interstellar absorption for energies $\lesssim$3 keV. Integrating $n(R,z)$ over the 1.6 deg^2 surveyed by *Chandra*, to a distance of $D = 3$ kpc from the Sun, we calculate that several tens of CVs, and perhaps of order 100, may have been detected. Therefore, CVs may make up a sizable fraction of the 1–3-keV sources in the WGL02 mosaic image.

Arguably, the most compelling hypothesis for the hard (>3 keV) Galactic X-ray sources detected by *Chandra* is that they are WNSs. Observed HMXBs exhibit a wide range of X-ray luminosities ($\sim 10^{33}$– 10^{38} ergs s^{-1}) and hard, nonthermal X-ray spectra that extend beyond 10 keV (Nagase 1989). Many ($\sim$40%) of these systems are transient, with short (less than several months) outburst phases where $L_{\rm X} \gtrsim 10^{36}$ ergs s^{-1}, and recurrence times that are often years or decades. During its essentially quiescent state, a transient HMXB may have $L_{\rm X} \lesssim 10^{35}$, due to steady accretion from the stellar wind by the NS, such as in the case of the Be/X-ray binary X Per/4U 0352+30 (Delgado-Martí et al. 2001). Theoretical calculations (e.g., Meurs & van den Heuvel 1989) indicate that tens of thousands of such low-luminosity WNSs may currently inhabit the Galaxy, implying that hundreds of WNSs may populate the $0.8^\circ \times 2^\circ$ field about the Galactic center. In the next section, we use binary population synthesis to estimate the number of potentially observable WNSs.

6.3 The X-ray Flux Distribution

An estimate of the number of WNSs with $S_{\rm X} > S_{\rm X,min}$ in the field surveyed by *Chandra* requires that we calculate their X-ray flux distribution. The X-ray luminosity of an individual source depends upon the parameters that characterize both the stellar wind and the binary system that contains the WNS. We have conducted a Monte Carlo population synthesis study of the formation of binaries that consist of a NS and a stellar companion. The three main steps of our population synthesis calculation are enumerated below. A more detailed description of massive binary stellar evolution and the elements of our population synthesis code is given in Chap. 2.

1) In the Galactic disk, each binary containing a NS descends from a massive *primordial binary*, where the initially more massive and less massive stars are hereafter referred to as the *primary* and *secondary*, respectively. We take the Galactic formation rate of massive binaries to be comparable to the core-collapse SN rate, $\mathcal{R}_{\rm SN} \sim 10^{-2}$ yr^{-1} (Cappellaro et al. 1999). The initial primary mass, taken to be $M_{1i} \geq 8\ M_\odot$, is chosen from a power-law IMF, $p(M_{1i}) \propto M_{1i}^{-2.5}$. The initial secondary mass, M_{2i}, is chosen from a flat distribution of mass ratios, $q_i \equiv M_{2i}/M_{1i} < 1$. For simplicity, we assume that the primordial binaries have circular orbits, and we choose the initial orbital separation, a_i, from a distribution that is flat in $\log a_i$.

2) If the orbit is sufficiently compact ($a_i \lesssim 5 - 10$ AU) that the primary evolves to fill its Roche lobe, we use analytic formulae (see § 2.4) to compute the orbital separation

following the subsequent phase of mass transfer. The mass ratio and the evolutionary state of the primary at the onset of Roche-lobe overflow are used to determine whether the mass transfer is *stable* or *dynamically unstable*. Given some critical mass ratio, which we take to be $q_c = 0.5$, the mass transfer is assumed to be stable if $q_i > q_c$ *and* the envelope of the primary is mostly radiative when mass transfer begins, and dynamically unstable if $q_i < q_c$ *or* the primary has a convective envelope. We assume that the entire hydrogen-rich envelope of the primary is removed during mass transfer, whether stable or dynamically unstable, leaving only the primary's hydrogen-depleted core. For stable mass transfer, we suppose that the secondary accretes a fraction, $\beta = 0.75$, of material donated by the primary, and that the remaining mass escapes the system with a specific angular momentum that is $\alpha = 1.5$ times the orbital angular momentum per unit reduced mass. The orbital separation increases or decreases during stable mass transfer by a modest factor of $\lesssim$5–10 for reasonable values of α and β (see § 2.4 and Fig. 2-3). We assume in all cases that the secondary is "rejuvenated" due to the accretion, so that it emerges following mass transfer on the ZAMS appropriate for its new mass. The minimum secondary mass following *stable* mass transfer is approximately (see § 2.4) $q_c 8\ M_\odot + \beta 6\ M_\odot = 8.5\ M_\odot$, where we have used our reference values of q_c and β, and 8 $M_\odot$ and 6 $M_\odot$ are, respectively, our chosen minimum value of M_{1i} and the corresponding envelope mass. Dynamically unstable mass transfer is accompanied by a common-envelope phase, wherein the secondary experiences a drag that causes the binary orbit to shrink in a time of $\lesssim 10^3$ yr. A fraction, $\eta_{\rm CE} \lesssim 1$, of the initial orbital energy is available to unbind the common envelope from the system. If insufficient energy is available, the two stars will merge. Otherwise, the envelope of the primary is dispersed, and the secondary emerges near the ZAMS, without having accreted any mass. The orbital separation may be $\sim$100 times smaller for binaries that survive dynamically unstable mass transfer. A merger results in nearly every case where $q_i < q_c$ and the primary's envelope is radiative when mass transfer starts. This implies that almost all systems that survive dynamically unstable mass transfer must have had initial orbital separations wide enough for the primary to grow to become a convective red supergiant.

3) Upon exhausting its remaining nuclear fuel, the exposed core of the primary explodes as a Type Ib or Ic SN. The impulsive mass loss and possibly large "kick" to the NS strongly perturb, and may unbind, the binary. We assume that both the mass loss and the kick are instantaneous, and that the orientations of the kicks are distributed isotropically. Two scenarios are considered for the distribution of kick speeds. Observations of *isolated* radio pulsars indicate that the mean NS kick speed may be $\gtrsim$100–300 km s^{-1} (e.g., Hansen & Phinney 1997; Arzoumanian et al. 2002). In our first kick scenario (hereafter, K1), we apply a Maxwellian distribution in kick speeds with a mean of $\sim$300 km s^{-1} to all NSs. Our second scenario (K2) was developed in Chap. 4 to account for a new class of HMXBs with long orbital periods ($P_{\rm orb} \gtrsim 30$ d) and low eccentricities ($e \lesssim 0.2$). For NS progenitors that are able to evolve into red supergiants (i.e., single stars and those in wide binaries), the kick speeds are drawn from a Maxwellian with a mean of $\sim$300 km s^{-1}, as in K1. Therefore, our arguments in the last paragraph imply that for post-SN binaries where $M_2 \lesssim 8\ M_\odot$, the NS has received the conventional large kick. If the NS progenitor is in a binary system,

and its envelope is removed while it is mostly radiative, which includes all systems where the mass transfer is stable, we utilize a Maxwellian distribution with a much lower mean of $\sim$30 km s^{-1}. Kick scenario K2 yields a much larger number of post-SN binaries containing massive companion stars ($\gtrsim$8 $M_\odot$), as compared to the number of surviving systems with $M_2 \lesssim 8\ M_\odot$.

The relevant output of the population synthesis code is the post-SN secondary mass, M_2, semimajor axis, a, and eccentricity, e, for each binary. We neglect tidal circularization during the main-sequence evolution of the secondary, although this is important for systems with $a(1-e) \lesssim$ 30–40 $R_\odot$. Our results will not be greatly modified if we include tidal circularization.

Each WNS accretes from the wind of a relatively unevolved stellar companion. Winds from early-type stars with masses of $\sim$3–20 $M_\odot$ are characterized by high speeds, $v_w \sim$ 1000 km s^{-1}, and low to moderate mass-loss rates, $\dot{M}_w \sim 10^{-11}$–$10^{-7}\ M_\odot$ yr^{-1}. Kudritzki & Puls (2000) give the asymptotic wind speeds for stars near the main sequence, which vary from $\sim$ 1.5 times the surface escape speed, v_e, for stellar masses of $\sim$3–10 $M_\odot$, and $\sim 2.5 v_e$ for hotter, more massive stars. The wind speeds are quite uncertain, however, and we thus consider two simple cases in our simulations, namely $v_w = v_e$ and $v_w = 2v_e$, independent of M_2. For $\dot{M}_w$, we utilize the fitting formula of Nieuwenhuijzen & de Jager (1990): $\dot{M}_w \propto M_2^{0.16} L_2^{1.24} R_2^{0.81}$, where L_2 and R_2 are, respectively, the luminosity and radius of the secondary. For both $\dot{M}_w$ and v_e, we substitute the time-averaged values of L_2 and R_2 during the main-sequence phase — roughly twice their ZAMS values for a wide range in M_2.

We apply the standard Bondi-Hoyle-Lyttleton accretion scenario (Hoyle & Lyttleton 1941; Bondi & Hoyle 1944) to obtain the X-ray luminosity of each WNS, specialized to the case where v_w is much larger than the orbital speed of the NS. We further assume that the wind is steady and spherically symmetric, so that the density varies as $\dot{M}_w r^{-2} v_w^{-1}$, where r is the instantaneous orbital separation. The orbital time-averaged X-ray luminosity then scales as $\langle L_X \rangle \propto \epsilon \dot{M}_w\, a^{-2}\, v_w^{-4}\, (1-e^2)^{-1/2}$. Here, $\epsilon \lesssim 1$ is the efficiency for converting gravitational energy into hard (1–10 keV) X-radiation. For $e = 0$, $a = 0.5$ AU, $v_w = 1000$ km s^{-1}, and $\dot{M}_w = 10^{-8}\ M_\odot$ yr^{-1}, we find, after including the multiplicative factors appropriate for an accreting NS, that $\langle L_X \rangle \sim \epsilon \cdot 10^{33}$ ergs s^{-1}. In the present work, we do not take into account the spin history of the NS and the centrifugal inhibition of accretion (e.g., Stella et al. 1986), although this should be incorporated into a more detailed study.

The X-ray flux distribution of the WNSs is obtained by convolving the distance and X-ray luminosity distributions, which we assume are independent in this study. Since the probability of observing a certain WNS should be roughly proportional to the main-sequence lifetime, $\tau_{MS}(M_2)$, of the secondary, we compute the distribution of intrinsic X-ray luminosities by accumulating the values of $\tau_{MS}(M_2)$ for each bin in $\langle L_X \rangle$. Using the same exponential form given in § 6.2 for the space density, $n(R,z)$, of WNSs, we obtain the distribution of distances, D, from the Sun, for sources located within a solid angle of 1.6 deg^2 centered on the Galactic center. We adopt fixed values of $R_0 = 4$ kpc and $z_0 = 200$ pc as being typical for the post-SN binaries. In reality, the effects of SN mass loss and NS kicks

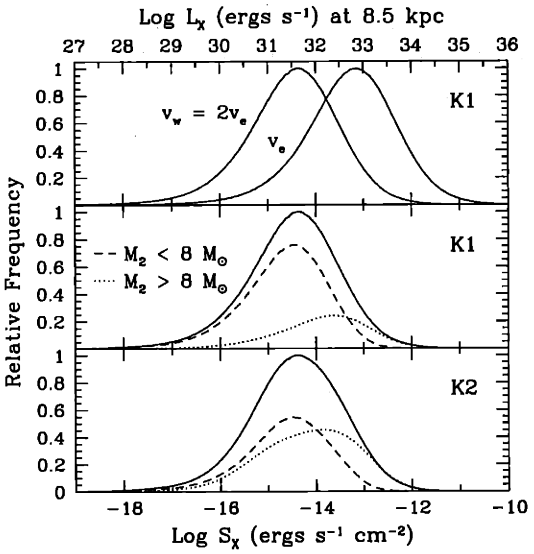

Figure 6-1: The X-ray flux distributions for a set of model assumptions. The top panel shows the distributions for $v_w = v_e$ (*right curve*) and $v_w = 2v_e$ (*left curve*), where kick scenario K1 was used. The middle panel shows the contributions of intermediate-mass (*short-dashed*) and high-mass (*dotted*) systems, for $v_e = 2v_w$ and kick scenario K1. The bottom panel is similar to the middle panel, but for kick scenario K2.

are such that, for a given kick speed, binaries with lower-mass secondaries will receive larger systemic velocities and reach greater distances from the Galactic midplane. A more detailed investigation should include the dynamical evolution of post-SN binaries in the Galaxy.

Our binary population synthesis calculation yields the formation efficiency, $\mathcal{F}_{\rm FE}$, for post-SN binaries with $M_2 > 3\ M_\odot$ (a somewhat arbitrary minimum mass), where the remainder of the massive binaries have ultimately merged or have been disrupted due to the SN. The secondary stars in the surviving systems have a mean main-sequence lifetime of $\langle\tau_{\rm MS}\rangle$, so that the total number of WNSs in the Galaxy is $\sim \langle\tau_{\rm MS}\rangle\mathcal{R}_{\rm SN}\mathcal{F}_{\rm FE}$. Multiplying this total Galactic number by the fraction, $\mathcal{F}_\Omega$, of systems encompassed by the observed solid angle, we obtain the intrinsic number of WNS in the surveyed field. If a fraction, $\mathcal{F}_{\rm X}$, of the WNSs have $S_{\rm X} > S_{\rm X,min}$, as determined from the X-ray flux distribution, *Chandra* should have detected roughly $\langle\tau_{\rm MS}\rangle\mathcal{R}_{\rm SN}\mathcal{F}_{\rm FE}\mathcal{F}_\Omega\mathcal{F}_{\rm X}$ such sources.

Here, we define intermediate- and high-mass post-SN binaries by $M_2 = 3$–$8\ M_\odot$ and $M_2 > 8\ M_\odot$, respectively. When we apply the conventional kick scenario, K1, we obtain $\mathcal{F}_{\rm FE} \sim 0.05$. The general importance of intermediate-mass secondaries is indicated by the rather large mean lifetime of $\langle\tau_{\rm MS}\rangle \sim 50$ Myr for the post-SN binaries. The formation efficiency in kick scenario K2 is $\mathcal{F}_{\rm FE} \sim 0.2$, and the mean lifetime is reduced to $\langle\tau_{\rm MS}\rangle \sim 30$ Myr. We find that $\mathcal{F}_\Omega \sim 0.01$, so that the total number of WNSs in the solid angle surveyed by *Chandra* is ~250 and ~600 for kick scenarios K1 and K2, respectively.

Examples of the X-ray flux distribution for the WNSs are shown in Fig. 1. The two curves in the top panel correspond to our two choices for the wind speed, both for kick scenario K1. Kick scenario K2 does not yield an appreciably different flux distribution, aside from the normalization factor $\mathcal{F}_{\rm FE}$. The middle and bottom panels of Fig. 1 show the contributions of intermediate- and high-mass systems, which change considerably in the two kick scenarios for reasons given earlier. The fraction of WNSs with $S_{\rm X} > S_{\rm X,min}$ depends very much on the prescription for the stellar wind speed. For $v_w = v_e$ and $v_w = 2v_e$, we

find that $\mathcal{F}_X \sim 0.4$ and $\sim$0.05, respectively, giving *detected* numbers of WNSs between ten and several hundred.

Figure 6-1 shows that WNSs with intermediate-mass companions may make a dominant contribution to the flux distribution over a wide range in S_X. This is largely due to the longer lifetimes and and lower wind speeds for lower secondary masses. While only a few of the observed so-called HMXBs (Liu et al. 2000) have the mid- to late-B spectral types consistent with unevolved intermediate-mass stars, it is certainly plausible that a much larger number of the known systems harbor such companions; in most cases the spectral subtype is not well constrained. Interestingly, the small fraction of these systems with $M_2 \lesssim 4\ M_\odot$ and $P_{\rm orb} \sim$ 1–10 d will appear as IMXBs (Podsiadlowski et al. 2002) when the secondary fills its Roche lobe and stably transfers matter to the NS. For longer periods and larger masses, the mass transfer is dynamically unstable. However, as essentially all of the NS binaries with $M_2 \lesssim 8\ M_\odot$ form in much the same way, the entire population of WNSs with intermediate-mass companions may provide unique statistical information regarding the formation of IMXBs.

6.4 Discussion

Chandra has detected $\sim$ 1000 X-ray sources about the Galactic center. The next step is to determine the nature of these sources. Based on the discussions and results presented in the last two sections, we are in a position to make suggestions regarding future observational work, especially as it pertains to WNSs.

A significant fraction — *perhaps the majority* — of the 3–8-keV point sources detected by *Chandra* may be WNSs located within several kiloparsecs of the Galactic center. We propose that an infrared observing campaign be undertaken to search for stellar counterparts. Our models indicate that the majority of WNSs have companions with mid-O to late-B spectral types, with unreddened K-band magnitudes of $\sim$11–16 at the distance of the Galactic center, assuming these stars are near the ZAMS. The intrinsic JHK colors of hot stars are nearly degenerate, and determination of their spectral subtypes thus requires a spectral-line classification system (e.g., Hanson et al. 1996). Purely photometric observations are an important first step, however, as they should allow one to distinguish between stars and background AGN, even with the effects of interstellar extinction.

We also suggest that it would be worthwhile to extend the *Chandra* survey in both sensitivity and angular coverage. The X-ray flux distributions shown in Fig. 1 indicate that a factor of 10 increase in sensitivity may gain a factor of $\sim$5–10 in the number of detected WNSs; of course, the number of AGN may likewise increase by a factor of several tens. Furthermore, extending the survey to Galactic latitudes $|b| \gtrsim 2^\circ$ may reveal a gradient in the density of point sources, and thus give the fraction that are Galactic.

Chapter 7

Summary and Outlook

In Chapters 3 through 6, we utilized massive binary population synthesis to investigate several classes of binary systems containing NSs. Our theoretical approach differs from most previous binary population synthesis studies in that it is directly motivated by observations of specific classes of X-ray binaries and binary radio pulsars. Where possible, we have made predictions and suggestions for future observational and theoretical work. We now summarize the key results and conclusions of each study presented in this thesis.

7.1 Low- and Intermediate-Mass X-ray Binaries

We describe in Chapter 3 the early stages of ongoing research on the Galactic population of LMXBs and IMXBs. The general statistical importance of IMXBs is emphasized. After a short ($\lesssim 10^7$ yr) phase of thermal-timescale mass transfer, many of the IMXBs eventually evolve to resemble standard LMXBs. In fact, with the inclusion of IMXBs in our study, we find using conventional model assumptions that luminous LMXBs at the current epoch are easily *overproduced* in comparison to the observed number. The actual number of systems formed depends very sensitively on the uncertain binding energy parameter λ for the common envelope. Smaller values of λ (more tightly bound common envelopes) lead to fewer systems in total and may severely reduce the number of binaries with low-mass secondaries.

In our study, we also find that NSs in L/IMXBs typically reach masses of $\gtrsim 2\ M_\odot$ by the current epoch if one adopts reasonable prescriptions for the accretion rate. Unless more than $\sim$50% of mass that could potentially be accreted onto the NS is ejected from the system, many NSs would likely collapse to low-mass ($\sim$2–3 $M_\odot$) black holes. Such systems have not yet been identified among observed LMXBs, although their existence is certainly plausible.

Our techniques will eventually be extended to study the population of binary millisecond radio pulsars, the supposed descendants of LMXBs. Furthermore, we plan to conduct a focused investigation of *ultracompact* ($P_{\rm orb} \lesssim 1$ hr) X-ray binaries in the Galaxy. Millisecond radio pulsars and ultracompact X-ray binaries are present in both the Galactic disk

and in globular clusters. In globular clusters, these systems form primarily as a result of binary-single star encounters, where generally the lighter component of a binary system is exchanged with a more massive NS in the field (e.g., Rasio et al. 2000). Preliminary studies of X-ray binary and binary pulsar formation in globular clusters have already been undertaken (Rasio et al. 2000; Rappaport et al. 2001), and will be greatly improved in the future.

7.2 A New Class of High-Mass X-ray Binaries

A new class of long-period ($P_{\rm orb} \sim$ 30–250 day), low-eccentricity ($e \lesssim 0.2$) HMXBs was investigated in Chapter 4. The 6 candidate members of the new class comprise ~20% of the HMXBs with measured orbital parameters. Long orbital periods and low eccentricities strongly suggest that (i) tidal circularization has not played a role, (ii) the NSs in these systems have received low natal kick speeds of $\lesssim$50 km s^{-1}, and (iii) the systems have not experienced the dramatic orbital shrinkage associated with the spiral-in during a CE phase. Such kick speeds are much smaller than those inferred from the proper motions of isolated pulsars and the population of LMXBs. Combining a reasonable spatial distribution of massive binaries in the Galactic disk with the detection sensitivities of satellites that have scanned or monitored the X-ray sky, we estimate a discovery probability of ~10^{-3} for members of the new class of HMXBs. Therefore, we require that there be several thousand wide, nearly circular HMXBs in the Galaxy at present in order to explain the handful of observed systems.

We describe an evolutionary scenario that adequately accounts for new class of HMXBs, as well as other known NS populations, such as HMXBs with eccentricities of ~0.3–0.5, isolated pulsars, and LMXBs. If the envelope of a NS progenitor in a binary system is removed before it has become deeply convective, then we propose that the exposed stellar core is likely to be rapidly rotating, and that the NS is born with a kick speed of $\lesssim$50 km s^{-1}. On the other hand, for NS progenitors that evolve to become deeply convective red supergiants, either in isolation or in wide binaries, we suppose that magnetic torques cause the core to spin down to the slow rotation rate of the giant envelope, and that the NS is born with the conventional large kick of $\gtrsim$100–200 km s^{-1}.

If the scenario discussed above is basically correct, then there are several important implications. First, our model suggests that rapidly rotating pre-SN stellar cores should preferentially yield NSs with small kicks, and conversely for slowly rotating cores; however, we cannot offer any compelling reasons for why this should be the case. Perhaps future three-dimensional hydrodynamical calculations of core-collapse with rapid rotation will offer an explanation of this dichotomy or disprove our hypothesis. Second, the reduced kick speeds of $\lesssim$50 km s^{-1} for many NSs result in a possible order-of-magnitude increase in the number of double NSs. Third, if a large fraction of NSs born in binary systems receive small kicks, then the severity of retention problem for NSs in globular clusters may be greatly reduced.

7.3 Neutron-Star Retention in Globular Clusters

Observational and theoretical results suggest that ~1000 NSs may be present in certain massive (~10^6 $M_\odot$) globular clusters, possibly representing $\gtrsim$10–20% of the total number of NSs formed in each cluster. Such a large NS retention fraction is seemingly at odds with the high NS kick speeds that are conventionally assumed, which range from roughly 5 to 10 times the central escape speeds of the most massive globular clusters. In Chapter 5, we carefully assess the possibility that this *retention problem* is solved if a large fraction of NSs are born in binary systems.

The preferred channel for retaining NSs involves stable mass transfer prior to NS formation, wherein the secondary becomes a massive star and the orbital separation changes by a relatively modest factor; both of these effects are in contrast to the results of dynamically unstable mass transfer. If a NS is formed with a massive binary companion, then there is a significant probability that the NS will remain bound to its companion following the SN explosion, and that the recoil speed of the system could be sufficiently small to allow it to be retained in the cluster. Our "standard model" involving the formation of NSs in binary systems predicts that at most ~5% of the NSs initially formed in a massive cluster can be retained. While binary systems reduce the severity of the retention problem, they do not appear to provide a robust solution.

We discuss several alternative solutions to the retention problem. Neutron-star formation via accretion-induced collapse is mentioned briefly, but it is not clear why NSs formed in this way should be less subject to the conventional large kicks. The dichotomous kick scenario proposed in Chapter 4, where NSs born with massive companions preferentially receive small natal kicks, increases the retention fraction by a large factor of ~5. Another very interesting possibility is that true retention fraction is ~1%, but many of the clusters we see at present are remnants of clusters that were initially $\gtrsim$10 times as massive, and thus $\gtrsim$10 times as many NSs were formed. Subsequent tidal stripping of an initially supermassive globular cluster dilutes the stellar population relative to the number of NSs.

7.4 Wind-Accreting Neutron Stars

The *Chandra X-ray Observatory* has revealed $\gtrsim$500 previously unknown X-ray sources in a 1.6 $\deg^2$ field about the Galactic center. We propose in Chapter 6 that many of these sources are NSs accreting from the winds of relatively unevolved stellar companions. Using massive binary population synthesis, we generate an ensemble of such systems, restricting our attention to secondary masses of 3–20 $M_\odot$. Combining standard wind mass-loss prescriptions and the standard Bondi-Hoyle-Lyttleton accretion formalism, we calculate the distribution of the intrinsic X-ray luminosities of these simulated objects. This luminosity distribution is then convolved with a reasonable spatial distribution for stars in the Galactic disk in order to obtain an X-ray flux distribution. Because of their longer main-sequence lifetimes, lower wind speeds, and smaller average orbital separation, systems with intermediate-mass (3–8 $M_\odot$) companions make a significant contribution to the X-ray flux distribution, and

may dominate over systems with massive (>8 $M_{\odot}$) companions. The uncertainty in the stellar wind speed leads to a large range of the theoretically calculated numbers of wind-accreting NSs in the *Chandra* field, from a small fraction to essentially all of the observed sources. Infrared photometric and spectroscopic observations will be required in order to search for possible stellar counterparts to the X-ray sources near the Galactic center.

Appendix A

Supernovae in Binary Systems

In this appendix, we present a flexible, computationally convenient formulation of the equations that describe a binary system following an asymmetric SN (SN) explosion of one of the components. We allow for the possibility that the pre-SN binary is eccentric, and we consider the effects of instantaneous mass loss from the exploding star and an impulsive kick delivered to the newly-formed compact remnant. Also included in our analysis is the effect of the SN blast wave on the companion to the exploding star. Furthermore, if the binary is disrupted following the SN, we calculate the asymptotic velocities of the components. Our approach differs from previous studies (e.g., Hills 1983; Brandt & Podsiadlowski 1995; Tauris & Takens 1998) in that we use mathematically compact vector expressions to describe the binary system after the explosion. It is straightforward to directly implement this vector formalism in a computer code, since vector arithmetic can be performed using simple array operations.

Consider a pre-SN binary system that consists of stars with masses M_1 and M_2 in an orbit with semimajor axis a and eccentricity e. The Keplerian orbital frequency is given by $\Omega = (GM_b/a^3)^{1/2}$, where $M_b = M_1 + M_2$. Relative to the center-of-mass (CM), the positions of the two stars at some time t are $\boldsymbol{r}_1(t)$ and $\boldsymbol{r}_2(t)$, and the corresponding velocities are $\boldsymbol{v}_1(t)$ and $\boldsymbol{v}_2(t)$. The relative positions and velocities are given by $\boldsymbol{r}(t) = \boldsymbol{r}_1(t) - \boldsymbol{r}_2(t)$ and $\boldsymbol{v}(t) = \boldsymbol{v}_1(t) - \boldsymbol{v}_2(t)$, respectively.

It is convenient to have a coordinate-independent description of the binary system. Such a description is provided by the two conserved vectors of the Kepler problem, namely the angular momentum per unit reduced mass, $\boldsymbol{h}$, and the Laplace-Runge-Lenz (LRL) vector, $\boldsymbol{e}$ (e.g., Goldstein 1980; Eggleton 1999):

$$\boldsymbol{h} = \boldsymbol{r} \times \boldsymbol{v} \quad ; \quad \boldsymbol{e} = \frac{\boldsymbol{v} \times \boldsymbol{h}}{GM_b} - \frac{\boldsymbol{r}}{r} \, . \tag{A.1}$$

Note that $\boldsymbol{h}$ points perpendicular to the orbital plane and has a magnitude $h = \Omega a^2(1 - e^2)^{1/2}$, and $\boldsymbol{e}$ points in the direction of periastron of star 1 and has a magnitude equal to the orbital eccentricity, e. By convention, boldfaced characters denote vectors, while the same characters with normal typeface denote the magnitudes of those vectors.

Since we allow for the possibility that the pre-SN binary is eccentric, we must take some care in computing $\boldsymbol{r}$ and $\boldsymbol{v}$ at the time of the explosion. We assume that there is no preferred position along the orbit for the explosion to take place; therefore, the explosion probability per unit time is constant. No closed form expressions exist for $\boldsymbol{r}$ and $\boldsymbol{v}$ as functions of time, and so we must be content with a parametric representation. Consider a Cartesian coordinate system with x-, y-, and z-axes defined by the directions of $\boldsymbol{e}$, $\boldsymbol{h} \times \boldsymbol{e}$, and $\boldsymbol{h}$, respectively. In terms of the eccentric anomaly, E, the dynamical equations read

$$\Omega t_p = E - e \sin E \ , \tag{A.2}$$

$$x = a(\cos E - e) \quad , \quad y = a(1 - e^2)^{1/2} \sin E \ , \tag{A.3}$$

$$v_x = -\frac{\Omega a^2}{r} \sin E \quad , \quad v_y = \frac{\Omega a^2}{r} (1 - e^2)^{1/2} \cos E \ , \tag{A.4}$$

where t_p is the time elapsed since periastron passage. With a randomly selected value for Ωt_p, the corresponding value of E is obtained by solving eq. (A.2) numerically, and the relative position and velocity vectors can be readily computed.

At the randomly selected time, star 1 undergoes a SN explosion. We assume that the explosion is an impulsive event, meaning that the direct dynamical influence of the explosion occurs over a time that is much shorter than the orbital period. In other words, it is assumed the SN explosion and the associated blast wave have an instantaneous effect on the masses and velocities of the binary components. The envelope of star 1 is ejected, exposing a remnant of mass M_1' with a new velocity $\boldsymbol{v}_1' = \boldsymbol{v}_1 + \Delta \boldsymbol{v}_1$, where $\Delta \boldsymbol{v}_1$ is the kick velocity. The magnitude and direction of the kick velocity are chosen from appropriate distributions. After a negligibly short time (the time it takes the blast wave to cross the orbit), a small fraction of the blast wave will interact with star 2, resulting in a new mass M_2' and velocity $\boldsymbol{v}_2' = \boldsymbol{v}_2 + \Delta \boldsymbol{v}_2$, where $\Delta \boldsymbol{v}_2$ is directed antiparallel to $\boldsymbol{r}$ (see Wheeler et al. 1975; Fryxell & Arnett 1981). If star 2 is still on the main sequence at the time of the explosion, it is expected the SN ejecta has only a small effect on star 2 and on the binary orbit. However, if star 2 is a giant at the time of the SN, a large fraction of its envelope may be stripped by the blast wave (see, however, Livne et al. 1992; Marietta et al. 2000), and so we consider this possibility in our mathematical formalism.

The combined effects of mass loss and the velocity perturbations received by the binary components yield a CM velocity

$$\begin{aligned} \boldsymbol{v}_{\rm CM}' &= \frac{1}{M_b'} (M_1' \boldsymbol{v}_1' + M_2' \boldsymbol{v}_2') \\ &= \left(-\frac{M_2}{M_b'} \frac{\Delta M_1}{M_b} + \frac{M_1}{M_b'} \frac{\Delta M_2}{M_b} \right) \boldsymbol{v} + \frac{M_1'}{M_b'} \Delta \boldsymbol{v}_1 + \frac{M_2'}{M_b'} \Delta \boldsymbol{v}_2 \ , \end{aligned} \tag{A.5}$$

where $\Delta M_1 = M_1 - M_1'$ is the mass of the ejected envelope of star 1, $\Delta M_2 = M_2 - M_2'$ is the mass stripped and ablated from star 2 (Wheeler et al. 1975), and $M_b' = M_1' + M_2'$. The orbital parameters following the explosion may differ dramatically from their initial values.

In fact, the explosion may disrupt the binary entirely. The post-SN orbital parameters are determined by the new specific angular momentum, $\boldsymbol{h}'$, and the new LRL vector, $\boldsymbol{e}'$:

$$\boldsymbol{h}' = \boldsymbol{r} \times \boldsymbol{v}' \;\; ; \;\; \boldsymbol{e}' = \frac{\boldsymbol{v}' \times \boldsymbol{h}'}{GM_b'} - \frac{\boldsymbol{r}}{r} \; . \tag{A.6}$$

The binary is gravitationally bound following the SN if $e' < 1$. In this case, the post-SN semimajor axis is given by

$$a' = \frac{h'^2}{GM_b'(1 - e'^2)} \; . \tag{A.7}$$

It is sometimes interesting to know the spin-orbit misalignment angle, γ, of the compact remnant or its companion following the SN (e.g., Brandt & Podsiadlowski 1995; Kalogera 2000). Star 2 will have the same rotation sense as the orbit following a phase of mass accretion. In this case, the spin of star 2 preserves the direction of the pre-SN orbital angular momentum, and the cosine of the misalignment angle is simply

$$\cos\gamma = \hat{\boldsymbol{h}} \cdot \hat{\boldsymbol{h}}' \; , \tag{A.8}$$

where hats denote unit vectors. Star 1 may likewise spin in the direction of the orbit owing to tidal coupling; however, this is not necessarily true for the remnant (see Spruit & Phinney 1998).

On the other hand, if $e' > 1$, the compact remnant and star 2 are not gravitationally bound, and we would like to compute the asymptotic speeds of the components relative to the pre-SN CM velocity. In the new CM frame, the two objects recede along hyperbolic trajectories. As a function of the true anomaly (also the polar angle in the new orbital plane), θ, the relative separation increases according to $r(\theta) \propto (1 + e'\cos\theta)^{-1}$. Clearly, r approaches infinity as $\cos\theta$ approaches the value $-1/e'$. For large r, the direction of the relative velocity is nearly radial, and so the relative velocity at infinity, $\boldsymbol{v}_\infty$, is given by

$$\boldsymbol{v}_\infty = v_\infty \left[-\frac{1}{e'}\hat{\boldsymbol{e}}' + \left(1 - \frac{1}{e'^2}\right)^{1/2} \hat{\boldsymbol{h}}' \times \hat{\boldsymbol{e}}' \right] \; , \tag{A.9}$$

where

$$v_\infty = \frac{GM_b'}{h'}(e'^2 - 1)^{1/2} \; . \tag{A.10}$$

Given $\boldsymbol{v}_\infty$ and $\boldsymbol{v}'_{\rm CM}$, the asymptotic velocities of the components relative to the pre-SN CM velocity can be computed:

$$\boldsymbol{v}_{1,\infty} = \frac{M_2'}{M_b'}\boldsymbol{v}_\infty + \boldsymbol{v}'_{\rm CM} \; ; \; \boldsymbol{v}_{2,\infty} = -\frac{M_1'}{M_b'}\boldsymbol{v}_\infty + \boldsymbol{v}'_{\rm CM} \; . \tag{A.11}$$

Appendix B

Binary Retention in Globular Clusters

A semi-analytic approach is used to compute the probability that a binary is bound following the SN explosion *and* is retained in a cluster with a given escape speed (see § 5.3). For an appropriate choice of pre-SN orbital separation and component masses, the calculated retention probability is a fair estimate of the net NS retention fraction contributed by all binary stellar evolution channels.

In what follows, we consider a circular pre-SN binary of total mass M_b and with separation a, so that the relative orbital speed is $v_{\rm orb} = (GM_b/a)^{1/2}$. We assume that the explosion is instantaneous and leaves a neutron star remnant of mass $M_{\rm NS}$. Furthermore, we neglect the effect of the SN ejecta on the secondary. The kick speed imparted to the NS is v_k and the systemic mass after the explosion is M_b'.

It is useful here to introduce a set of dimensionless variables. All speeds are expressed in units of the pre-SN relative orbital speed, $v_{\rm orb}$, and are denoted by the variable w with an appropriate subscript (e.g., $w_k \equiv v_k/v_{\rm orb}$ is the dimensionless kick speed). The fractional mass loss in the explosion is given by $\Delta \equiv 1 - M_b'/M_b$. In place of the secondary mass M_2, we use the post-SN mass ratio $q' \equiv M_2/M_{\rm NS}$. Finally, the variable u represents the cosine of the angle between the direction of the kick and the direction of the pre-SN relative orbital velocity.

The orbital energy, E', of the post-SN binary is proportional to the dimensionless quantity (e.g., Hills 1983; Brandt & Podsiadlowski 1995)

$$E' \propto -1 + 2\Delta + w_k^2 + 2u\,w_k \ . \tag{B.1}$$

For the purposes of § 5.3 it is sufficient to consider $\Delta < 1/2$, in which case there is a minimum kick, $w_{k,\rm min}$, required to unbind the system, realized when $u = 1$:

$$w_{k,\rm min} = -1 + [2(1-\Delta)]^{1/2} \ . \tag{B.2}$$

Likewise, for there to be a finite probability that the system remains bound, w_k must be less than some large value, $w_{k,\max}$, corresponding to $E' = 0$ and $u = -1$ in eq. (B.1):

$$w_{k,\max} = 1 + [2(1-\Delta)]^{1/2} \ . \tag{B.3}$$

If $w_k > w_{k,\max}$, the system is guaranteed to be disrupted. For a given $w_{k,\min} < w_k < w_{k,\max}$ and $\Delta < 1/2$, u must be less than a maximum value, $u_{\max}$, for the binary to remain bound following the explosion:

$$u < u_{\max} \equiv \frac{1}{2w_k}(1 - 2\Delta - w_k^2) \ . \tag{B.4}$$

When the kick speed is large ($w_k \gtrsim 1$), we see that $u_{\max} < 0$. Therefore, if the directions of the kicks are preferentially aligned perpendicularly to the orbital plane (i.e., $u \sim 0$), rather than distributed isotropically, we expect somewhat fewer bound and retained systems for a mean kick speed that is larger than the typical orbital speed (see Brandt & Podsiadlowski 1995). Conversely, if the mean kick speed is small, perpendicular kicks tend to yield an increase in the number of retained binaries, although the baseline retention fraction (for isotropic kicks) is also larger in this case.

The center-of-mass (CM) speed of a bound binary determines whether or not the system will be retained in the cluster. The CM speed, $w_{\rm CM}$, following the explosion is given by

$$w_{\rm CM} = \frac{1}{1+q'}[(q'\Delta)^2 - 2q'\Delta\, u\, w_k + w_k^2]^{1/2} \ . \tag{B.5}$$

If $w_{\rm esc}$ is the dimensionless central escape speed of the cluster, then the probability that a bound post-SN binary is retained is simply a step function, $S(w_{\rm esc} - w_{\rm CM})$, equal to unity for $w_{\rm esc} - w_{\rm CM} > 0$ and vanishing otherwise. Taking Δ, q', and $w_{\rm esc}$ to be fixed parameters, we obtain the retention probability, P_r, as a function of w_k by integrating over u:

$$P_r(w_k; \Delta, q', w_{\rm esc}) = \int_{-1}^{\min(1,u_{\max})} du\, p(u)\, S(w_{\rm esc} - w_{\rm CM}) \ , \tag{B.6}$$

where $\min(1, u_{\max})$ is the minimum of 1 and $u_{\max}$. For isotropically distributed kick directions, the distribution function for u is simply $p(u) = 1/2$. Convolution of P_r with the distribution in dimensionless kick speeds, $p(w_k)$, yields the total probability, $P_{r,\rm tot}$, that a bound binary is retained in the cluster after the SN:

$$P_{r,\rm tot}(\Delta, q', w_{\rm esc}) = \int_0^{w_{k,\max}} dw_k\, p(w_k)\, P_r(w_k; \Delta, q', w_{\rm esc}) \ . \tag{B.7}$$

Bibliography

Abt, H. A. & Levy, S. G. (1978). Binaries among B2-B5 IV, V absorption and emission stars. *The Astrophysical Journal Supplement Series*, **36**, 241.

Acheson, D. J. (1978). Unknown. *Solar Physics*, **62**, 23.

Apparao, K. M. V., Bradt, H. V., Dower, R. G., Doxsey, R. E., Jernigan, J. G., & Li, F. (1978). Positions of galactic X-ray sources - l/II/ between 320 and 340 deg. *Nature*, **271**, 225.

Arzoumanian, Z., Chernoff, D. F., & Cordes, J. M. (2002). The Velocity Distribution of Isolated Radio Pulsars. *The Astrophysical Journal*, **568**, 289.

Bacon, D., Sigurdsson, S., & Davies, M. B. (1996). Close approach during hard binary-binary scattering. *Monthly Notices of the Royal Astronomical Society*, **281**, 830.

Bhattacharya, D. & van den Heuvel, E. P. J. (1991). Formation and evolution of binary and millisecond radio pulsars. *Physics Reports*, **203**, 1.

Bildsten, L., Chakrabarty, D., Chiu, J., Finger, M. H., Koh, D. T., Nelson, R. W., Prince, T. A., Rubin, B. C., Scott, D. M., Stollberg, M., Vaughan, B. A., Wilson, C. A., & Wilson, R. B. (1997). Observations of Accreting Pulsars. *The Astrophysical Journal Supplement Series*, **113**, 367.

Binney, J. & Tremaine, S. (1987). *Galactic Dynamics*. Princeton, NJ, Princeton University Press.

Blaauw, A. (1961). On the origin of the O- and B-type stars with high velocities (the "run-away" stars), and some related problems. *Bulletin of the Astronomical Institute of the Netherlands*, **15**, 265+.

Blundell, K. M., Mioduszewski, A. J., Muxlow, T. W. B., Podsiadlowski, P., & Rupen, M. P. (2001). Images of an Equatorial Outflow in SS 433. *The Astrophysical Journal Letters*, **562**, L79.

Boersma, J. (1961). Mathematical theory of the two-body problem with one of the masses decreasing with time. *Bulletin of the Astronomical Institute of the Netherlands*, **15**, 291.

Bondi, H. & Hoyle, F. (1944). On the mechanism of accretion by stars. *Monthly Notices of the Royal Astronomical Society*, **104**, 273.

Bonnell, I. A., Bate, M. R., & Zinnecker, H. (1998). On the formation of massive stars. *Monthly Notices of the Royal Astronomical Society*, **298**, 93.

Borozdin, K., Gilfanov, M., Sunyaev, R., Churazov, E., Loznikov, V., Yamburenko, N., Skinner, G. K., Patterson, T. G., Willmore, A. P., Emam, O., Brinkman, A. C., Heise, J., Int-Zand, J. J. M., & Jager, R. (1990). KS:1947+300 - a New Transient X-Ray Source in Cygnus. *Soviet Astronomy Letters*, **16**, 345.

Brandt, N. & Podsiadlowski, P. (1995). The effects of high-velocity supernova kicks on the orbital properties and sky distributions of neutron-star binaries. *Monthly Notices of the Royal Astronomical Society*, **274**, 461.

Brandt, W. N., Alexander, D. M., Hornschemeier, A. E., Garmire, G. P., Schneider, D. P., Barger, A. J., Bauer, F. E., Broos, P. S., Cowie, L. L., Townsley, L. K., Burrows, D. N., Chartas, G., Feigelson, E. D., Griffiths, R. E., Nousek, J. A., & Sargent, W. L. W. (2001). The Chandra Deep Field North Survey. V. 1 Ms Source Catalogs. *The Astronomical Journal*, **122**, 2810.

Braun, H. & Langer, N. (1995). Effects of accretion onto massive main sequence stars. *Astronomy and Astrophysics*, **297**, 483.

Brisken, W. F., Benson, J. M., Beasley, A. J., Fomalont, E. B., Goss, W. M., & Thorsett, S. E. (2000). Measurement of the Parallax of PSR B0950+08 Using the VLBA. *The Astrophysical Journal*, **541**, 959.

Brown, G. E., Lee, C.-H., & Bethe, H. A. (2000). Hypercritical Advection-dominated Accretion Flow. *The Astrophysical Journal*, **541**, 918.

Camilo, F., Lorimer, D. R., Freire, P., Lyne, A. G., & Manchester, R. N. (2000). Observations of 20 Millisecond Pulsars in 47 Tucanae at 20 Centimeters. *The Astrophysical Journal*, **535**, 975.

Cappellaro, E., Evans, R., & Turatto, M. (1999). A new determination of supernova rates and a comparison with indicators for galactic star formation. *Astronomy and Astrophysics*, **351**, 459.

Casares, J., Charles, P. A., & Kuulkers, E. (1998). The Mass of the Neutron Star in Cygnus X-2 (V1341 Cygni). *The Astrophysical Journal Letters*, **493**, L39.

Chen, K. & Leonard, P. J. T. (1993). Does the coalescence of white dwarfs produce millisecond pulsars in globular clusters? *The Astrophysical Journal Letters*, **411**, L75.

Chernoff, D. F. & Weinberg, M. D. (1990). Evolution of globular clusters in the Galaxy. *The Astrophysical Journal*, **351**, 121.

Chevalier, R. A. (1993). Neutron star accretion in a stellar envelope. *The Astrophysical Journal Letters*, **411**, L33.

Chevalier, R. A. (1996). Neutrino-cooled Accretion: Rotation and Stellar Equation of State. *The Astrophysical Journal*, **459**, 322.

Cordes, J. M. & Chernoff, D. F. (1998). Neutron Star Population Dynamics. II. Three-dimensional Space Velocities of Young Pulsars. *The Astrophysical Journal*, **505**, 315.

Cowley, A. P. (1969). The VV Cephei Stars. *Publications of the Astronomical Society of the Pacific*, **81**, 297.

Cowley, A. P., Hutchings, J. B., & Popper, D. M. (1977). The masses of cool supergiants : the interacting eclipsing system AZ Cas. *Publications of the Astronomical Society of the Pacific*, **89**, 882.

D'Amico, N., Possenti, A., Manchester, R. N., Sarkissian, J., Lyne, A. G., & Camilo, F. (2001a). An Eclipsing Millisecond Pulsar with a Possible Main-Sequence Companion in NGC 6397. *The Astrophysical Journal Letters*, **561**, L89.

D'Amico, N., Possenti, A., Manchester, R. N., Sarkissian, J., Lyne, A. G., & Camilo, F. (2001b). New Millisecond Pulsars in Globular Clusters. In *20th Texas Symposium on relativistic astrophysics*, page 526.

Davies, M. B. (1995). The binary zoo: the calculation of production rates of binaries through 2+1 encounters in globular clusters. *Monthly Notices of the Royal Astronomical Society*, **276**, 887.

Davies, M. B. & Hansen, B. M. S. (1998). Neutron star retention and millisecond pulsar production in globular clusters. *Monthly Notices of the Royal Astronomical Society*, **301**, 15.

De Greve, J.-P. & De Loore, C. (1977). The evolution of massive close binaries. V - Systems containing primaries with masses between 10 solar mass and 15 solar mass. *Astrophysics and Space Science*, **50**, 75.

Delgado, A. J. & Thomas, H.-C. (1981). Mass transfer in a binary system - The evolution of the mass-giving helium star. *Astronomy and Astrophysics*, **96**, 142.

Delgado-Martí, H., Levine, A. M., Pfahl, E., & Rappaport, S. A. (2001). The Orbit of X Persei and Its Neutron Star Companion. *The Astrophysical Journal*, **546**, 455.

Deutsch, E. W., Margon, B., & Anderson, S. F. (2000). Ultracompact X-Ray Binaries in Globular Clusters: Variability of the Optical Counterpart of X1832-330 in NGC 6652. *The Astrophysical Journal Letters*, **530**, L21.

Dewey, R. J. & Cordes, J. M. (1987). Monte Carlo simulations of radio pulsars and their progenitors. *The Astrophysical Journal*, **321**, 780.

Dewi, J. D. M. & Tauris, T. M. (2000). On the energy equation and efficiency parameter of the common envelope evolution. *Astronomy and Astrophysics*, **360**, 1043.

Dewi, J. D. M. & Tauris, T. M. (2001). On the λ-Parameter of the Common Envelope Evolution. In *ASP Conf. Ser. 229: Evolution of Binary and Multiple Star Systems*, page 255.

Di Stefano, R. & Rappaport, S. (1992). Production of recycled pulsars in globular clusters via two-body tidal capture. *The Astrophysical Journal*, **396**, 587.

Drukier, G. A. (1996). Retention fractions for globular cluster neutron stars. *Monthly Notices of the Royal Astronomical Society*, **280**, 498.

Duquennoy, A. & Mayor, M. (1991). Multiplicity among solar-type stars in the solar neighbourhood. II - Distribution of the orbital elements in an unbiased sample. *Astronomy and Astrophysics*, **248**, 485.

Eggleton, P. (1999). *Evolutionary in Binary and Multiple Stars.* Cambridge, UK, Cambridge University Press, in preparation.

Eggleton, P. P. (1983). Approximations to the radii of Roche lobes. *The Astrophysical Journal*, **268**, 368.

Fabian, A. C., Pringle, J. E., & Rees, M. J. (1975). Tidal capture formation of binary systems and X-ray sources in globular clusters. *Monthly Notices of the Royal Astronomical Society*, **172**, 15P.

Faulkner, J. (1971). Ultrashort-Period Binaries, Gravitational Radiation, and Mass Transfer. I. The Standard Model, with Applications to WZ Sagittae and Z Camelopardalis. *The Astrophysical Journal Letters*, **170**, L99.

Flannery, B. P. & van den Heuvel, E. P. J. (1975). On the origin of the binary pulsar PSR 1913 + 16. *Astronomy and Astrophysics*, **39**, 61.

Freire, P. C., Camilo, F., Lorimer, D. R., Lyne, A. G., & Manchester, R. N. (2000). Millisecond Pulsars in 47 Tucanae. In *ASP Conf. Ser. 202: IAU Colloq. 177: Pulsar Astronomy - 2000 and Beyond*, page 87.

Fryer, C. L. & Heger, A. (2000). Core-Collapse Simulations of Rotating Stars. *The Astrophysical Journal*, **541**, 1033.

Fryer, C. L., Benz, W., & Herant, M. (1996). The Dynamics and Outcomes of Rapid Infall onto Neutron Stars. *The Astrophysical Journal*, **460**, 801.

Fryxell, B. A. & Arnett, W. D. (1981). Hydrodynamic effects of a stellar explosion on a binary companion star. *The Astrophysical Journal*, **243**, 994.

Fukuda, I. (1982). A statistical study of rotational velocities of the stars. *Publications of the Astronomical Society of the Pacific*, **94**, 271.

Garmany, C. D., Conti, P. S., & Massey, P. (1980). Spectroscopic studies of O type stars. IX - Binary frequency. *The Astrophysical Journal*, **242**, 1063.

Goldstein, H. (1980). *Classical Mechanics.* Reading, MA, Addison-Wesley.

Grindlay, J. E., Heinke, C. O., Edmonds, P. D., Murray, S. S., & Cool, A. M. (2001a). Chandra Exposes the Core-collapsed Globular Cluster NGC 6397. *The Astrophysical Journal Letters*, **563**, L53.

Grindlay, J. E., Heinke, C., Edmonds, P. D., & Murray, S. S. (2001b). High-Resolution X-ray Imaging of a Globular Cluster Core: Compact Binaries in 47Tuc. *Science*, **292**, 2290.

Habets, G. M. H. J. (1986a). The evolution of a single and a binary helium star of 2.5 solar masses up to neon ignition. *Astronomy and Astrophysics*, **165**, 95.

Habets, G. M. H. J. (1986b). The evolution of helium stars in the mass range 2.0 to 4.0 solar masses. *Astronomy and Astrophysics*, **167**, 61.

Han, Z. (1998). The formation of double degenerates and related objects. *Monthly Notices of the Royal Astronomical Society*, **296**, 1019.

Hansen, B. M. S. & Phinney, E. S. (1997). The pulsar kick velocity distribution. *Monthly Notices of the Royal Astronomical Society*, **291**, 569.

Hanson, M. M., Conti, P. S., & Rieke, M. J. (1996). A Spectral Atlas of Hot, Luminous Stars at 2 Microns. *The Astrophysical Journal Supplement Series*, **107**, 281.

Harmanec, P., Habuda, P., Štefl, S., Hadrava, P., Korčáková, D., Koubský, P., Krtička, J., Kubát, J., Škoda, P., Šlechta, M., & Wolf, M. (2000). Properties and nature of Be stars. XX. Binary nature and orbital elements of Hbeta Cas. *Astronomy and Astrophysics*, **364**, L85.

Harrison, E. R. & Tademaru, E. (1975). Acceleration of pulsars by asymmetric radiation. *The Astrophysical Journal*, **201**, 447.

Heger, A., Langer, N., & Woosley, S. E. (2000). Presupernova Evolution of Rotating Massive Stars. I. Numerical Method and Evolution of the Internal Stellar Structure. *The Astrophysical Journal*, **528**, 368.

Hills, J. G. (1976). The formation of binaries containing black holes by the exchange of companions and the X-ray sources in globular clusters. *Monthly Notices of the Royal Astronomical Society*, **175**, 1P.

Hills, J. G. (1983). The effects of sudden mass loss and a random kick velocity produced in a supernova explosion on the dynamics of a binary star of arbitrary orbital eccentricity - Applications to X-ray binaries and to the binary pulsars. *The Astrophysical Journal*, **267**, 322.

Hjellming, M. S. & Webbnik, R. F. (1987). Thresholds for rapid mass transfer in binary systems. I - Polytropic models. *The Astrophysical Journal*, **318**, 794.

Howarth, I. D., Siebert, K. W., Hussain, G. A. J., & Prinja, R. K. (1997). Cross-correlation characteristics of OB stars from IUE spectroscopy. *Monthly Notices of the Royal Astronomical Society*, **284**, 265.

Howell, S. B., Nelson, L. A., & Rappaport, S. (2001). An Exploration of the Paradigm for the 2-3 Hour Period Gap in Cataclysmic Variables. *The Astrophysical Journal*, **550**, 897.

Hoyle, F. & Lyttleton, R. A. (1941). On the accretion theory of stellar evolution. *Monthly Notices of the Royal Astronomical Society*, **101**, 227.

Hurley, J. R., Pols, O. R., & Tout, C. A. (2000). Comprehensive analytic formulae for stellar evolution as a function of mass and metallicity. *Monthly Notices of the Royal Astronomical Society*, **315**, 543.

Hut, P., Murphy, B. W., & Verbunt, F. (1991). The formation rate of low-mass X-ray binaries in globular clusters. *Astronomy and Astrophysics*, **241**, 137.

Iben, I. (1982). Hot accreting white dwarfs in the quasi-static approximation. *The Astrophysical Journal*, **259**, 244.

In't Zand, J. J. M., Corbet, R. H. D., & Marshall, F. E. (2001). Discovery of a 75 Day Orbit in XTE J1543-568. *The Astrophysical Journal Letters*, **553**, L165.

Israel, G. L., Covino, S., Campana, S., Polcaro, V. F., Roche, P., Stella, L., Di Paola, A., Lazzati, D., Mereghetti, S., Giallongo, E., Fontana, A., & Verrecchia, F. (2000). The discovery of the optical/IR counterpart of the 12-s transient X-ray pulsar GS 0834-43. *Monthly Notices of the Royal Astronomical Society*, **314**, 87.

Janka, H.-T. & Mueller, E. (1994). Neutron star recoils from anisotropic supernovae. *Astronomy and Astrophysics*, **290**, 496.

Johnston, H. M. (1996). An Observational Approach to Binary Population Synthesis. In *NATO ASIC Proc. 477: Evolutionary Processes in Binary Stars*, page 385.

Johnston, H. M. & Verbunt, F. (1996). The globular cluster population of low-luminosity X-ray sources. *Astronomy and Astrophysics*, **312**, 80.

Johnston, S., Manchester, R. N., Lyne, A. G., Bailes, M., Kaspi, V. M., Qiao, G., & D'Amico, N. (1992). PSR 1259-63 - A binary radio pulsar with a Be star companion. *The Astrophysical Journal Letters*, **387**, L37.

Joshi, K. J., Nave, C. P., & Rasio, F. A. (2001). Monte Carlo Simulations of Globular Cluster Evolution. II. Mass Spectra, Stellar Evolution, and Lifetimes in the Galaxy. *The Astrophysical Journal*, **550**, 691–702.

Kalogera, V. (2000). Spin-Orbit Misalignment in Close Binaries with Two Compact Objects. *The Astrophysical Journal*, **541**, 319.

Kalogera, V. & Webbink, R. F. (1996). Formation of Low-Mass X-Ray Binaries. I. Constraints on Hydrogen-rich Donors at the Onset of the X-Ray Phase. *The Astrophysical Journal*, **458**, 301.

Kalogera, V. & Webbink, R. F. (1998). Formation of Low-Mass X-Ray Binaries. II. Common Envelope Evolution of Primordial Binaries with Extreme Mass Ratios. *The Astrophysical Journal*, **493**, 351.

Kaspi, V. M., Johnston, S., Bell, J. F., Manchester, R. N., Bailes, M., Bessell, M., Lyne, A. G., & D'Amico, N. (1994). A massive radio pulsar binary in the Small Magellanic Cloud. *The Astrophysical Journal Letters*, **423**, L43.

Kaspi, V. M., Bailes, M., Manchester, R. N., Stappers, B. W., & Bell, J. F. (1996). Evidence from a precessing pulsar orbit for a neutron-star birth kick. *Nature*, **381**, 584.

Katz, J. I. (1983). Stellar collapse, pulsars, and globular clusters. *Astronomy and Astrophysics*, **128**, L1.

Kelley, R. L., Rappaport, S., & Ayasli, S. (1983). Discovery of 9.3 S X-ray pulsations from 2S 1553-542 and a determination of the orbit. *The Astrophysical Journal*, **274**, 765.

King, A. R. & Ritter, H. (1999). Cygnus X-2, super-Eddington mass transfer, and pulsar binaries. *Monthly Notices of the Royal Astronomical Society*, **309**, 253.

Kolb, U., Davies, M. B., King, A., & Ritter, H. (2000). The violent past of Cygnus X-2. *Monthly Notices of the Royal Astronomical Society*, **317**, 438.

Koyama, K., Kondo, H., Makino, F., Nagase, F., Takano, S., Tawara, Y., Turner, M. J. L., & Warwick, R. S. (1989). Are there many Be star binary X-ray pulsars in the galactic ridge? *Publications of the Astronomical Society of Japan*, **41**, 483.

Kraicheva, Z. T., Popova, E. I., Tutukov, A. V., & Iungelson, L. R. (1978). Some properties of spectroscopic binary stars. *Soviet Astronomy*, **22**, 670.

Kroupa, P., Tout, C. A., & Gilmore, G. (1993). The distribution of low-mass stars in the Galactic disc. *Monthly Notices of the Royal Astronomical Society*, **262**, 545.

Kudritzki, R. & Puls, J. (2000). Winds from Hot Stars. *Annual Review of Astronomy and Astrophysics*, **38**, 613.

Landau, L. D. & Lifshitz, E. M. (1975). *The classical theory of fields.* Oxford: Pergamon Press, 1975, 4th Revised English Edition.

Langer, N. (1989). Mass-dependent mass loss rates of Wolf-Rayet stars. *Astronomy and Astrophysics*, **220**, 135.

Langer, N. & Maeder, A. (1995). The problem of the blue-to-red supergiant ratio in galaxies. *Astronomy and Astrophysics*, **295**, 685.

Levine, A. M., Rappaport, S. A., & Zojcheski, G. (2000). Orbital Decay in LMC X-4. *The Astrophysical Journal*, **541**, 194.

Lewin, W. H. G., van Paradijs, J., & Taam, R. E. (1993). X-Ray Bursts. *Space Science Reviews*, **62**, 223.

Lipunov, V. M., Postnov, K. A., & Prokhorov, M. E. (1997). Formation and coalescence of relativistic binary stars: the effect of kick velocity. *Monthly Notices of the Royal Astronomical Society*, **288**, 245.

Liu, Q. Z., van Paradijs, J., & van den Heuvel, E. P. J. (2000). A catalogue of high-mass X-ray binaries. *Astronomy and Astrophysics Supplement Series*, **147**, 25.

Liu, Q. Z., van Paradijs, J., & van den Heuvel, E. P. J. (2001). A catalogue of low-mass X-ray binaries. *Astronomy and Astrophysics*, **368**, 1021.

Livne, E., Tuchman, Y., & Wheeler, J. C. (1992). Explosion of a supernova with a red giant companion. *The Astrophysical Journal*, **399**, 665.

Lyne, A. G. & Lorimer, D. R. (1994). High Birth Velocities of Radio Pulsars. *Nature*, **369**, 127.

Maeder, A. (1992). Stellar yields as a function of initial metallicity and mass limit for black hole formation. *Astronomy and Astrophysics*, **264**, 105.

Manchester, R. N., Johnston, S., Lyne, A. G., D'Amico, N., Bailes, M., & Nicastro, L. (1995). Period evolution of PSR B1259-63: Evidence for propeller-torque spindown. *The Astrophysical Journal Letters*, **445**, L137.

Marietta, E., Burrows, A., & Fryxell, B. (2000). Type IA Supernova Explosions in Binary Systems: The Impact on the Secondary Star and Its Consequences. *The Astrophysical Journal Supplement Series*, **128**, 615.

Marigo, P., Girardi, L., Chiosi, C., & Wood, P. R. (2001). Zero-metallicity stars. I. Evolution at constant mass. *Astronomy and Astrophysics*, **371**, 152.

Mason, B. D., Gies, D. R., Hartkopf, W. I., Bagnuolo, W. G., Brummelaar, T. T., & McAlister, H. A. (1998). ICCD speckle observations of binary stars. XIX - an astrometric/spectroscopic survey of O stars. *The Astronomical Journal*, **115**, 821.

McGary, R. S., Brisken, W. F., Fruchter, A. S., Goss, W. M., & Thorsett, S. E. (2001). Proper-Motion Measurements with the VLA. I. Wide-Field Imaging and Pulse-gating Techniques. *The Astronomical Journal*, **121**, 1192.

Meurs, E. J. A. & van den Heuvel, E. P. J. (1989). The number of evolved early-type close binaries in the Galaxy. *Astronomy and Astrophysics*, **226**, 88.

Meyer, F. & Meyer-Hofmeister, E. (1979). Formation of cataclysmic binaries through common envelope evolution. *Astronomy and Astrophysics*, **78**, 167.

Meylan, G., Sarajedini, A., Jablonka, P., Djorgovski, S. G., Bridges, T., & Rich, R. M. (2001). Mayall II=G1 in M31: Giant Globular Cluster or Core of a Dwarf Elliptical Galaxy? *The Astronomical Journal*, **122**, 830.

Miller, G. E. & Scalo, J. M. (1979). The initial mass function and stellar birthrate in the solar neighborhood. *The Astrophysical Journal Supplement Series*, **41**, 513.

Nagase, F. (1989). Accretion-powered X-ray pulsars. *Publications of the Astronomical Society of Japan*, **41**, 1.

Negueruela, I., Marco, A., Speziali, R., & Israel, G. L. (2000). KS 1947+300. *IAU Circ.*, **7541**, 2.

Nelemans, G., Yungelson, L. R., Portegies Zwart, S. F., & Verbunt, F. (2001). Population synthesis for double white dwarfs . I. Close detached systems. *Astronomy and Astrophysics*, **365**, 491.

Nelson, C. A. & Eggleton, P. P. (2001). A Complete Survey of Case A Binary Evolution with Comparison to Observed Algol-type Systems. *The Astrophysical Journal*, **552**, 664.

Nieuwenhuijzen, H. & de Jager, C. (1990). Parametrization of stellar rates of mass loss as functions of the fundamental stellar parameters M, L, and R. *Astronomy and Astrophysics*, **231**, 134.

Nomoto, K. (1982). Accreting white dwarf models for type I supernovae. I - Presupernova evolution and triggering mechanisms. *The Astrophysical Journal*, **253**, 798.

Nomoto, K. (1987). Neutron Star Formation in Theoretical Supernovae - Low Mass Stars and White Dwarfs. In *IAU Symp. 125: The Origin and Evolution of Neutron Stars*, volume 125, page 281.

Nomoto, K. & Iben, I. (1985). Carbon ignition in a rapidly accreting degenerate dwarf - A clue to the nature of the merging process in close binaries. *The Astrophysical Journal*, **297**, 531.

Nomoto, K. & Kondo, Y. (1991). Conditions for accretion-induced collapse of white dwarfs. *The Astrophysical Journal Letters*, **367**, L19.

Ögelman, H. & Swank, J. H. (1974). Neutron stars with main sequence binary companions as low luminosity X-ray sources. *Astronomy and Astrophysics*, **37**, 101.

Orosz, J. A. & Kuulkers, E. (1999). The optical light curves of Cygnus X-2 (V1341 Cyg) and the mass of its neutron star. *Monthly Notices of the Royal Astronomical Society*, **305**, 132.

Paczyński, B. (1976). Common Envelope Binaries. In *IAU Symp. 73: Structure and Evolution of Close Binary Systems*, volume 73, page 75.

Paczyński, B. (1990). A test of the galactic origin of gamma-ray bursts. *The Astrophysical Journal*, **348**, 485.

Paczyński, B. & Sienkiewicz, R. (1972). Unknown. *Acta Astronomica*, **22**, 73.

Pfahl, E. & Rappaport, S. (2001). Bondi-Hoyle-Lyttleton Accretion Model for Low-Luminosity X-Ray Sources in Globular Clusters. *The Astrophysical Journal*, **550**, 172.

Phinney, E. S. & Sigurdsson, S. (1991). Ejection of pulsars and binaries to the outskirts of globular clusters. *Nature*, **349**, 220.

Podsiadlowski, P. & Rappaport, S. (2000). Cygnus X-2: The Descendant of an Intermediate-Mass X-Ray Binary. *The Astrophysical Journal*, **529**, 946.

Podsiadlowski, P., Joss, P. C., & Hsu, J. J. L. (1992). Presupernova evolution in massive interacting binaries. *The Astrophysical Journal*, **391**, 246.

Podsiadlowski, P., Hsu, J. J. L., Joss, P. C., & Ross, R. R. (1994). Formation and Evolution of Neutron Stars and Black Holes in Binaries. In *Circumstellar Media in the Late Stages of Evolution*, page 187.

Podsiadlowski, P., Cannon, R. C., & Rees, M. J. (1995). The evolution and final fate of massive Thorne-Zytkow objects. *Monthly Notices of the Royal Astronomical Society*, **274**, 485.

Podsiadlowski, P., Rappaport, S., & Pfahl, E. D. (2002). Evolutionary sequences for low- and intermediate-mass X-ray binaries. *The Astrophysical Journal*, **565**, 1107.

Pols, O. R. (1994). Case A evolution of massive close binaries: formation of contact systems and possible reversal of the supernova order. *Astronomy and Astrophysics*, **290**, 119.

Portegies Zwart, S. F. & Yungelson, L. R. (1998). Formation and evolution of binary neutron stars. *Astronomy and Astrophysics*, **332**, 173.

Preibisch, T., Hofmann, K.-H., Schertl, D., Weigelt, G., Balega, Y., Balega, I., & Zinnecker, H. (2000). Multiplicity of the young O- and B-type stars in the Orion Nebula cluster. In *IAU Symposium*, volume 200, page 106P.

Price, N. M. & Podsiadlowski, P. (1995). Dynamical interactions between young stellar objects and a collisional model for the origin of the stellar mass spectrum. *Monthly Notices of the Royal Astronomical Society*, **273**, 1041.

Pylyser, E. & Savonije, G. J. (1988). Evolution of low-mass close binary sytems with a compact mass accreting component. *Astronomy and Astrophysics*, **191**, 57.

Pylyser, E. H. P. & Savonije, G. J. (1989). The evolution of low-mass close binary systems with a compact component. II - Systems captured by angular momentum losses. *Astronomy and Astrophysics*, **208**, 52.

Rappaport, S. & van den Heuvel, E. P. J. (1982). X-ray observations of Be stars. In *IAU Symp. 98: Be Stars*, volume 98, page 327.

Rappaport, S., Joss, P. C., & Webbink, R. F. (1982). The evolution of highly compact binary stellar systems. *The Astrophysical Journal*, **254**, 616.

Rappaport, S., Joss, P. C., & Verbunt, F. (1983). A new technique for calculations of binary stellar evolution, with application to magnetic braking. *The Astrophysical Journal*, **275**, 713.

Rappaport, S., Di Stefano, R., & Smith, J. D. (1994). Formation and evolution of luminous supersoft X-ray sources. *The Astrophysical Journal*, **426**, 692.

Rappaport, S., Podsiadlowski, P., Joss, P. C., di Stefano, R., & Han, Z. (1995). The relation between white dwarf mass and orbital period in wide binary radio pulsars. *Monthly Notices of the Royal Astronomical Society*, **273**, 731.

Rappaport, S., Pfahl, E., Rasio, F. A., & Podsiadlowski, P. (2001). Formation of Compact Binaries in Globular Clusters. In *ASP Conf. Ser. 229: Evolution of Binary and Multiple Star Systems*, page 409.

Rasio, F. A. & Shapiro, S. L. (1991). Collisions of giant stars with compact objects - Hydrodynamical calculations. *The Astrophysical Journal*, **377**, 559.

Rasio, F. A. & Shapiro, S. L. (1995). Hydrodynamics of binary coalescence. 2: Polytropes with gamma = 5/3. *The Astrophysical Journal*, **438**, 887.

Rasio, F. A., Pfahl, E. D., & Rappaport, S. (2000). Formation of Short-Period Binary Pulsars in Globular Clusters. *The Astrophysical Journal Letters*, **532**, L47.

Rieutord, M. & Zahn, J. (1997). Ekman Pumping and Tidal Dissipation in Close Binaries: A Refutation of Tassoul's Mechanism. *The Astrophysical Journal*, **474**, 760.

Romani, R. W. (1998). A census of low mass black hole binaries. *Astronomy and Astrophysics*, **333**, 583.

Salpeter, E. E. (1955). The Luminosity Function and Stellar Evolution. *The Astrophysical Journal*, **121**, 161.

Sandquist, E. L., Taam, R. E., & Burkert, A. (2000). On the Formation of Helium Double Degenerate Stars and Pre-Cataclysmic Variables. *The Astrophysical Journal*, **533**, 984.

Scalo, J. M. (1986). The stellar initial mass function. *Fundamentals of Cosmic Physics*, **11**, 1.

Secchi, A. (1867). Unknown. *Astron. Nachr.*, **68**, 63.

Shirey, R. E. (1998). Mass Transfer and Accretion in the Eccentric Neutron-Star Binary Circinus X-1. *Ph.D. Thesis*.

Sigurdsson, S. & Phinney, E. S. (1993). Binary–Single Star Interactions in Globular Clusters. *The Astrophysical Journal*, **415**, 631.

Sigurdsson, S. & Phinney, E. S. (1995). Dynamics and Interactions of Binaries and Neutron Stars in Globular Clusters. *The Astrophysical Journal Supplement Series*, **99**, 609.

Skumanich, A. (1972). Time Scales for CA II Emission Decay, Rotational Braking, and Lithium Depletion. *The Astrophysical Journal*, **171**, 565.

Slettebak, A. (1988). The Be stars. *Publications of the Astronomical Society of the Pacific*, **100**, 770.

Smith, M. A. (1979). Rotational studies of lower main-sequence stars. *Publications of the Astronomical Society of the Pacific*, **91**, 737.

Smith, M. A., Robinson, R. D., & Corbet, R. H. D. (1998). A Multiwavelength Campaign on gamma Cassiopeiae. I. The Case for Surface X-Ray Flaring. *The Astrophysical Journal*, **503**, 877.

Spruit, H. C. (1998). Origin of the rotation rates of single white dwarfs. *Astronomy and Astrophysics*, **333**, 603.

Spruit, H. C. (1999). Differential rotation and magnetic fields in stellar interiors. *Astronomy and Astrophysics*, **349**, 189.

Spruit, H. C. (2002). Dynamo action by differential rotation in a stably stratified stellar interior. *Astronomy and Astrophysics*, **381**, 923.

Spruit, H. C. & Phinney, E. S. (1998). Birth kicks as the origin of pulsar rotation. *Nature*, **393**, 139.

Stairs, I. H., Manchester, R. N., Lyne, A. G., Kaspi, V. M., Camilo, F., Bell, J. F., D'Amico, N., Kramer, M., Crawford, F., Morris, D. J., Possenti, A., McKay, N. P. F., Lumsden, S. L., Tacconi-Garman, L. E., Cannon, R. D., Hambly, N. C., & Wood, P. R. (2001). PSR J1740-3052: a pulsar with a massive companion. *Monthly Notices of the Royal Astronomical Society*, **325**, 979.

Stella, L., White, N. E., & Rosner, R. (1986). Intermittent stellar wind accretion and the long-term activity of Population I binary systems containing an X-ray pulsar. *The Astrophysical Journal*, **308**, 669.

Taam, R. E., Bodenheimer, P., & Ostriker, J. P. (1978). Double core evolution. I - A 16 solar mass star with a 1 solar mass neutron-star companion. *The Astrophysical Journal*, **222**, 269.

Takahashi, K. & Portegies Zwart, S. F. (2000). The Evolution of Globular Clusters in the Galaxy. *The Astrophysical Journal*, **535**, 759.

Tauris, T. M. & Savonije, G. J. (1999). Formation of millisecond pulsars. I. Evolution of low-mass X-ray binaries with orbital periods greater than 2 days. *Astronomy and Astrophysics*, **350**, 928.

Tauris, T. M. & Takens, R. J. (1998). Runaway velocities of stellar components originating from disrupted binaries via asymmetric supernova explosions. *Astronomy and Astrophysics*, **330**, 1047.

Tauris, T. M., van den Heuvel, E. P. J., & Savonije, G. J. (2000). Formation of Millisecond Pulsars with Heavy White Dwarf Companions:Extreme Mass Transfer on Subthermal Timescales. *The Astrophysical Journal Letters*, **530**, L93.

Tayler, R. J. (1973). The adiabatic stability of stars containing magnetic fields-I.Toroidal fields. *Monthly Notices of the Royal Astronomical Society*, **161**, 365.

Thorne, K. S. & Zytkow, A. N. (1975). Red giants and supergiants with degenerate neutron cores. *The Astrophysical Journal Letters*, **199**, L19.

Thorne, K. S. & Zytkow, A. N. (1977). Stars with degenerate neutron cores. I - Structure of equilibrium models. *The Astrophysical Journal*, **212**, 832.

Torra, J., Fernández, D., & Figueras, F. (2000). Kinematics of young stars. I. Local irregularities. *Astronomy and Astrophysics*, **359**, 82.

Toscano, M., Britton, M. C., Manchester, R. N., Bailes, M., Sandhu, J. S., Kulkarni, S. R., & Anderson, S. B. (1999). Parallax of PSR J1744-1134 and the Local Interstellar Medium. *The Astrophysical Journal Letters*, **523**, L171.

Tutukov, A. V., Fedorova, A. V., Ergma, E. V., & Yungelson, L. R. (1985). Evolution of Low-Mass Close Binaries - the Minimum Orbital Period. *Soviet Astronomy Letters*, **11**, 52.

van den Heuvel, E. P. J. (1987). Millisecond pulsar formation and evolution. In *IAU Symp. 125: The Origin and Evolution of Neutron Stars*, volume 125, pages 393–404.

van den Heuvel, E. P. J., Bhattacharya, D., Nomoto, K., & Rappaport, S. A. (1992). Accreting white dwarf models for CAL 83, CAL 87 and other ultrasoft X-ray sources in the LMC. *Astronomy and Astrophysics*, **262**, 97.

van den Heuvel, E. P. J., Portegies Zwart, S. F., Bhattacharya, D., & Kaper, L. (2000). On the origin of the difference between the runaway velocities of the OB-supergiant X-ray binaries and the Be/X-ray binaries. *Astronomy and Astrophysics*, **364**, 563.

van der Klis, M. (2000). Millisecond Oscillations in X-ray Binaries. *Annual Review of Astronomy and Astrophysics*, **38**, 717.

van der Kruit, P. C. (1987). Comparison of the Galaxy with external spiral galaxies. In *NATO ASIC Proc. 207: The Galaxy*, page 27.

Verbunt, F. (2001). A census with ROSAT of low-luminosity X-ray sources in globular clusters. *Astronomy and Astrophysics*, **368**, 137.

Verbunt, F. & Hasinger, G. (1998). Nine X-ray sources in the globular cluster 47 Tucanae. *Astronomy and Astrophysics*, **336**, 895.

Verbunt, F. & van den Heuvel, E. P. J. (1995). Formation and Evolution of Neutron Stars and Black Holes in Binaries. In *X-ray Binaries*, page 457.

Wang, Q. D., Gotthelf, E. V., & Lang, C. C. (2002). A faint discrete source origin for the highly ionized iron emission from the Galactic Centre region. *Nature*, **415**, 148.

Webbink, R. F. (1984). Double white dwarfs as progenitors of R Coronae Borealis stars and Type I supernovae. *The Astrophysical Journal*, **277**, 355.

Wellstein, S., Langer, N., & Braun, H. (2001). Formation of contact in massive close binaries. *Astronomy and Astrophysics*, **369**, 939.

Wheeler, J. C., Lecar, M., & McKee, C. F. (1975). Supernovae in binary systems. *The Astrophysical Journal*, **200**, 145.

Wilson, C. A., Finger, M. H., Harmon, B. A., Scott, D. M., Wilson, R. B., Bildsten, L., Chakrabarty, D., & Prince, T. A. (1997). A Sequence of Outbursts from the Transient X-Ray Pulsar GS 0834-430. *The Astrophysical Journal*, **479**, 388.

Zahn, J.-P. (1977). Tidal friction in close binary stars. *Astronomy and Astrophysics*, **57**, 383.